

**NASA CONTRACTOR  
REPORT**

**NASA CR-150324**

**(NASA-CR-150324) SOLID-PROPELLANT ROCKET  
MOTOR INTERNAL BALLISTIC PERFORMANCE  
VARIATION ANALYSIS, PHASE 2 Final Report  
(Auburn Univ.) 127 p HC A07/MF A01 CSCL 21H**

**N77-28213**

**Unclas**

**G3/20 39225**

**SOLID-PROPELLANT ROCKET MOTOR INTERNAL BALLISTIC  
PERFORMANCE VARIATION ANALYSES (PHASE TWO)**

**By Richard H. Sforzini and Winfred A. Foster, Jr.  
Aerospace Engineering Department  
Auburn University  
Auburn, Alabama**

**Final Report**

**September 1976**



**Prepared for**

**NASA - GEORGE C. MARSHALL SPACE FLIGHT CENTER  
Marshall Space Flight Center, Alabama 35812**

TECHNICAL REPORT STANDARD TITLE PAGE

1. REPORT NO. NASA CR-150324	2. GOVERNMENT ACCESSION NO.	3. RECIPIENT'S CATALOG NO.	
4. TITLE AND SUBTITLE Solid-Propellant Rocket Motor Internal Ballistic Performance Variation Analysis (Phase Two)		5. REPORT DATE September 1976	6. PERFORMING ORGANIZATION CODE
7. AUTHOR(S) Richard H. Sforzini and Winfred A. Foster, Jr.		8. PERFORMING ORGANIZATION REPORT #	
9. PERFORMING ORGANIZATION NAME AND ADDRESS Auburn University School of Engineering Auburn, Alabama		10. WORK UNIT NO.	11. CONTRACT OR GRANT NO. NCA8-00120 & NCA8-00124
12. SPONSORING AGENCY NAME AND ADDRESS National Aeronautics and Space Administration Washington, D. C. 20546		13. TYPE OF REPORT & PERIOD COVERED Contractor Report Final	
14. SPONSORING AGENCY CODE		15. SUPPLEMENTARY NOTES	
16. ABSTRACT The report presents the results of continued research aimed at improving the assessment of off-nominal internal ballistics performance including thrust imbalance between two large solid-rocket motors (SRMs) firing in parallel. Previous analyses by the authors using the Monte Carlo technique (NASA Contractor Reports NASA CR-120700 and CR-144264) have been extended to permit detailed investigation of thrust imbalance and its first time derivative throughout the burning times of SRM pairs. Comparison of results with flight performance data from Titan IIIC SRMs shows good agreement. Statistical correlations of the thrust imbalance at various times with corresponding nominal trace slopes suggest several alternative methods of predicting thrust imbalance to that presented in earlier reports. A separate investigation of the effect of circular-perforated grain deformation on internal ballistics is discussed, and a modified design analysis computer program which permits such an evaluation is presented. Comparisons with SRM firings indicate that grain deformation may account for a portion of the so-called scale factor on burning rate between large motors and strand burners or small ballistic test motors. Thermoelastic effects on burning rate are also investigated. Burning surface temperature is calculated by coupling the solid phase energy equation containing a strain rate term with a model of the gas phase combustion zone using the Zeldovich-Novozhilov technique. Comparisons of solutions with and without the strain rate term indicate a small but possibly significant effect of the thermoelastic coupling. An approach is suggested for using the Monte Carlo program to assess the degree of predictability of SRM performance at various phases in a development program; however, it has been determined that the type of data needed for the assessment is not generally available. A number of changes to the computer programs listed in CR-144264 that have been made to improve their accuracy and flexibility are presented.			
17. KEY WORDS		18. DISTRIBUTION STATEMENT Unclassified-Unlimited  <i>A. A. McCool</i> A. A. McCool Director, Structures & Propulsion Lab.	
19. SECURITY CLASSIF. (of this report) Unclassified	20. SECURITY CLASSIF. (of this page) Unclassified	21. NO. OF PAGES 117	22. PRICE NTIS

## ACKNOWLEDGEMENTS

The authors express appreciation to personnel at the George C. Marshall Space Flight Center for their many useful suggestions which materially aided this investigation and in particular to Messrs. B. W. Shackelford, Jr. (NASA Project Coordinator) and E. P. Jacobs.

The suggestion of Dr. L. H. Caveny of Princeton University to use the Zeldovich-Novozhilov technique for modeling transient burning rate phenomena proved quite useful in the thermoelastic analysis and is also gratefully acknowledged.

The participation of the following from the Aerospace Engineering Department at Auburn University is likewise appreciated: Mr. D. F. Smith, graduate student, who assisted in modification of the design analysis computer program for the effects of grain deformation and in the evaluation of sample cases, and who developed the closed form approximation of grain deformation which was used in the program; Ms. L. S. Garrick, graduate research assistant, who performed the statistical computations and prepared a number of figures, Mr. H. Aultman, Jr., applications EDP programmer, who assisted in obtaining and plotting computer results; and Mrs. M. N. McGee who typed the bulk of the manuscript.

## TABLE OF CONTENTS

List of Figures . . . . .	v
List of Tables . . . . .	vii
Nomenclature . . . . .	viii
I. Introduction and Summary . . . . .	1
II. The Monte Carlo Evaluation of Performance Parameters . . . . .	4
The Imbalance Analysis Computer Programs. . . . .	4
Correlation of Thrust Imbalance with Thrust Imbalance Rate. . . . .	14
Correlation of Thrust Imbalance with Nominal Thrust Rate . . . . .	14
III. Effect of Grain Deformation on Internal Ballistics . . . . .	20
Analysis of Grain Deformation Effects . . . . .	20
Simplified Determination of Grain Deformation . . . . .	23
Modification of the Design Analysis Computer Program . . . . .	24
Comparison of Theoretical and Experimental Results. . . . .	27
IV. Thermoelastic Analysis . . . . .	32
Basic Theory. . . . .	32
Numerical Solution Procedure . . . . .	36
Numerical Results and Discussion . . . . .	41
V. Performance Predictability Investigation . . . . .	49
VI. Changes to Previous Computer Programs . . . . .	51
VII. Concluding Remarks . . . . .	60
References . . . . .	61

<b>Appendices . . . . .</b>	<b>63</b>
<b>A. A Computer Program for Analysis of SRM Pair Imbalance         Data During Specified Time Intervals . . . . .</b>	<b>64</b>
<b>B. A Computer Program for Analysis of SRM Pair Imbalance         Data at Specified Times During Operation . . . . .</b>	<b>70</b>
<b>C. The SRM Design Analysis Computer Program with Option         Permitting Evaluation of Grain Deformation Effects . . . . .</b>	<b>75</b>

## LIST OF FIGURES

Fig. II-1	CalComp plot of thrust imbalance versus time from 0 to 100 secs. for 30 pairs of theoretical Titan IIIC SRMs. . . . .	6
Fig. II-2	Tolerance limits for thrust imbalance from 0 to 100 secs. for 30 pairs of theoretical Titan IIIC SRMs (Probability 0.90 for 99.7% of the distribution). . . .	8
Fig. II-3	Tolerance limits for first time derivative of thrust imbalance from 0 to 100 secs. for 30 pairs of theoretical Titan IIIC SRMs (Probability 0.90 for 99.7% of the distribution). . . . .	9
Fig. II-4	Comparison of Monte Carlo tolerance limits for 30 pairs of Titan III-C SRMs with flight test analysis for 21 pairs (K = 3.68 and 3.86, respectively; probability of 0.90 for 99.7% of the distribution . . . . .	11
Fig. II-5	Comparison of contractor's thrust imbalance during web action time analysis (Ref. 7) with tolerance limits obtained by the Monte Carlo program for 30 space shuttle type SRM pairs (0.90 probability for 99.7% of distribution). . . . .	12
Fig. II-6	Thrust imbalance versus time from 0 to 105 secs. for 30 theoretical pairs of Space Shuttle type SRMs obtained from the Monte Carlo program . . . . .	13
Fig. II-7	Correlation coefficients between thrust imbalance and thrust imbalance rate at various times during operation for 30 pairs of Titan IIIC SRMs . . . . .	15
Fig. II-8	Scatter diagram: mean of absolute values of thrust imbalance for 30 theoretical Titan IIIC SRM pairs versus the absolute value of mean time rate of change of thrust for the 60 motors . . . . .	17
Fig. II-9	Scatter diagram: standard deviation of thrust imbalance for 30 theoretical Titan IIIC SRM pairs versus the absolute value of the mean time rate of change of thrust for the 60 motors. . . . .	18
Fig. III-1	Sector of cross-section of solid propellant with and without pressurization and combustion. . . . .	21

LIST OF FIGURES (Continued)

Fig. III-2	Grain geometry notation for analysis of solid-propellant strains. The insulation and liner may be considered a part of the propellant . . . . .	21
Fig. III-3a	Comparison of approximate solution for tangential bore strain (Ref. 4) with finite element solution method of Ref. 9 . . . . .	25
Fig. III-3b	Continued comparison of approximate solution for tangential bore strain (Ref. 4) with finite element solution method of Ref. 9 . . . . .	26
Fig. III-4	Comparison of theoretical and experimental results for a Titan IIIC/D SRM with no scale factor on strand burning rate . . . . .	29
Fig. III-5	Comparison of theoretical and experimental results for a Castor TX 354-5 SRM with no scale factor on small ballistic test motor burning rate. . . . .	30
Fig. IV-1	Typical finite element for axisymmetric problem. . . .	37
Fig. IV-2	Schematic of finite element model (no scale) . . . . .	40
Fig. IV-3	Comparison of results with increased pressurization rate to baseline example . . . . .	45
Fig. IV-4	Comparison of results with increased elastic modulus to baseline solution . . . . .	47

## LIST OF TABLES

Table II-1	Sample printout for time interval imbalance analysis computer program . . . . .	5
Table II-2	Sample printout for time slice imbalance analysis computer program . . . . .	10
Table II-3	Results of correlation and regression analysis of Monte Carlo thrust imbalance and thrust imbalance rate for Titan IIIC SRMs ( $\Delta F = b \Delta \bar{r} + c$ ) . . . . .	16
Table IV-1	Baseline example data . . . . .	42
Table IV-2	Results for baseline example . . . . .	43
Table IV-3	Results for modified pressurization rate example. . .	44
Table IV-4	Results for modified elastic modulus example. . . . .	46
Table A-1	Computer program for analysis of SRM pair imbalance data during specified time intervals. . . .	65
Table B-1	Computer program for analysis of SRM pair imbalance data at specified times during operation . . . . .	71
Table C-1	Example data sheets for design analysis program with grain deformation . . . . .	77
Table C-2	Sample computer printout for design analysis program with grain deformation . . . . .	79
Table C-3	SRM design and performance analysis . . . . .	80



## NOMENCLATURE

<u>English Symbol</u>	<u>Definition</u>	<u>Units Used</u>
a	Propellant burning rate coefficient.	in/sec-psi <sup>n</sup>
c	Specific heat.	in-lbf/lbm°F
C <sub>v</sub>	Coefficient of variation; i.e., the ratio of the standard deviation to the mean.	—
e <sub>ij</sub>	Strain tensor.	—
E	Modulus of elasticity.	lbf/in <sup>2</sup>
F	Thrust.	lbf
K	Statistical confidence coefficient.	—
I <sub>t</sub>	Total impulse.	lbf-sec
l	Length of propellant grain.	in.
m	Mass or ratio of inside to outside radius.	slugs or —
$\dot{m}_G$	Mass of propellant gases generated per unit time.	slugs/sec
n	Burning rate exponent or number of observations of a statistically distributed variable.	—
P	Pressure.	lbf/in <sup>2</sup>
r	Burning rate.	in/sec
r <sub>c</sub>	Correlation coefficient.	—
R	Radius.	in.
s	Standard deviation of a sample of a statistically distributed variable.	units vary
s <sub>o</sub>	Square root of the second moment of a sample distribution about an assumed zero mean.	units vary
S	Burning perimeter.	in.
t	Time.	sec.

NOMENCLATURE (Continued)

<u>English Symbol</u>	<u>Definition</u>	<u>Units Used</u>
T	Temperature in thermoelastic analysis.	°R
$T_{Gr}, T_{ref}$	Grain temperature and standard grain temperature, respectively.	°F
x	Radial coordinate in thermoelastic analysis.	in.
$\bar{X}$	Value of general statistically distributed variable.	units vary
$\gamma, \gamma'$	Distance propellant has burned from initial lateral surface of circular perforated grain and from other initial surfaces, respectively.	in.
 <u>Greek Symbol</u>		
$\alpha$	Linear coefficient of thermal expansion	/°F
$\beta$	Volumetric coefficient of thermal expansion	/°F
$\delta_{ij}$	The Kronecker delta (1 when $i=j$ , 0 when $i \neq j$ )	—
$\Delta$	Change or difference in quantity.	units vary
$\epsilon$	Strain.	—
$\eta$	Compressibility.	$\text{in}^2/\text{lbf}$
$\lambda$	Thermal conductivity.	$\text{in-lbf/in-sec } ^\circ\text{F}$
$\nu$	Poisson's ratio.	—
$\rho$	Density.	$\text{slugs/in}^3$
$\sigma$	The standard deviation of a statistically distributed variable; i.e., the square root of the second moment about its mean value.	units vary
$\sigma_p$	Temperature sensitivity of burning rate at constant pressure.	/°R
$\tau$	Thickness.	in.

NOMENCLATURE (Continued)

<u>Subscripts</u>	<u>Definition</u>
av	Average or mean value.
c	Motor case or compressed state of propellant just outside the heat-affected zone.
e	Grain exterior surface position.
i	Grain exterior surface position or initial condition.
max	Maximum value.
o	Unpressurized and unheated state of propellant or in the thermoelastic analysis the ambient transient condition.
p	Propellant.
r	Radial coordinate.
s	Surface condition.
ss	Steady state
t	Transient
w	Propellant web.
y	Distance burned.
z	Axial coordinate.
$\theta$	Tangential coordinate.

## I. INTRODUCTION AND SUMMARY

This report presents the results of research performed at Auburn University during the period October 28, 1975, to September 30, 1976, under Modifications Nos. 17 and 18 to the Cooperative Agreement, dated February 11, 1969, between NASA Marshall Space Flight Center (MSFC) and Auburn University. The principal objective of the research was to further develop techniques for theoretical assessment of solid rocket motor (SRM) internal ballistic performance to include statistical investigation of thrust imbalance of pairs of SRMs firing in parallel as on the booster stage of the Space Shuttle.

The theoretical thrust imbalance of motor pairs has been previously investigated statistically by application of the Monte Carlo technique (Refs. 1-3). The results of this investigation include a computer program which selects sets of significant variables on a probability basis and calculates the performance characteristics for a large number of motor pairs using a mathematical model of the internal ballistics. Comparison of such a statistical analysis for TITAN IIIC motor pairs with test results shows the theory underpredicts the standard deviation in maximum thrust imbalance by 20% with variability in burning times matched within 2% (Ref. 1).

The referenced research disclosed a number of ways in which both nominal and off-nominal performance predictions for single and pairs of SRMs could be improved. The present report deals with the results of research to produce these improvements.

Recent efforts by MSFC to describe thrust imbalance characteristics to be anticipated in a concise way that would be meaningful for systems performance studies have indicated that the Monte Carlo program would be useful for this purpose. Two supplementary computer programs are included in this report to permit the critical imbalance parameters to be determined on a statistical basis throughout the operating times of the SRMs. The principal critical imbalance parameters are the thrust imbalance and its first time derivative. Data for these and other parameters of interest; e.g., impulse imbalance; are generated by the Monte Carlo program and stored on magnetic tape. One program is used to determine the maximum values of the parameters of interest during specified time periods. The second program computes statistical tolerance limits as a function of time based on the Monte Carlo sample. CalComp plots of the parameters of interest versus time are obtainable for both individual SRM pairs overlaid on each other and for the tolerance limits. These are illustrated in the report. Comparison of program results with flight test results for Titan IIIC are given and show good agreement.

The correlation coefficients between thrust imbalance and its time derivative were determined at various times. The results show considerable variation in the goodness of the correlation at various operating

times. A linear regression analysis shows little generalization is possible as to the relation between these variables at the various operating times. On the other hand, there appears to be excellent correlation between thrust imbalance and the nominal slope of the thrust time trace which suggests several alternative approaches to that used in Refs. 1 and 2 for determining thrust imbalance.

Another portion of this research treats certain effects of grain deformation on the internal ballistics of SRMs. The report explains how the deformation can affect the burning rate of the propellant and account for a significant portion of the "scale factor" between large and small motor burning rate. The important factor is the tangential strain of the burning surface of the propellant grain. A method developed by Smith (Ref. 4) has been used to estimate the strain at various times. The method was coupled with the design analysis computer program (Ref. 2) to analyze the effects on internal ballistics for circular-perforated grains. Comparisons are presented of the internal ballistic results with and without grain deformation and with actual test data for two different SRMs. The modified design analysis computer program is listed in the report along with a sample solution. Variations in the propellant and motor case properties (especially variation in the propellant modulus) could produce variations in the grain deformation causing each SRM of a pair to perform differently. However, further verification of the deformation analysis is in order before the results are incorporated into the Monte Carlo program.

A third general aspect of the present investigation is that of changes in grain temperatures produced by high strain rates. Previous research (Ref. 2) indicated that thermoelastic coupling could have a significant effect upon the grain temperature distribution near the burning surface during highly transient chamber pressure conditions. This evaluation was based upon the assumption of a specified fixed surface temperature. However, during transient conditions the surface temperature is not fixed but depends upon both the combustion chamber pressure and the thermoelastic coupling itself which will alter the heat transfer from the combustion zone. Also, the previous analysis considered the effect of surface regression on the energy balance only in an approximate and intuitive way. In the present work, the problem was solved more rigorously. The surface regression term is included in the energy equation along with the strain rate (thermoelastic) term. The surface temperature is calculated by coupling the energy equation with a model of the combustion zone. This is accomplished using the Zeldovich-Novozhilov (Z-N) technique (Ref. 5) which relates the transient heat flux at the surface to steady state burning rate data. The Z-N method has the advantage over other approaches considered of not requiring detailed knowledge of the flame structure which would involve quantities that are difficult to measure.

Solution of the differential equation for the energy balance of the solid propellant grain subject to the appropriate boundary conditions yields the temperature distribution and the surface regression rate. The solutions are obtained using the numerical technique of Foster (Refs. 2 and 6) applied to a circular-perforated case-bonded grain of finite length subjected to an increasing chamber pressure.

Comparisons are made of the results with and without thermoelastic coupling. It is concluded from the comparison that the effect of thermoelastic coupling is very slight. However, it may not be insignificant. Additional research is indicated, particularly with respect to possible viscoelastic effects.

Another facet of internal ballistic performance variation considered is the ability to assess the quality of ballistic predictions. It is important to know the confidence with which the performance of an SRM as a function of time may be predicted at any phase of a motor development program. In general, predictability will improve as more motors of a single type are manufactured and tested. As shown in this report, the Monte Carlo program provides an approach to assessing the degree of predictability both for single SRMs and pairs at various phases in the development program. However, further investigation has shown that it may prove impractical to obtain the type of design and manufacturing data necessary to establish predictability by this method.

The final portion of the report identifies additions and other changes that have been made to the two computer programs listed in Ref. 2: the Monte Carlo program and the design analysis program. Each change is identified by page number and line, as listed in Ref. 2. The changes are for the most part refinements in analysis or program logic. A few minor errors in the programs have been found and corrected. The most extensive addition is the improvement of the use of tabular values for burning surface area during tailoff in the Monte Carlo program. This had been accomplished earlier for the design analysis program.

## II. THE MONTE CARLO EVALUATION OF PERFORMANCE PARAMETERS

The ability to predict the thrust imbalance between a pair of SRMs firing in parallel, such as on the Space Shuttle or Titan IIIC, as a function of time is essential to the total vehicle system design. To do this with a reasonable degree of accuracy without large scale testing programs has obvious economic advantage. As has been discussed in Refs. 1-3, the Monte Carlo technique provides a reasonably accurate and economical means of predicting the performance variations of pairs of SRMs. In the present work, the utility of the Monte Carlo program has been extended to permit further evaluation of performance parameters. The Monte Carlo technique is used to generate, as in Refs. 1-3, the performance of a theoretical population of motor pairs. Provision has now been made, however, for the data generated by the Monte Carlo program to be in the form of a magnetic tape containing the thrust imbalance versus time data for each SRM pair. The changes to the Monte Carlo program necessary to produce the tape are listed in Section VI of this report.

The tape generated by the Monte Carlo program may be analyzed with respect to certain critical performance characteristics by the use of two new computer programs described in this section of the report. Such an analysis is extended for a sample case to a separate investigation of statistical correlations for a number of sets of performance parameters. As is discussed, one particular correlation may have important general practical application.

### The Imbalance Analysis Computer Programs

Because of the various possible applications for the statistical analysis of the thrust imbalance versus time data and to maintain a certain amount of generality, the analysis was done in two parts.

The objective of the first part of the analysis was, given any time interval during which the motors are firing, to determine the mean value and the standard deviation about this mean of the absolute value of the maximum thrust imbalance and of the time within the prescribed interval when this thrust imbalance occurs. This is calculated using a data search routine which is compatible with the data tape generated by the Monte Carlo program. The same calculations were also made for the time rate of change of thrust imbalance within the prescribed time interval.

The computer program for the analysis of imbalance data during specified time intervals is listed in Appendix A. A sample of the computer output is shown in Table II-1. In addition, computer generated plots may be made by superimposing curves representing the thrust imbalances and thrust imbalance rates for each motor pair of the population. This feature is quite useful in determining the limits and general behavior of the imbalances for a particular population of motor pairs. An example of this graphical output is given in Figure II-1. The latter example is based upon a tape of the

Table II-1. Sample printout for time interval imbalance analysis computer program.

THIS IS TIME INTERVAL NUMBER 1  
 THERE ARE 30 SETS OF DATA FOR THIS TIME INTERVAL  
 THIS TIME INTERVAL BEGINS AT 0.0 SECS AND ENDS AT 100.00 SECS

THE ABSOLUTE VALUE OF THE MAXIMUM THRUST IMBALANCE FOR MOTOR PAIR NUMBER 1 IS 1.5809E 04 LBF  
 THIS IMBALANCE OCCURS AT 7.82 SECS

THE ABSOLUTE VALUE OF THE MAXIMUM THRUST IMBALANCE FOR MOTOR PAIR NUMBER 2 IS 2.6190E 03 LBF  
 THIS IMBALANCE OCCURS AT 8.99 SECS

.....

THE ABSOLUTE VALUE OF THE MAXIMUM THRUST IMBALANCE FOR MOTOR PAIR NUMBER 30 IS 7.9540E 03 LBF  
 THIS IMBALANCE OCCURS AT 1.97 SECS

THE ABSOLUTE VALUE OF THE MAXIMUM THRUST IMBALANCE DURING THIS TIME INTERVAL IS 3.4488E 04 LBF  
 THIS IMBALANCE OCCURS AT 8.04 SECS

THE MEAN VALUE OF  
 THE ABSOLUTE VALUE OF THE MAXIMUM THRUST IMBALANCE DURING THIS TIME INTERVAL IS 1.0357E 04 LBF

THE STANDARD DEVIATION OF  
 THE ABSOLUTE VALUE OF THE MAXIMUM THRUST IMBALANCE DURING THIS TIME INTERVAL IS 7.6735E 03 LBF

THE MEAN VALUE OF THE TIME FOR THIS IMBALANCE IS 22.89 SECS

THE STANDARD DEVIATION OF THE TIME FOR THIS IMBALANCE IS 38.16 SECS

THE ABSOLUTE VALUE OF THE MAXIMUM THRUST IMBALANCE RATE FOR MOTOR PAIR NUMBER 1 IS 7.0044E 04 LBF/SEC  
 THIS IMBALANCE RATE OCCURS AT 0.23 SECS

THE ABSOLUTE VALUE OF THE MAXIMUM THRUST IMBALANCE RATE FOR MOTOR PAIR NUMBER 2 IS 8.5780E 03 LBF/SEC  
 THIS IMBALANCE RATE OCCURS AT 0.22 SECS

THE ABSOLUTE VALUE OF THE MAXIMUM THRUST IMBALANCE RATE FOR MOTOR PAIR NUMBER 3 IS 1.4061E 04 LBF/SEC  
 THIS IMBALANCE RATE OCCURS AT 0.24 SECS

THE ABSOLUTE VALUE OF THE MAXIMUM THRUST IMBALANCE RATE FOR MOTOR PAIR NUMBER 4 IS 3.2273E 04 LBF/SEC

.....

ORIGINAL PAGE IS  
OF POOR QUALITY



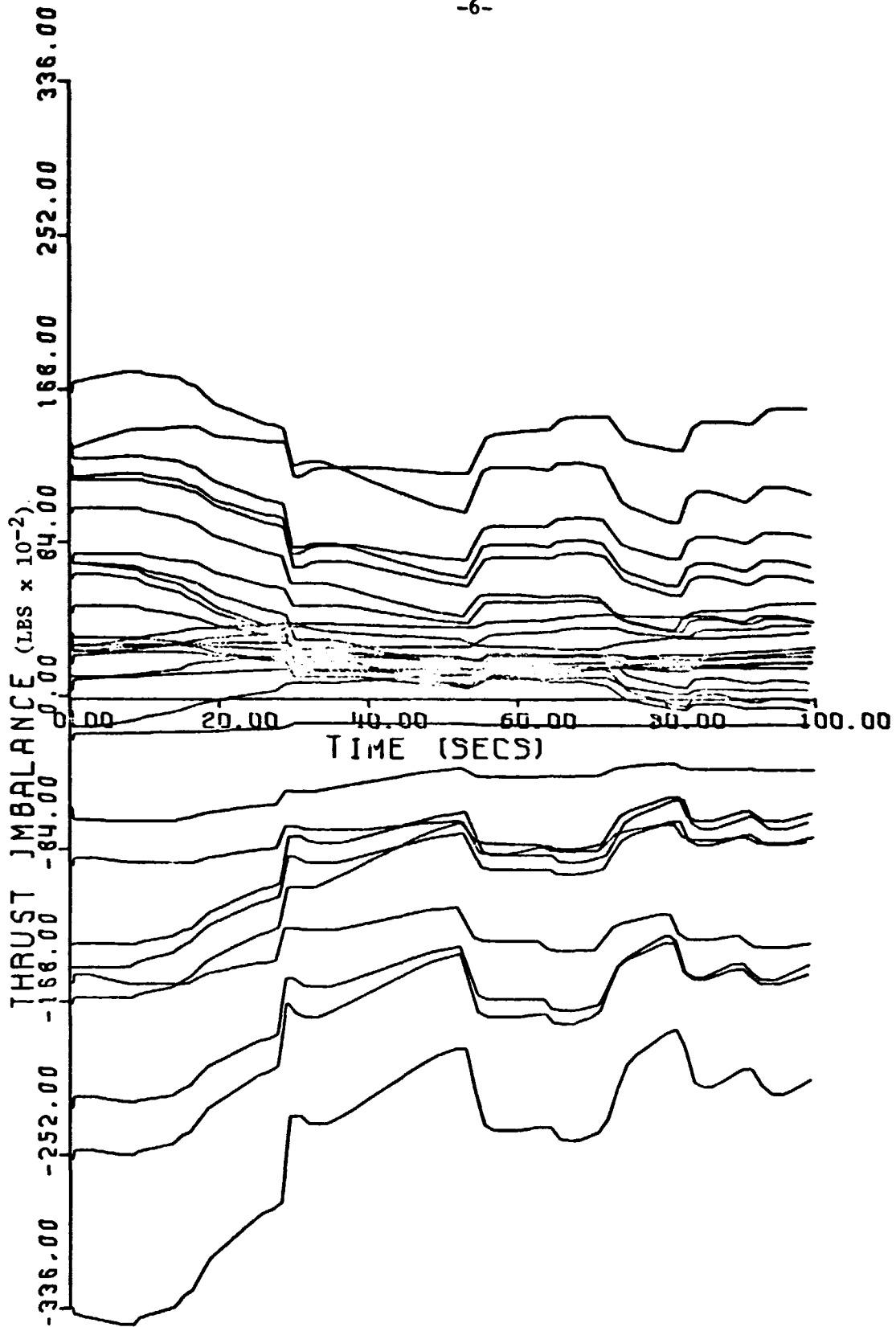


Figure II-1. CalComp plot of thrust imbalance versus time from 0 to 100 secs. for 30 pairs of theoretical Titan IIIC SRMs.

performance of 30 pairs of Titan IIIC SRMs prepared using the input values described in Table 2 of Ref. 1.

Any number of intervals may be specified for analysis. Also, similar data is obtained as output for the absolute value of the maximum impulse imbalance and the times at which they occur. The absolute impulse imbalance is defined by the relation,

$$(\Delta I_t)_{Abs} = \int_0^t |F_1 - F_2| dt \quad (II-1)$$

where  $F_1$  and  $F_2$  are the thrusts of the two motors of a pair. The maximum absolute impulse imbalance clearly occurs at the last tabulated time point within the interval.

The objective of the second part of the analysis was, given any time during which the motors are firing, to determine the statistical limits of the thrust imbalance and the first time derivative of the imbalance. In this analysis these limits are taken to be  $\pm K_2 s_0$ , where  $s_0$  is the second moment of the distribution about an assumed zero mean and  $K_2$  is the two-sided tolerance factor determined by the size of the sample being considered and the specified probability that a specified percentage of the distribution will be included within the limits. A separate data search routine is used to make these calculations and the results are presented in the form of computer generated plots. These plots determine a statistical imbalance envelope for the population. Sample plots are shown in Figures II-2 and II-3 based again on the 30 Titan IIIC pairs. Table II-2 illustrates the computer printout for this data. The computer program used for the time slice analysis is listed in Appendix B.

The second program also generates data similar to that described above on impulse imbalance and absolute impulse imbalance. In the case of the absolute impulse imbalance the upper limit is taken as  $\bar{x} + K_1 s$  where  $K_1$  is the one-sided tolerance limit,  $s$  is the sample standard deviation, and  $\bar{x}$  is the true mean because the  $\pm K_2 s_0$  limits would have little significance in this case.

In order to establish the validity of this analysis, a comparison was made between a sample of 30 Titan IIIC SRM pairs obtained from the Monte Carlo program and data furnished by MSFC on 21 Titan IIIC flight tests. Figure II-4 shows that good agreement was obtained. Another comparison was made between 30 Space Shuttle type SRM pairs from the Monte Carlo program and the contractor's preliminary predicted imbalance envelope (Ref. 7) during web action time. This comparison also showed good agreement with regard to the shape of the envelope as can be seen in Figure II-5. Individual SRM pair results are shown in Figure II-6 for the period 0 to 105 seconds for the Monte Carlo evaluation. The contractor's prediction was based on the estimated 3 sigma spread between matched motors considered

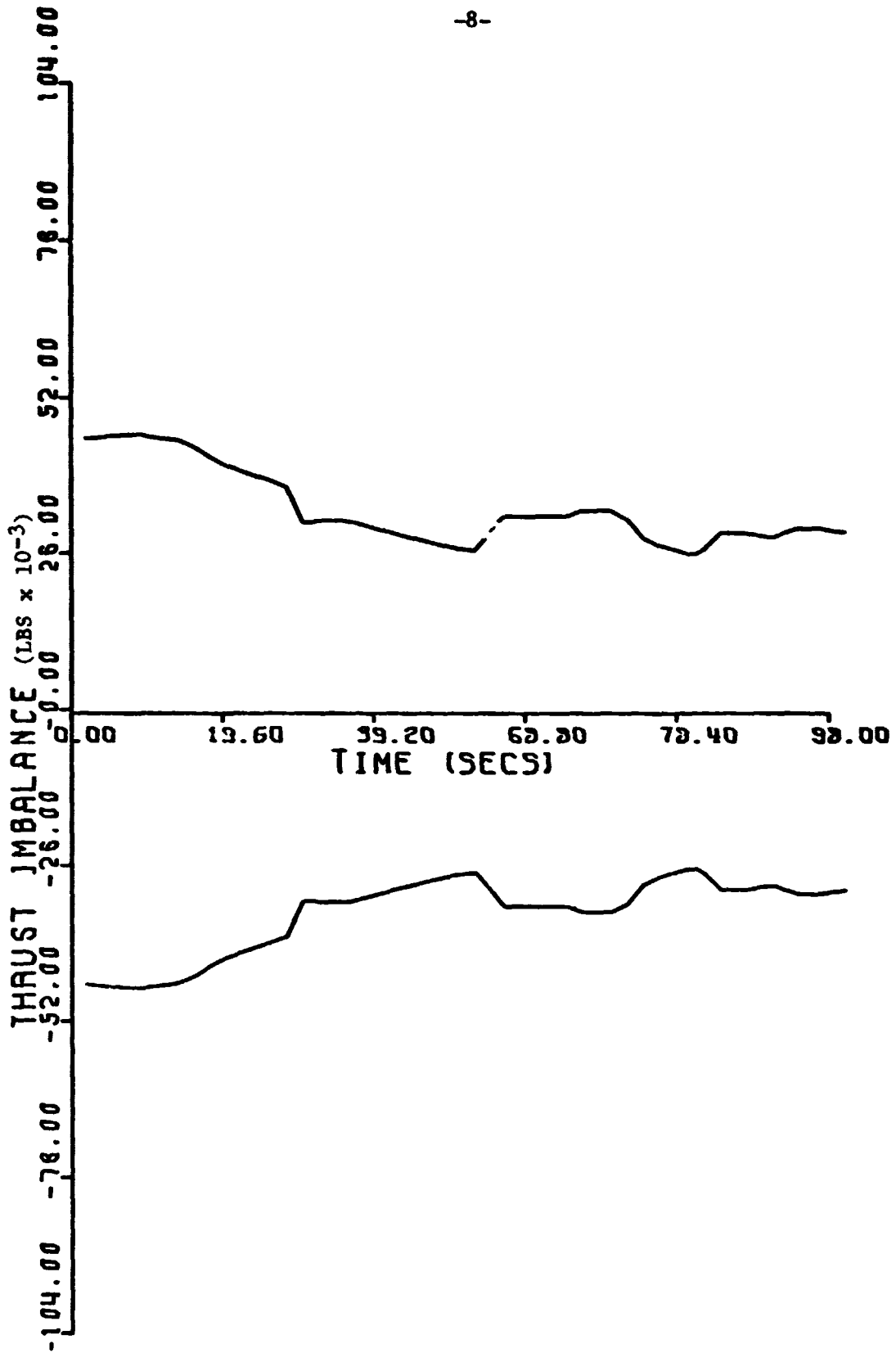


Figure II-2. Tolerance limits for thrust imbalance from 0 to 100 secs. for 30 pairs of theoretical Titan IIIC SRMs (Probability 0.90 for 99.7% of the distribution).

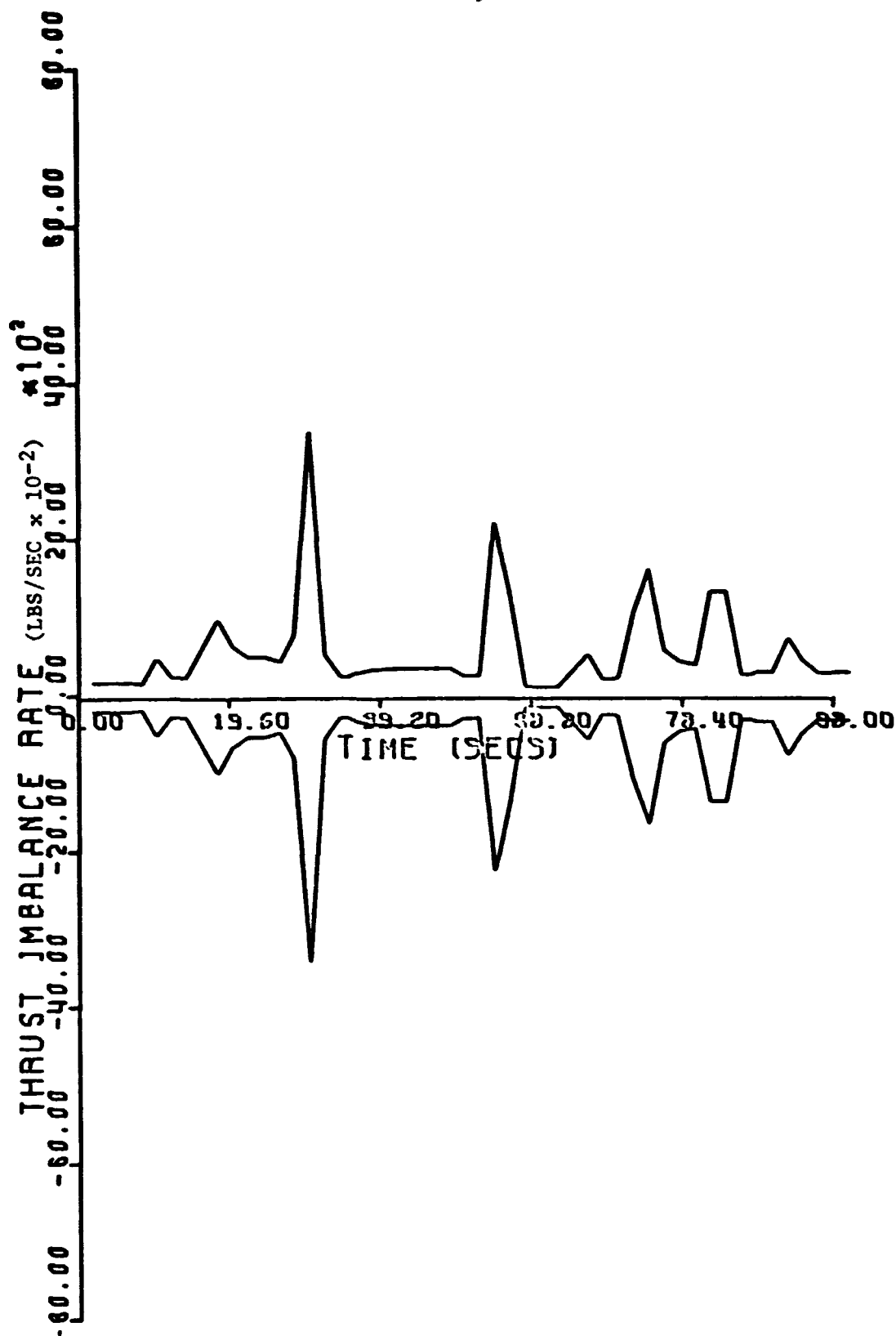


Figure II-3. Tolerance limits for first time derivative of thrust imbalance from 0 to 100 secs. for 30 pairs of theoretical Titan IIC SRMs (Probability 0.90 for 99.7% of the distribution).

Table II-2. Sample printout for time slice imbalance analysis computer program.

THERE ARE 30 SETS OF MOTOR PAIR DATA  
THE ONE SIDED K FACTOR (K1) FOR THIS SAMPLE SIZE IS 3.500  
THE TWO SIDED K FACTOR (K2) FOR THIS SAMPLE SIZE IS 3.680  
THE RESULTS ARE CALCULATED AT 34 TIME SLICES

THIS TIME SLICE WAS TAKEN AT 0.50 SECS  
THE + OR - K2\*SIGMA LIMIT ABOUT A ZERO MEAN FOR THE THRUST IMBALANCE IS 4.5587E 04 LBF  
THE + OR - K2\*SIGMA LIMIT ABOUT A ZERO MEAN FOR THE THRUST IMBALANCE RATE IS 6.6956E 03 LBF/SEC

THIS TIME SLICE WAS TAKEN AT 5.00 SECS  
THE + OR - K2\*SIGMA LIMIT ABOUT A ZERO MEAN FOR THE THRUST IMBALANCE IS 4.6219E 04 LBF  
THE + OR - K2\*SIGMA LIMIT ABOUT A ZERO MEAN FOR THE THRUST IMBALANCE RATE IS 2.1601E 02 LBF/SEC

THIS TIME SLICE WAS TAKEN AT 10.00 SECS  
THE + OR - K2\*SIGMA LIMIT ABOUT A ZERO MEAN FOR THE THRUST IMBALANCE IS 4.5652E 04 LBF  
THE + OR - K2\*SIGMA LIMIT ABOUT A ZERO MEAN FOR THE THRUST IMBALANCE RATE IS 5.0566E 02 LBF/SEC

THIS TIME SLICE WAS TAKEN AT 15.00 SECS  
THE + OR - K2\*SIGMA LIMIT ABOUT A ZERO MEAN FOR THE THRUST IMBALANCE IS 4.4337E 04 LBF  
THE + OR - K2\*SIGMA LIMIT ABOUT A ZERO MEAN FOR THE THRUST IMBALANCE RATE IS 6.0350E 02 LBF/SEC

THIS TIME SLICE WAS TAKEN AT 20.00 SECS  
THE + OR - K2\*SIGMA LIMIT ABOUT A ZERO MEAN FOR THE THRUST IMBALANCE IS 4.0753E 04 LBF  
THE + OR - K2\*SIGMA LIMIT ABOUT A ZERO MEAN FOR THE THRUST IMBALANCE RATE IS 6.3203E 02 LBF/SEC

THIS TIME SLICE WAS TAKEN AT 25.00 SECS  
THE + OR - K2\*SIGMA LIMIT ABOUT A ZERO MEAN FOR THE THRUST IMBALANCE IS 3.8476E 04 LBF  
THE + OR - K2\*SIGMA LIMIT ABOUT A ZERO MEAN FOR THE THRUST IMBALANCE RATE IS 4.8870E 02 LBF/SEC

THIS TIME SLICE WAS TAKEN AT 30.00 SECS  
THE + OR - K2\*SIGMA LIMIT ABOUT A ZERO MEAN FOR THE THRUST IMBALANCE IS 3.1354E 04 LBF  
THE + OR - K2\*SIGMA LIMIT ABOUT A ZERO MEAN FOR THE THRUST IMBALANCE RATE IS 3.4029E 03 LBF/SEC

THIS TIME SLICE WAS TAKEN AT 35.00 SECS  
THE + OR - K2\*SIGMA LIMIT ABOUT A ZERO MEAN FOR THE THRUST IMBALANCE IS 3.1627E 04 LBF  
THE + OR - K2\*SIGMA LIMIT ABOUT A ZERO MEAN FOR THE THRUST IMBALANCE RATE IS 2.9476E 02 LBF/SEC

THIS TIME SLICE WAS TAKEN AT 40.00 SECS  
THE + OR - K2\*SIGMA LIMIT ABOUT A ZERO MEAN FOR THE THRUST IMBALANCE IS 2.9979E 04 LBF  
THE + OR - K2\*SIGMA LIMIT ABOUT A ZERO MEAN FOR THE THRUST IMBALANCE RATE IS 3.8533E 02 LBF/SEC

THIS TIME SLICE WAS TAKEN AT 45.00 SECS  
THE + OR - K2\*SIGMA LIMIT ABOUT A ZERO MEAN FOR THE THRUST IMBALANCE IS 2.8266E 04 LBF  
THE + OR - K2\*SIGMA LIMIT ABOUT A ZERO MEAN FOR THE THRUST IMBALANCE RATE IS 3.5842E 02 LBF/SEC

THIS TIME SLICE WAS TAKEN AT 50.00 SECS  
THE + OR - K2\*SIGMA LIMIT ABOUT A ZERO MEAN FOR THE THRUST IMBALANCE IS 2.6809E 04 LBF  
THE + OR - K2\*SIGMA LIMIT ABOUT A ZERO MEAN FOR THE THRUST IMBALANCE RATE IS 2.5000E 02 LBF/SEC

.....

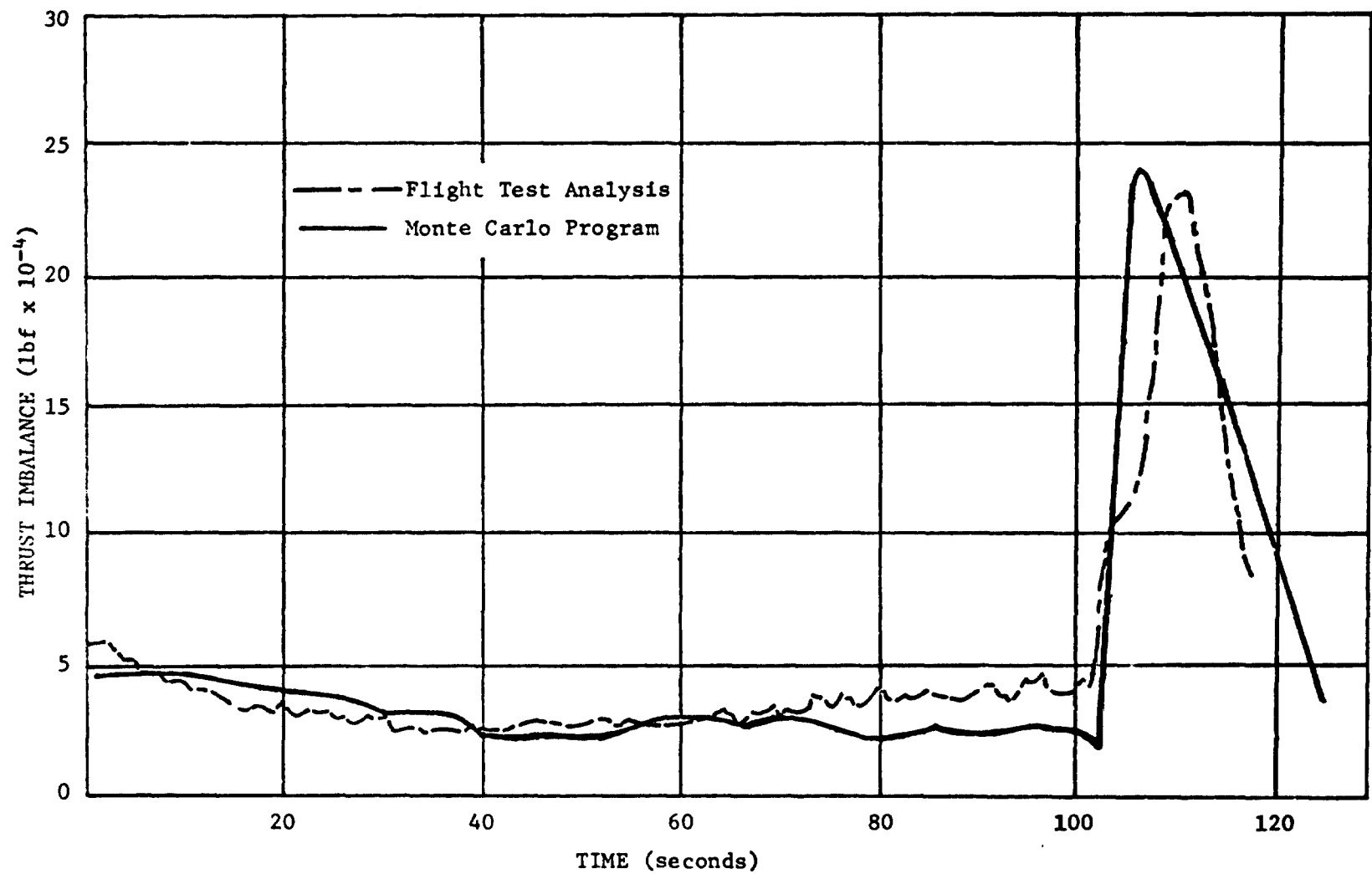


Figure II-4. Comparison of Monte Carlo tolerance limits for 30 pairs of Titan III-C SRMs with flight test analysis for 21 pairs (K = 3.68 and 3.86 respectively; probability 0.90 for 99.7% of the distribution).

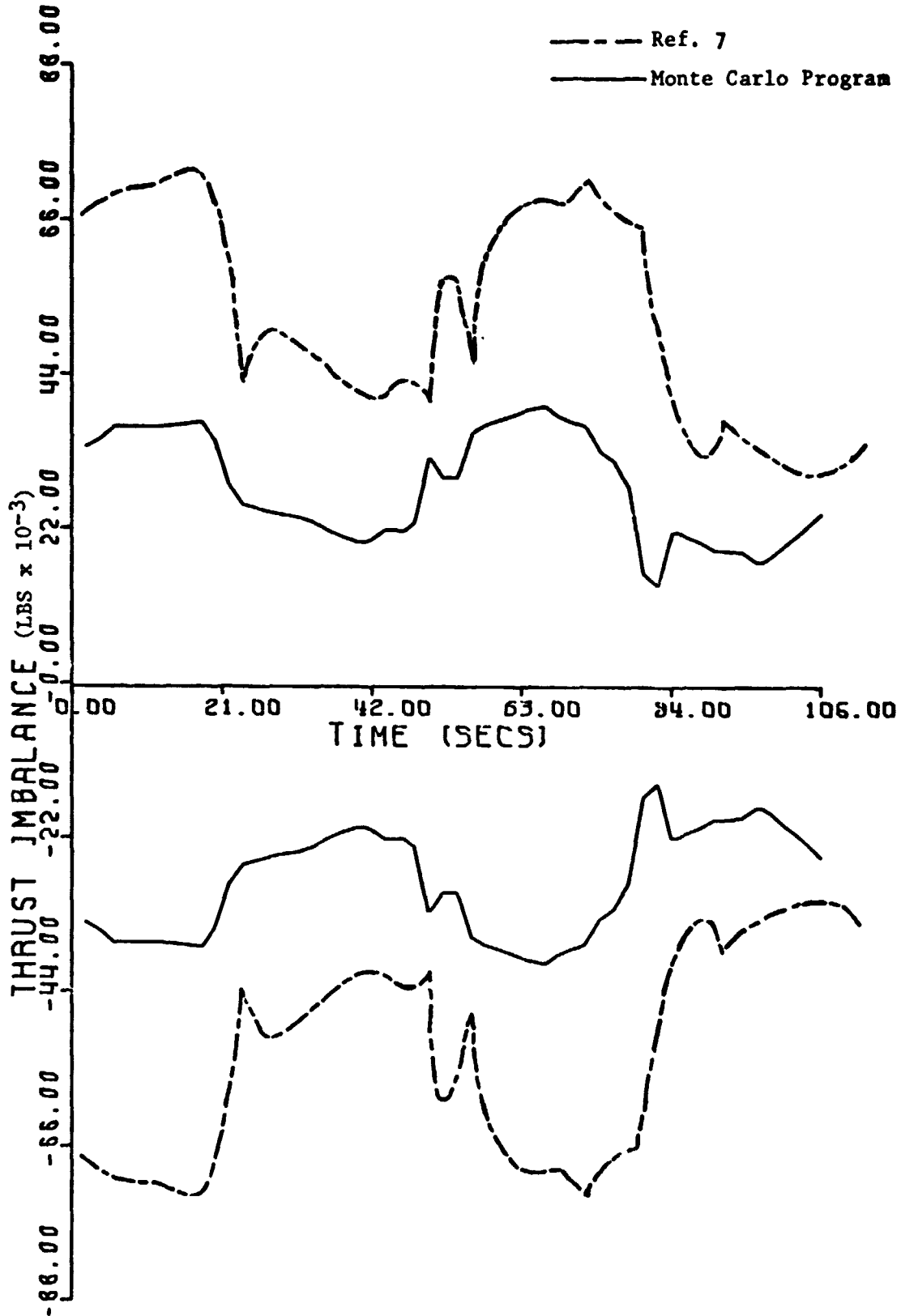
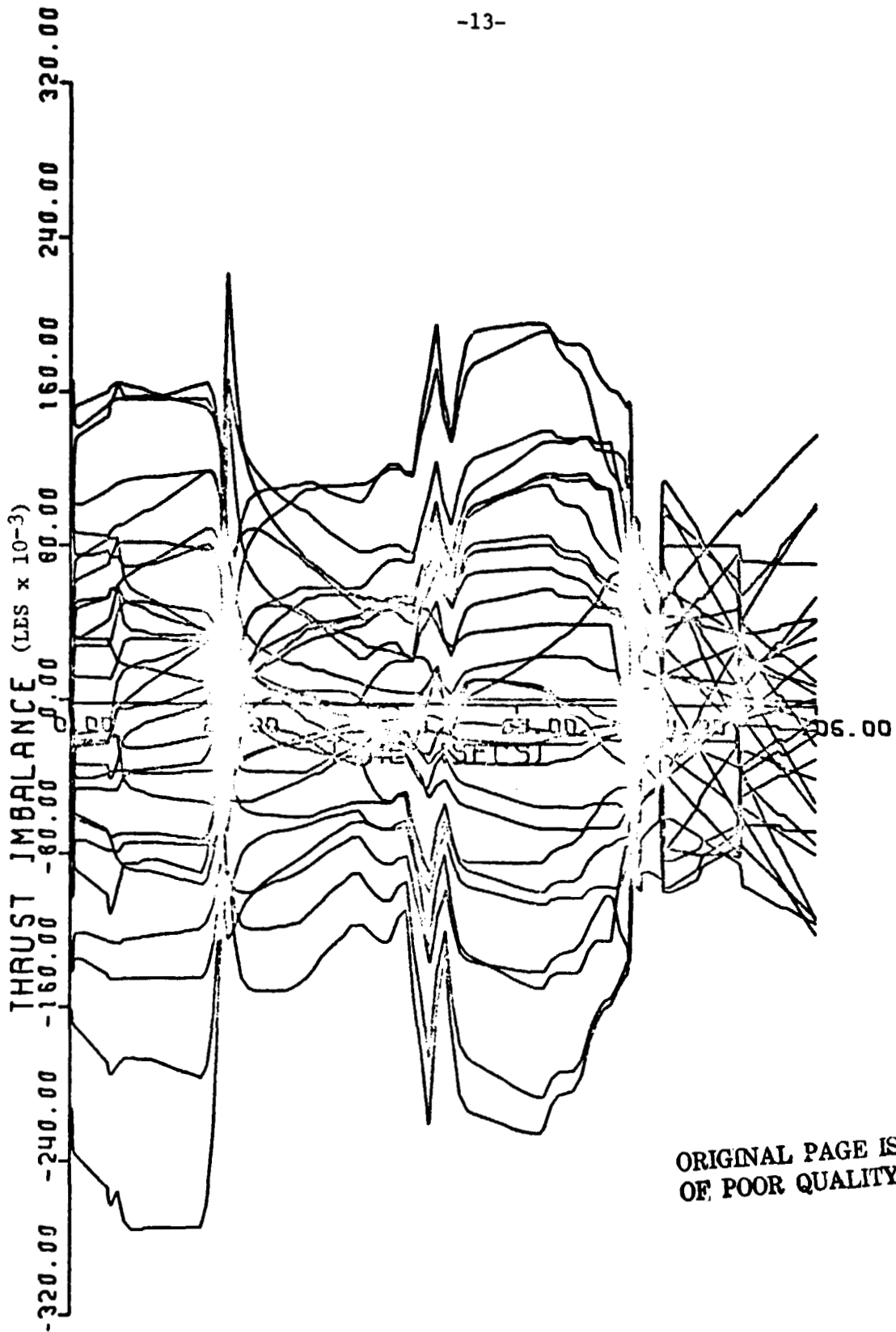


Figure II-5. Comparison of contractor's thrust imbalance during web action time analysis (Ref. 7) with tolerance limits obtained by the Monte Carlo program for 30 space shuttle type SRM pairs (0.99 probability for 99.7% of distribution).



ORIGINAL PAGE IS  
OF POOR QUALITY

Figure II-6. Thrust imbalance versus time from 0 to 105 secs. for 30 theoretical pairs of Space Shuttle type SRMs obtained from the Monte Carlo program.



possible in throat erosion rate, delivered specific impulse, burn rate, and propellant weight. The combination of the variations produced a 2.0% burn time differential which is high with respect to the 0.85% differential predicted by the Monte Carlo program. We attribute the difference in the two results primarily to the much higher burn rate difference ( $C_V=0.42\%$ ) used by the contractor with respect to that used in the Monte Carlo program ( $C_V=0.06\%$ ).

#### Correlation of Thrust Imbalance with Thrust Imbalance Rate

For possible use in systems performance analysis, the correlation between thrust imbalance and its first time derivative was investigated at various operating times. This was done for both algebraic and absolute values of the variables using the data from the Monte Carlo program for the 30 pairs of theoretical Titan IIIC SRMs. At each of the 20 time points considered the correlation coefficient  $r_c$  between the variables was determined. The results are given in Figure II-7. Also, a linear regression line was established for each time point. The slopes and intercepts of the linear regression lines are listed in Table II-3.

Examination of the results shows that there is a better correlation of the algebraic values than the absolute values in the region from 10 to 80 seconds, but the correlation coefficient for the algebraic values changes sign shortly before web time (107 seconds). Both the algebraic and absolute values show poor correlation during the 15 seconds preceding and excellent correlation for the 15 seconds following web time. The varying characteristics of the regression lines at the various time points prevent further generalization of the results.

It is possible that better correlation might be obtained by examining the relationship between thrust imbalance at one time and the thrust imbalance rate at a slightly earlier time. Such correlations have not been attempted because the potential applications of such works have not developed as originally anticipated. However, the analysis has suggested correlations between other variables which may have important consequences as discussed below.

#### Correlation of Thrust Imbalance with Nominal Thrust Rate

Investigation of the correlation between thrust imbalance and nominal thrust-time trace characteristics have revealed some interesting results. The mean of the absolute values of thrust imbalance at a given time was found to have a correlation coefficient of 0.976 with the absolute value of the nominal slope of the thrust-time trace at the same time. This is based on analysis of the previously discussed Titan IIIC Monte Carlo data. A similar correlation of the standard deviation of the absolute values of thrust imbalance with the nominal slope of the thrust-time trace gives a sample correlation coefficient of 0.954. Figures II-8 and 9 are scatter diagrams for the variables. When the thrust imbalance was correlated with both thrust slope and thrust, the correlation was not significantly improved.

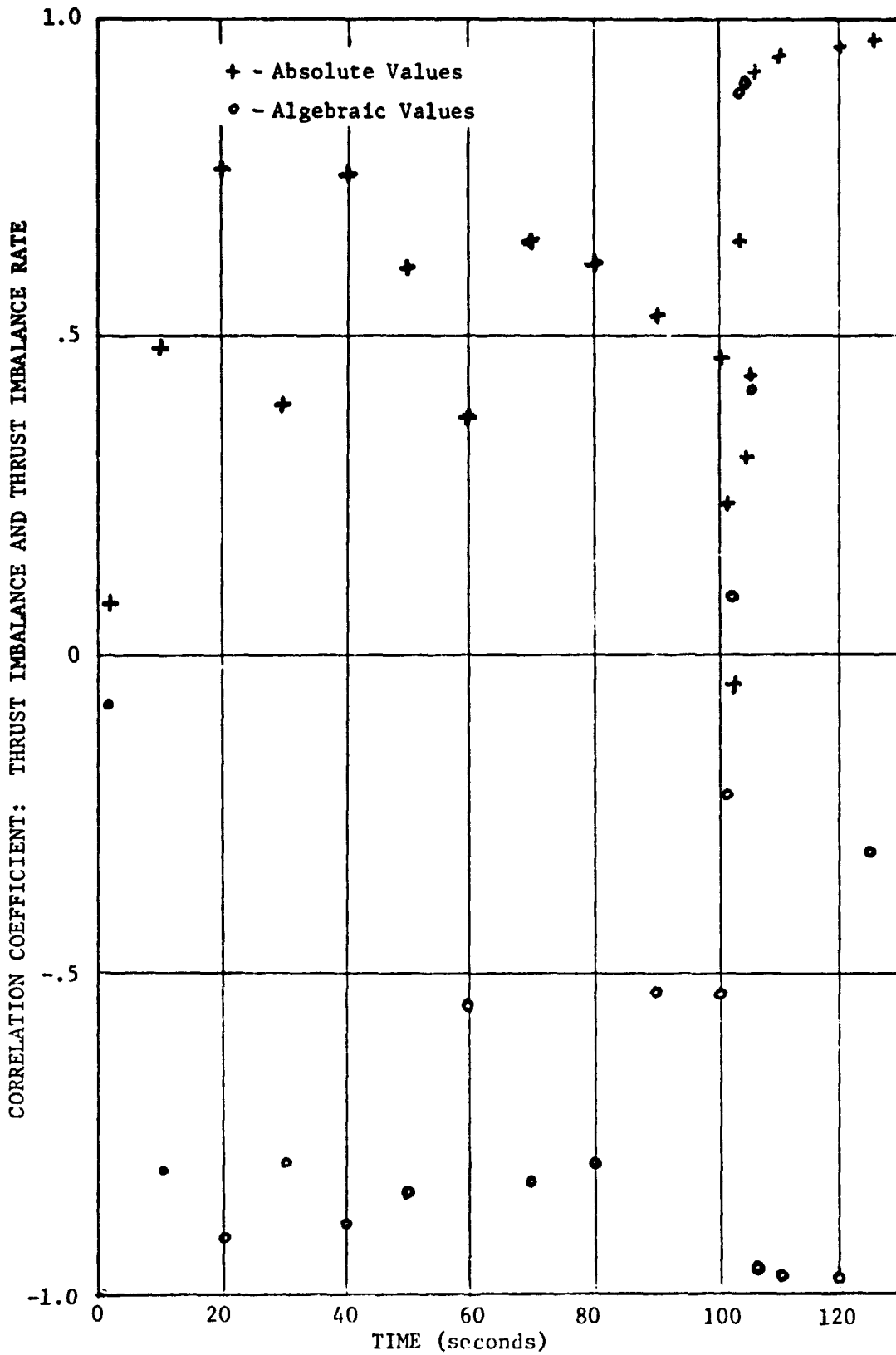


Figure II-7. Correlation coefficients between thrust imbalance and thrust imbalance rate at various times during operation for 30 pairs of Titan IIIC SRMs.

Table II-3. Results of correlation and regression analysis of Monte Carlo thrust imbalance and thrust imbalance rate for Titan IIIC SRMs ( $\Delta F = b \Delta F + c$ ).

Time(sec)	Algebraic Values			Absolute Values		
	b	c	r <sub>c</sub>	b	c	r <sub>c</sub>
0.5	-0.6900	-179	-0.0774	1.1291	8114	0.1590
10.0	-74.5114	-2895	-0.8109	50.6067	3871	0.4905
20.0	-59.8190	-1872	-0.9242	56.6595	528	0.7763
30.0	-7.9085	-3215	-0.8043	3.3994	4329	0.4001
40.0	-70.3361	-241	-0.9054	6.0127	1434	0.7739
50.0	-90.7287	-820	-0.8476	67.9270	1960	0.6126
60.0	-147.0134	-463	-0.5535	101.9460	4138	0.3736
70.0	-101.8451	171	-0.8339	88.4369	1603	0.6678
80.0	-54.3596	-412	-0.8092	44.2926	1659	0.6154
90.0	-46.6494	-1049	-0.5239	46.2998	2862	0.5319
100.0	-53.3827	-992	-0.5424	47.8907	3028	0.4708
107.0	-4.5988	-232	-0.2110	3.6304	5542	0.2421
108.0	-0.0436	1187	-0.0907	-0.0171	4989	-0.0526
103.0	0.5521	3362	0.7057	0.5111	4803	0.6596
104.0	0.7497	13709	0.7070	0.3391	22439	0.3124
105.0	1.2287	3778	0.4265	0.8371	42578	0.4449
106.0	-27.8496	2534	-0.9731	26.9581	2929	0.9324
110.0	-21.2082	1279	-0.9858	21.1880	273	0.9651
120.0	-7.4078	-141	-0.9863	7.4302	-123	0.9670
125.0	-0.5615	3520	-0.3174	0.2900	4899	0.1642

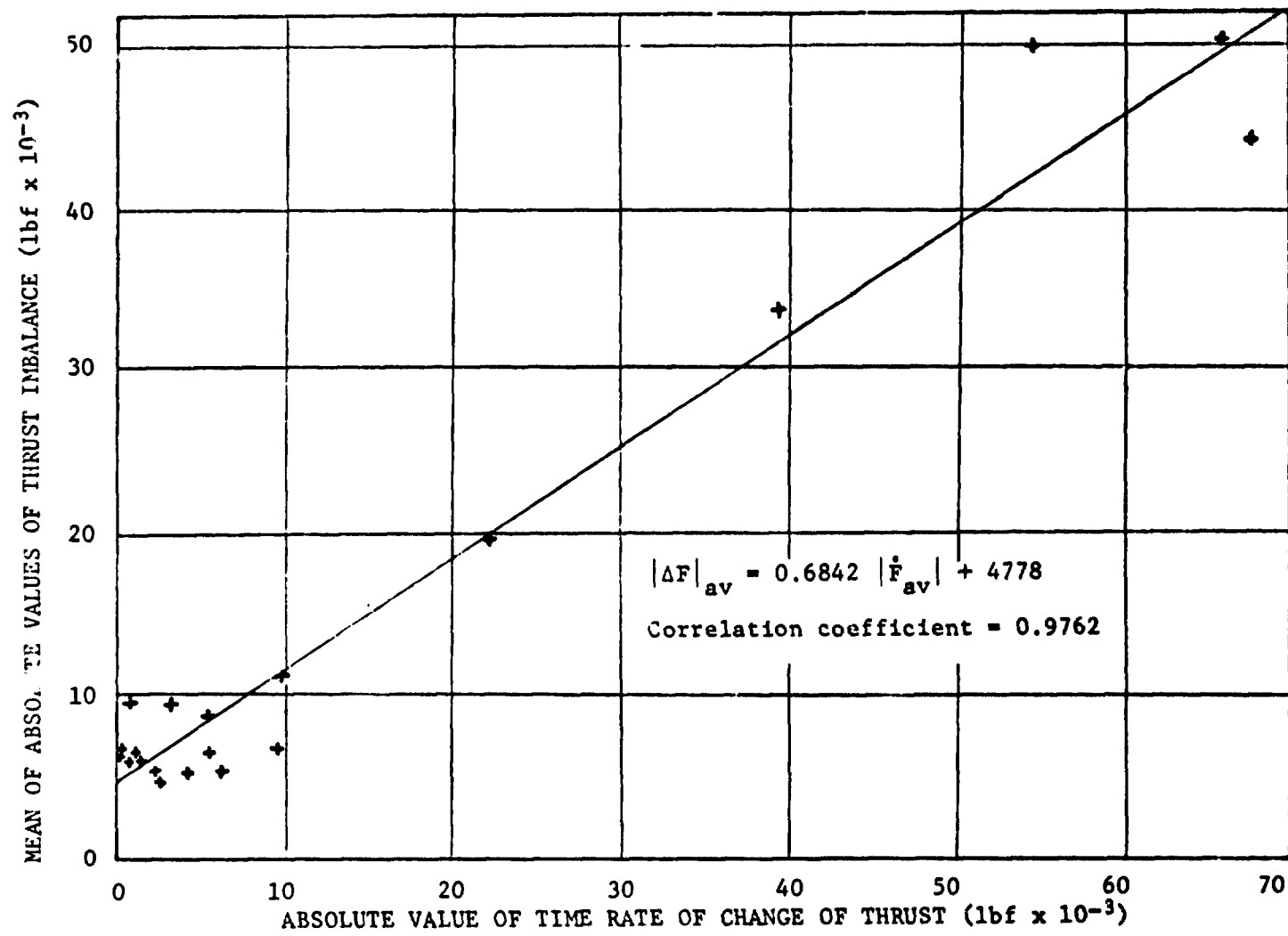


Figure II-8. Scatter diagram: mean of absolute values of thrust imbalance for 30 theoretical Titan IIIC SRM pairs versus the absolute value of mean time rate of change of thrust for the 60 motors.

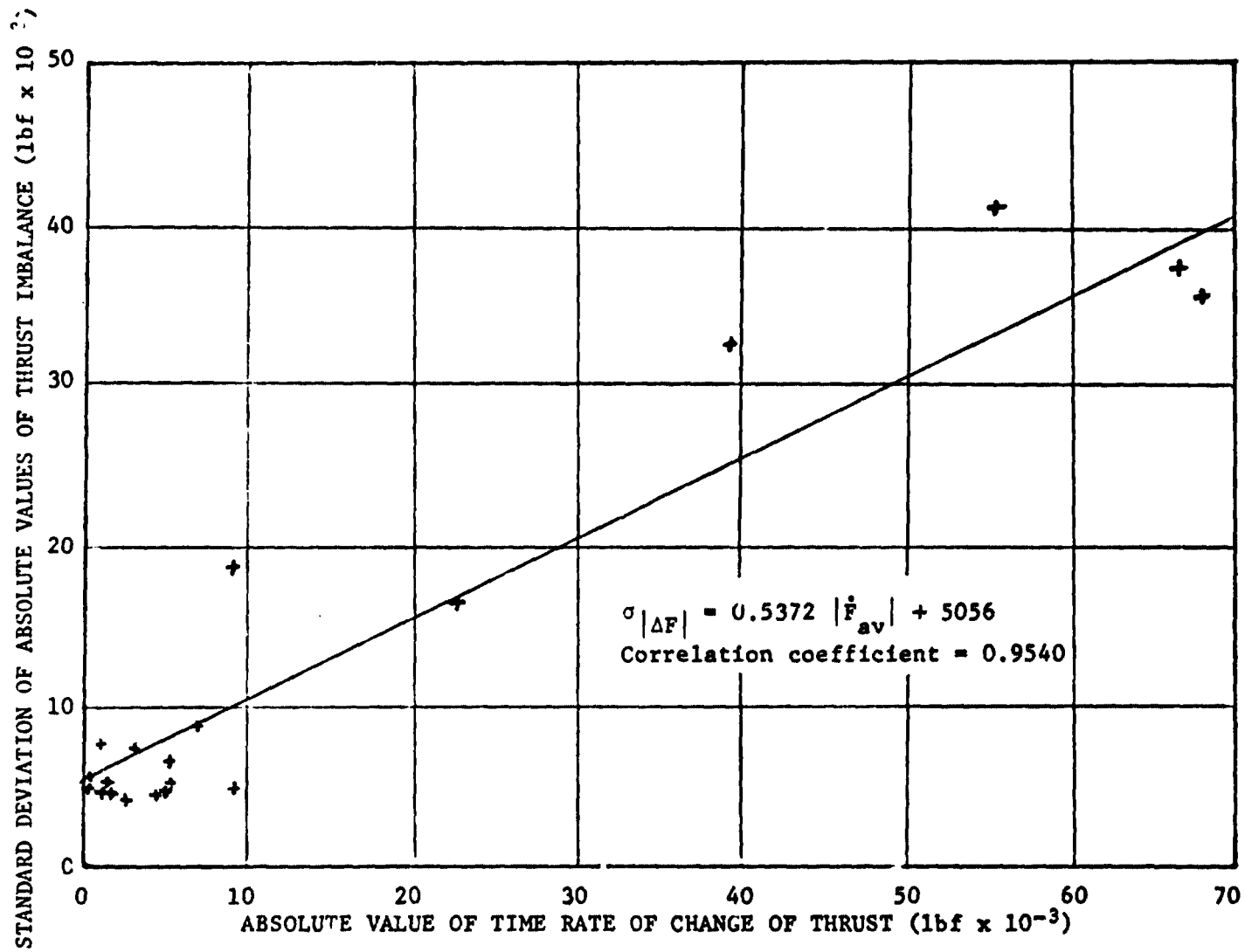


Figure II-9. Scatter diagram: standard deviation of thrust imbalance for 30 theoretical Titan IIIC SRM pairs versus the absolute value of the mean time rate of change of thrust for the 60 motors.

The nominal slopes of the thrust-time trace were determined by computing the mean of the slopes for the 60 SRMs at each time point.

It should be noted that the 20 time points on which the latter correlations were based were not randomly selected; they were selected to cover all portions of the trace for the previous analysis of the relationship between thrust imbalance and imbalance rate. Although the time points were not selected with a knowledge of the values of the present variables of interest, the manner of selection introduces a question on the random nature of the variables (thrust imbalance and thrust slope), so that further investigation of the correlation should be accomplished before attempting additional statistical analysis. However, it appears that there is a strong relationship between the variables in question.

The relationship between the thrust imbalance and the slope of the thrust-time trace has at least two important potential applications. The first can be accomplished only if the regression analysis proves to be general, that is, it must be shown that it is reasonable to expect that the same regression line fits all SRMs or at least members of a family of SRMs. If it does, the thrust imbalance predictions could be based directly on the slope of the trace of a new SRM without Monte Carlo evaluation. Also, although it has been shown (for Titan IIIC's, at least) that the Monte Carlo program gives reasonable representation of the SRM pair imbalance, it would be a logical step to test the correlation directly against actual performance data. This suggests a second application - that of using the regression analysis to establish imbalance scaling relationships between different SRMs. The regression analysis for the Monte Carlo program would be compared to that for the actual motor to establish the scaling relationship. The result would then be applied to a regression analysis of a Monte Carlo evaluation for a new SRM (e.g., the Space Shuttle) to establish the imbalance limits for the new SRM pairs. This could be done whether or not the same regression line fits the two types of SRMs. Investigation of these applications is beyond the scope of the current research.

### III. EFFECT OF GRAIN DEFORMATION ON INTERNAL BALLISTICS

The circular-perforated (c.p.) portion of the grain of an SRM of the Space Shuttle type may deform as much as 1.2 inch in the radial direction under pressurization from the chamber gases. At a 30-inch bore radius, this results in as much as a 4% increase in the initial burning perimeter of the grain bore. This can affect the chamber pressure and the apparent burning rate of the propellant. The effects will decrease as burning of the propellant web progresses because the displacement of the burning surface relative to its unpressurized position will decrease. The ability to quantitatively assess these particular effects of grain deformation on internal ballistics should improve predictability of performance of individual motors, especially for the first motor of a new design where the "scale factor" on burning rate is uncertain.

#### Analysis of Grain Deformation Effects

The underlying hypothesis on which the ballistic effects of the grain deformation is based is that at fixed pressure the regression rate  $r_c$  of the pressurized propellant surface just beneath the heat-affected zone is independent of the state of strain. To show that this is plausible, first consider the burning perimeter of a sector of solid propellant. The burning perimeter consists of a thin zone (liquid and/or solid) in which the physical properties are degraded to a state where the propellant develops negligible shear stresses. Therefore the regression rate of this zone ( $r_m$ ) should be independent of the precise state of strain calculated just beneath the degraded zone which will be somewhat thinner than the solid phase heat-affected zone. The concept needs experimental verification, but appears consistent with the known features of the solid-gas transition region.

In the present analysis, it is assumed the thermoelastic coupling discussed in Section IV on this report is absent. Thermoelastic coupling may possibly alter the depth of and the temperature distribution within the heat-affected zone and thereby make burning rate sensitive to strain. However, as discussed in Section IV, it is expected to be significant only during highly transient conditions; i.e., during ignition and very rapid depressurization.

If we now consider a control surface (See Fig. III-1) separating the region of degraded propellant from the remaining propellant, a quasi-steady state mass balance across the heat-affected zone, which for the purpose of this analysis is considered of zero thickness, yields

$$r_c = r_m \rho_m / \rho_{pc} \quad (\text{III-1})$$

where  $\rho_m$  is the density of the degraded propellant and  $\rho_{pc}$  is the density of the unheated propellant just outside the heat-affected zone. It is apparent that  $r_m$  and  $\rho_m$  are pressure dependent but should not depend on the state of strain underneath the degraded surface. Also, when as in the principal case of interest here, Poisson's ratio  $\nu$  is close to 0.5, it is intuitively clear and may easily be shown that the density of the unheated propellant can be expressed as a function of pressure (and modulus) only since

$$(1+\epsilon_r) (1+\epsilon_\theta) (1+\epsilon_z) = [1-P(1-2\nu)/E]^3 \quad (\text{III-2})$$

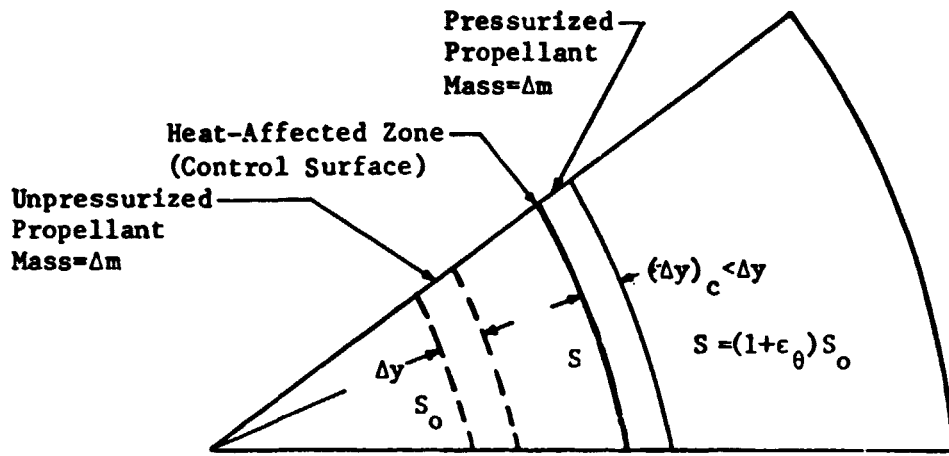


Figure III-1. Sector of cross-section of solid propellant with and without pressurization and combustion.

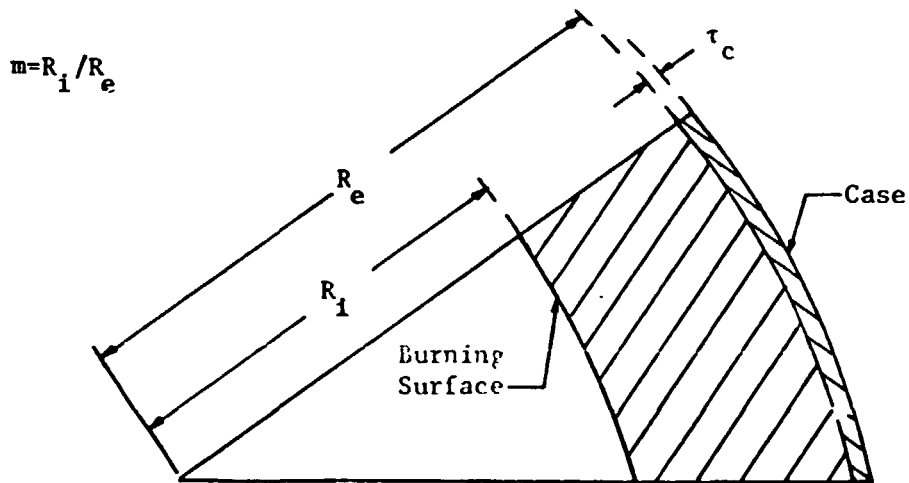


Figure III-2. Grain geometry notation for analysis of solid-propellant strains. The insulation and liner may be considered a part of the propellant.



where  $\epsilon$  is strain,  $P$  is pressure,  $E$  is modulus of elasticity and  $\theta$ ,  $r$  and  $z$  refer to the tangential, radial and axial directions, respectively. Thus Eq. III-1 should govern the burning rate of the propellant regardless of the state of strain and  $r_c$  is a function of pressure only (for fixed initial grain temperature and erosive burning characteristics).

Next, the effect of the deformation on internal ballistics is examined. We consider only a circular-perforated grain for which  $\epsilon_\theta$  is independent of the tangential coordinate at one axial position. The mass generated per unit time per unit length at the control surface separating the heat-affected zone of the propellant from the unheated propellant is given by

$$m_G/l = S_o (1 + \epsilon_o) \rho_{po} r_c / \{ [1 - P(1 - 2\nu)] / E [1 + \alpha(T_{Gr} - T_{Ref})] \}^3 \quad (III-3)$$

where  $S$  is the burning perimeter,  $\alpha$  is the linear coefficient of thermal expansion and the subscript  $o$  refers to the unpressurized and unheated (reference grain temperature) state of the propellant. The approximation of Eq. III-2 has been used in Eq. III-3 to determine the effect of pressurization on the unpressurized density, and that density has been further modified for the small effect of thermal expansion between the standard temperature  $T_{Ref}$  at which density is measured and the actual grain temperature  $T_{Gr}$ .

A second modification of customary ballistic analysis is the way the time  $\Delta t$  required to burn an increment  $\Delta y$  normal to the surface is calculated. The usual relationship is

$$\Delta t = \Delta y / r_o \quad (III-4)$$

where  $r_o$  is the burning rate deduced from strand burners or small ballistic test motors modified with a "scale factor" reflecting the estimate of the change in burning rate between the strands or test motors and the SRM under consideration. The comparable equation to Eq. III-3 used with Eq. III-4 is

$$m_G/l = S_p \rho_{po} r_o \quad (III-5)$$

For the present we disregard any scale factors and devise an appropriate relationship for  $\Delta t$  in terms of  $\Delta y$  and  $r_c$  applicable to the deformed grain problem. First, note that the  $r_o$  should be the rate at which the unpressurized and unheated propellant regresses because the  $\Delta y$  is to be used for further computations of surface area as an increment of undeformed propellant. Next, it is assumed that the changes in length ( $l$ ) of the grain produced by pressure and thermal loading are negligible. As shown in Ref. 4, longitudinal (axial) grain strain due to pressurization is on the average over the length of the grain approximately a half order of magnitude less than the corresponding tangential strains. The axial strains are negative while the tangential strains are positive. Although a quantitative assessment has not been made, when heating of the surface of the propellant is considered, the axial strain at the point of interest; i.e., just beneath the heat-affected zone, will become less negative because of the restraint of the unheated propellant to the expansion of the heat-affected propellant. This will decrease the extent of any change in length of the propellant relative to the increase in perimeter over that due to pressurization alone.

Referring to Fig. III-1, we obtain from a mass balance between deformed and undeformed propellant

$$\rho_{po} S_o^2 r_o = \rho_{pc} S_o^2 (1+\epsilon_\theta) r_c \quad (III-6)$$

or

$$r_o = r_c (1+\epsilon_\theta) / \{ [1-P(1-2\nu)/E] [1+\alpha(T_{Gr} - T_{ref})] \}^3 \quad (III-7)$$

The same result may also be obtained by direct combination of Eqs. III-3 and III-5. With this  $r_o$ , Eq. III-4 then applies to the deformed grain situation.

Data to give  $r_c$  are obtained from ballistic test motors or strand burners. As previously noted, no scale factor is considered. Indeed, it is suggested that the grain deformation may account for a significant portion of the scale factor. The strands are under essentially a state of hydrostatic compression. The same is very nearly true for the typical ballistic test motor because of the rigidity of the relatively thick cases and the relatively thin webs. It should be recalled that  $r_c$  should be independent of the state of strain. However, the burning rate of small test motors (or strands) is deduced by dividing the undistorted web thickness (or strand length) by time. Therefore, to determine  $r_c$ , the regression rate of the propellant surface just beneath the heat-affected zone of the SRM, the test motor (or strand) rate must be reduced by the multiplying factor  $[1-P(1-2\nu)/E]$ . The  $r_c$ , of course, is subject to the usual laws governing its relationship with initial grain temperature, pressure and velocity (erosive burning).

#### Simplified Determination of Grain Deformation

For a first analysis of the effect of grain deformation on internal ballistics, a simplified model of the deformation was developed. We are concerned for the present only with the modification of the internal burning surface of a circular-perforated grain for which it has been shown that the important parameter is the tangential bore strain  $\epsilon_\theta$ . The  $\epsilon_\theta$  will change as burning progresses and also will vary in general with axial position. Smith (Ref. 4) working under the direction of this project has shown that as an approximation the  $\epsilon_\theta$  may be considered independent of axial position. Smith extended the method used by Vandenkerckhove (Ref. 8) for calculation of grain stresses in case-bonded propellant with rigid motor cases to the calculation of propellant strains in non-rigid motor cases. His results for tangential strains at the bore are given by

$$\begin{aligned} E_p \epsilon_\theta / P_i = & \{ [1+m^2 + \nu_p (1-m^2 - 2m^2\nu_p)] / (1-m^2) \} \\ & + (P_e / P_i) \{ [2(\nu_p^2 - 1) / (1-m^2)] + E_p R_p \nu_p / E_c \tau_c \} \end{aligned} \quad (III-8)$$

where  $P_e$  is the radial stress at the propellant-case interface as given by

$$\begin{aligned} P_e / P_i = & [2m^2(1-\nu_p^2) / (1-m^2)] / \{ [E_p R_p (1-\nu_c \nu_p) / E_c \tau_c] - \nu_p (1+\nu_p) \\ & + (1-\nu_p^2) (1+m^2) / (1-m^2) \} \end{aligned} \quad (III-9)$$

Here the geometric notation is given by Fig. III-2,  $P_i$  is internal pressure,  $\nu$  is Poisson's ratio and  $E$  is modulus of elasticity. The subscripts  $p$  and  $c$  refer to the propellant and motor case, respectively. Details of the analysis are given in Ref. 4.

Smith compares results for tangential, radial and axial strain with a more exact solution obtained using a computer program devised by Brisbane (Ref. 9). The two solutions for the tangential strain are illustrated in Figs. III-3a and b for a 140-inch diameter motor segment 300 inches long for various web thicknesses. The results are given in non-dimensional form and are applicable to motors of various sizes with the same ratios  $\tau_w/R_e$ ,  $\tau_c/R_e$  and  $l/R_e$  and material properties. Study of Figs. III-3a and b shows that the simplified solution, which assumes the same strain at all axial positions, in general, overestimates the strain with respect to the more exact solution. The worse case is at the largest web thickness to outside radius ratio ( $\tau_w/R_e$ ). Here, the strains calculated by the two methods are within 30% over two-thirds of the grain length and the comparison improves rapidly with decreasing web thickness (increasing distance burned). It should be noted that the strains calculated by both Refs. 4 and 9 are those due to pressure loadings only. Expansion of the propellant in the heat-affected zone will tend to produce additional tension of the solid surface just outside the heat-affected zone (the surface of interest). This will compensate somewhat for the apparently excessive strains calculated by Eq. III-8.

We feel that the approximate analysis is adequate for a first approach to analysis of the described effect of deformation on internal ballistics. It will permit rapid calculation of the bore strains for various configurations, material properties and distances burned. Additional investigation performed by the authors under this project using the program of Brisbane shows that tangential bore strain, the quantity of primary importance in the analysis, is changed by less than 5% by solid-phase thermal gradients so that thermal effects may be neglected in this first analysis. The reason the thermal gradient changes the tangential bore strain so little is that the gradients are confined to only a very thin zone at the surface. The bulk of the strain is due to pressurization of the entire propellant web.

#### Modification of the Design Analysis Computer Program

The design analysis computer program of Ref. 2 has been modified to permit computation of the internal ballistics with the deformed grain. The program is listed in Appendix C along with instructions on preparation of new input data cards and a sample problem solution.

Bore deformation of c.p. grains or grain segments is evaluated by the simplified approach discussed earlier. Only deformation of the internal burning surface of c.p. grains or segments is considered. The calculation of the deformations of the ends of c.p. grains and star grains is a formidable task. Any solution would appear to be inconsistent with the simplified analysis of deformation and internal ballistics being presented and well beyond the scope of the present research. The design analysis treats the ends of c.p. grains and star grains with an unmodified burning ratio. This is accomplished by computing a separate burned increment  $\Delta y'$  applicable to c.p. grain ends and the entire star grain. The  $\Delta y'$  (computer symbol YETA)

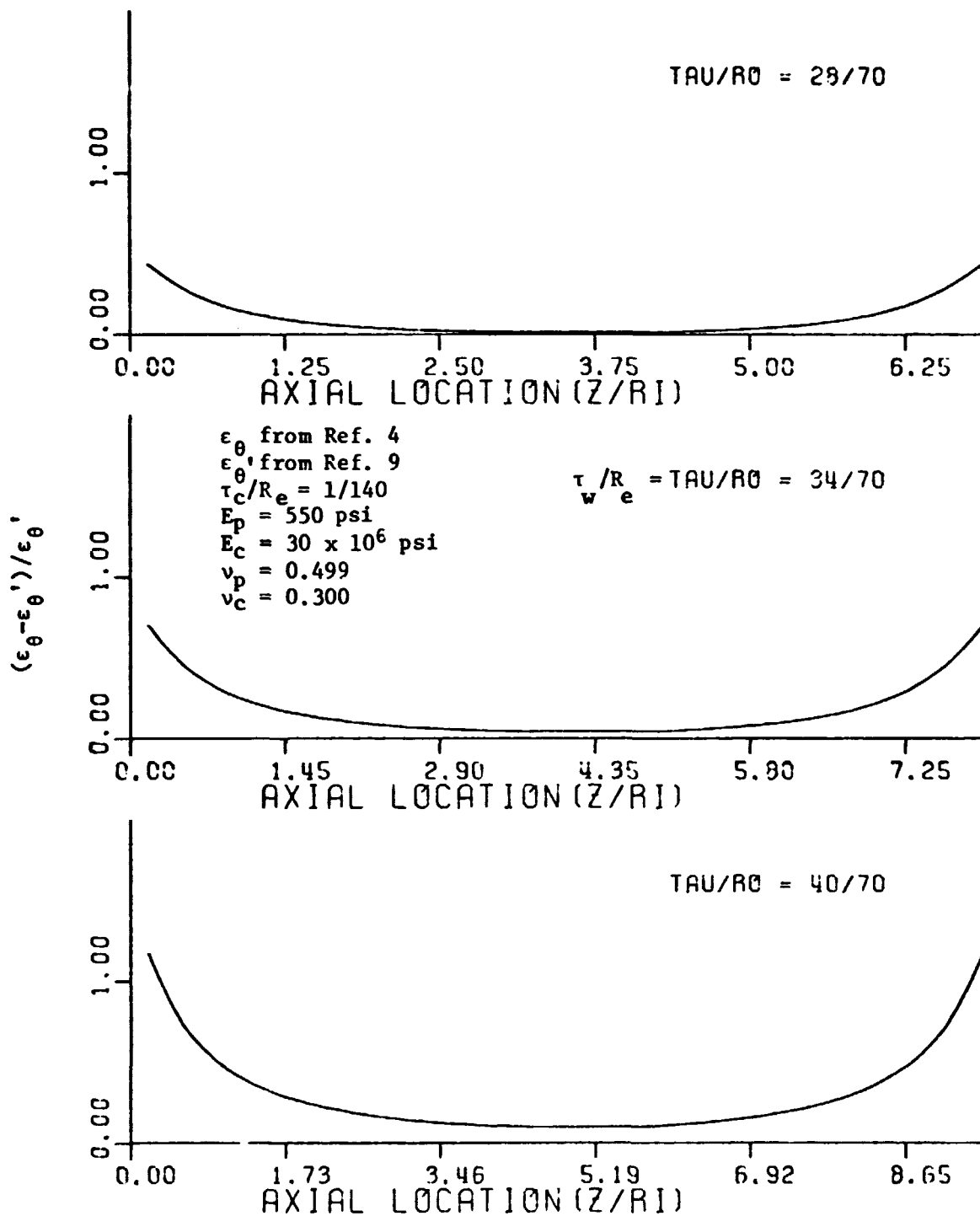


Figure III-3a. Comparison of approximate solution for tangential bore strain (Ref. 4) with finite element solution method of Ref. 9.

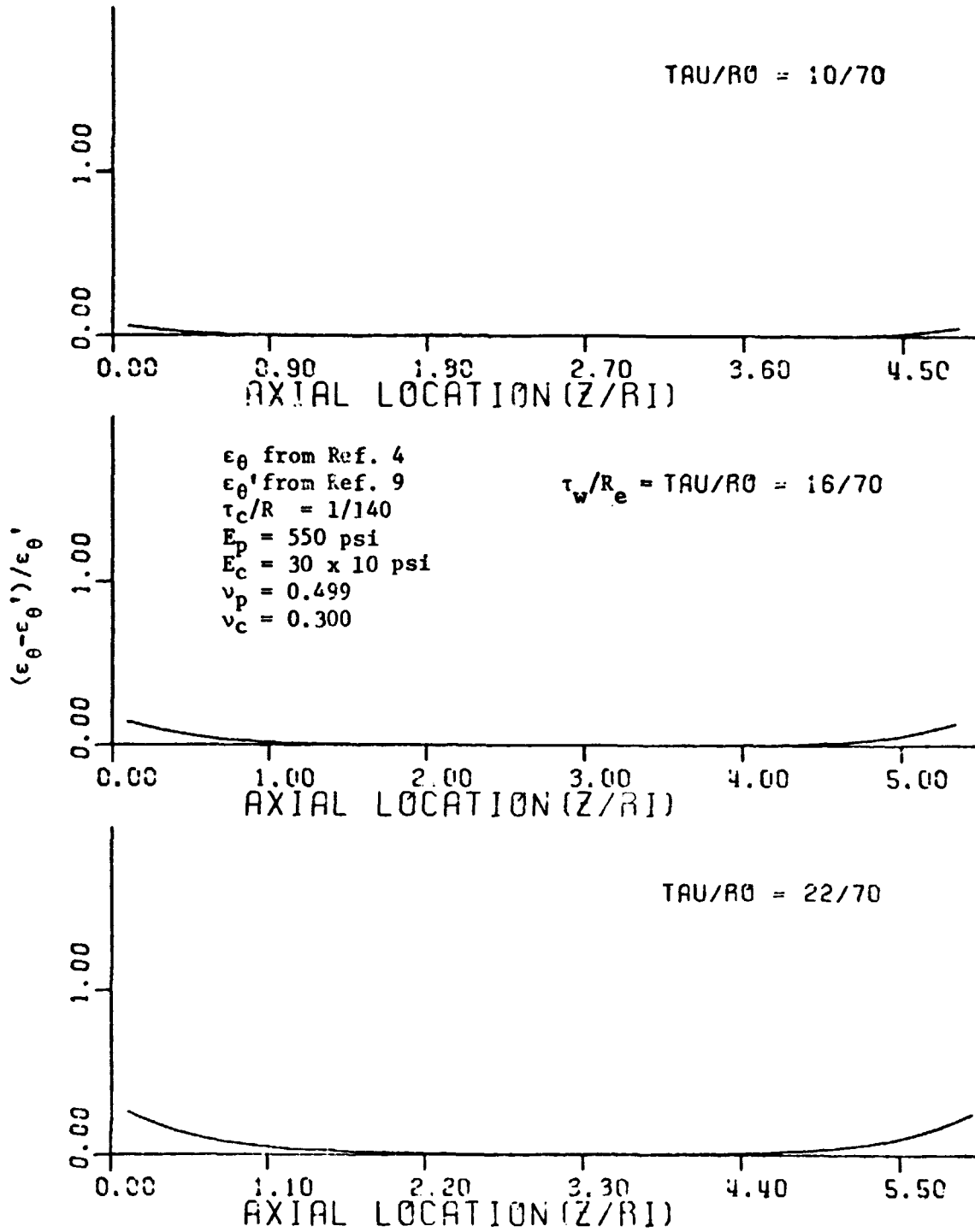


Figure III-3b. Continued comparison of approximate solution for tangential bore strain (Ref. 4) with finite element solution method of Ref. 9.

is related to the  $\Delta y$  applicable to the c.p. grain lateral surface by the equation

$$\Delta y' = \Delta y \left\{ \left[ \frac{1 + P(1 - 2\nu_p)}{E_p} \right] \left[ 1 + \alpha(T_{Gr} - T_{ref}) \right] \right\}^3 / (1 + \epsilon_\theta) \quad (\text{III-10})$$

The  $\Delta y'$  thus calculated gives the regression of the star grain surfaces and ends of the c.p. grain in the same time increment that the c.p. lateral surface regresses a distance  $\Delta y$ . The modification of the bore surface of the c.p. grain due to deformation is accounted for in the mass generated equation by the use of the program variable XETH which is the fraction of the total burning bore surface associated with the c.p. grain. The factor  $(1 + XETH * ETHETA)$ , where  $ETHETA = \epsilon_\theta$ , multiplies the undeformed total burning bore surface area when the deformation option is elected by setting  $ISO=1$ . The program will calculate the internal ballistics without grain deformation when  $ISO=0$ . The program changes that have been made in the design analysis of Ref. 2 to permit the alternative computations are identified by the symbol  $\blacktriangleright$  in the left-hand margin of the listing. Also, the modifications of the design analysis program discussed in Section VI of this report have been incorporated into the program listed in Appendix C.

In modifying the program, it was found convenient for the purposes of minimizing the number of modifications and for preserving the ability of the program to make calculations with no deformation to change the usage of SUMAB in the program. Before the modification (or presently when  $ISO=0$ ) SUMAB represents the surface area at a given distance  $y$  burned normal to the entire surface. With the modification (when  $ISO=1$ ) because of the difference between  $y$  and  $y'$  the SUMAB represents the area at a distance  $y$  burned over a part of the surface and  $y'$  over another part. This creates an error in the calculation of the weight of propellant burned (WP2) which is obtained by integration of SUMAB with respect to  $y$  alone. Therefore the calculation of WP2 should be disregarded when  $ISO=1$ . To calculate WP, the arithmetic average of WP2 and the weight of propellant burned (WP1) calculated from the mass discharged rate, the program now sets  $WP2=WP1$  when  $ISO=1$ . Comparisons of weights calculated by the two methods can still be made by comparing WP1 calculated with  $ISO=1$  with WP2 calculated with  $ISO=0$ . The latter is still a valid calculation for total weight of propellant burned even with grain deformation. Also comparisons have been made for the two sample cases discussed next and the WP1 is not significantly different for  $ISO=0$  and  $ISO=1$ .

#### Comparison of Theoretical and Experimental Results

To test the validity of the hypothesis regarding the effect of grain deformation on internal ballistics, the modified program was used to predict the performance of two entirely different rocket motors and the results compared with actual performance data. In each case the burning rate used to predict the performance was that obtained from ballistic test motors or strand burners; no scale factor was applied.

The first comparison made was for a Titan IIIC/D configuration. The basic input parameters used for the prediction are those given by the mean values in Table 2 of Ref. 1 with the following exceptions: The propellant density had been changed to  $0.06325 \text{ lbm/in}^3$  because additional data on this has become available. The strand burning rate coefficient obtained from a number of batches of propellant loaded into the same SRM (No. D5) for which

the comparison is to be made was used for the prediction. The burning rate coefficient used (0.06466 with no scale factor) was deduced from Ref. 10. Five burning slot faces were assumed in the program calculations. A table of tabular values was prepared so that the burning surface areas calculated by the unmodified program more nearly match the known geometric surface versus distance burned characteristics of the Titan IIIC/D configuration over web action time. Aft-end closure propellant surface representation was included in the tabular values.

Propellant and motor case properties used in the analysis of the deformed propellant grain are given on Fig. III-4. The figure is a comparison of the program results for aft-end stagnation chamber pressure versus time with and without deformation and with the results of analysis of actual test data given for Titan IIIC/D motor number D5, in Ref. 10. This particular motor was selected because its performance is more or less typical of the Titan IIIC/D and because of availability of strand burning results on the same propellant loaded into the large motor.

A similar comparison of theoretical and experimental results was made for the Castor TX354-5 SRM. This is a 31-in. dia. motor with an entirely c.p. slotted grain which is described in detail in Ref. 11. The SRM is also described briefly in Ref. 12 where input parameters applicable to an early version of the design analysis program are identified. A complete listing of input values for the modified design analysis is given in Table C-1 of the present report where the Castor motor is used as a sample problem to illustrate use of the program. The input values differ from those used in Ref. 12 because of the program changes that have been made and because we have improved our representation of the grain geometry, particularly with respect to use of tabular values. Again, the burning rate coefficient used has no scale factor between the Castor motor and the small ballistic motor data from which the coefficient was deduced. Vacuum thrust results are compared (See Fig. III-5) for the Castor motor. The vacuum thrust results for the actual motor were based on analysis of static test results and are tabulated in Ref. 11 as typical performance values. The strand burning rate data is also typical but are not otherwise identifiable with the specific large motor.

Analysis of the two comparisons shows that the theoretical predictions are substantially improved by consideration of the deformations. Additional comparisons are needed to confirm the efficacy of the new model. Modification of other parameters can also make improvements in prediction possible. A prime example is the use of the burning rate scale factor. However, the scale factor is most often applied without specific theoretical justification and usually is only accurate after data on actual SRM firings has been obtained. On the other hand, the deformation effect has a basis in theory. If it can be further validated, it will not only by itself improve prediction capabilities but also clear the way for more accurate assessment of other specific ballistic phenomena such as erosive burning and nozzle throat erosion. For example, consider the discrepancy between the prediction with grain deformation and the test results for the Titan IIIC/D. It is obvious that the areas under the two traces are not the same. This is suggestive of a difference between the nozzle throat erosion rate used in the theoretical prediction (time independent, pressure and size dependent) and the actual erosion rate. The application of a scale factor to the theoretical burning rate coefficients

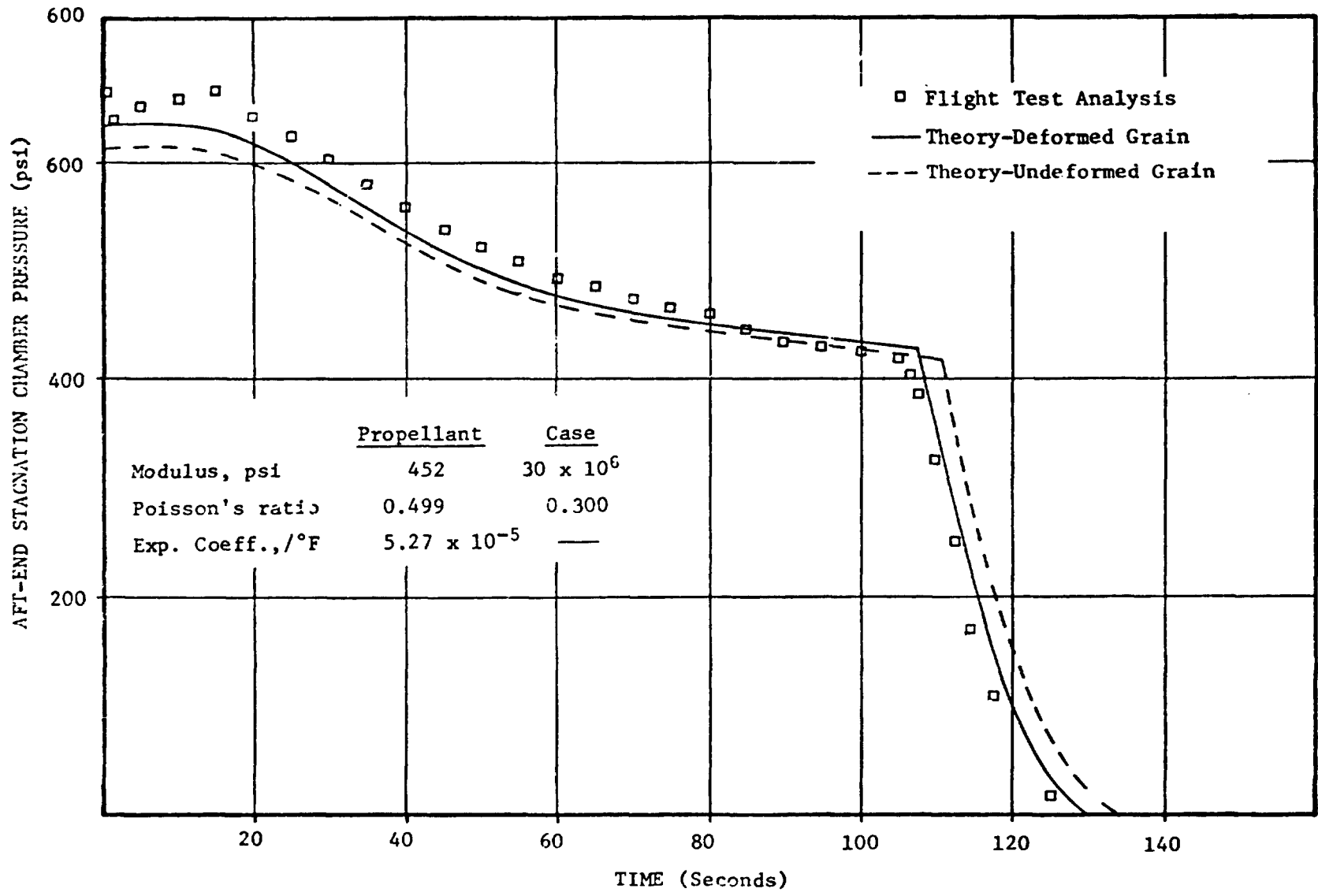


Figure III-4. Comparison of theoretical and experimental results for a Titan IIIC/D SRM with no scale factor on strand burning rate.



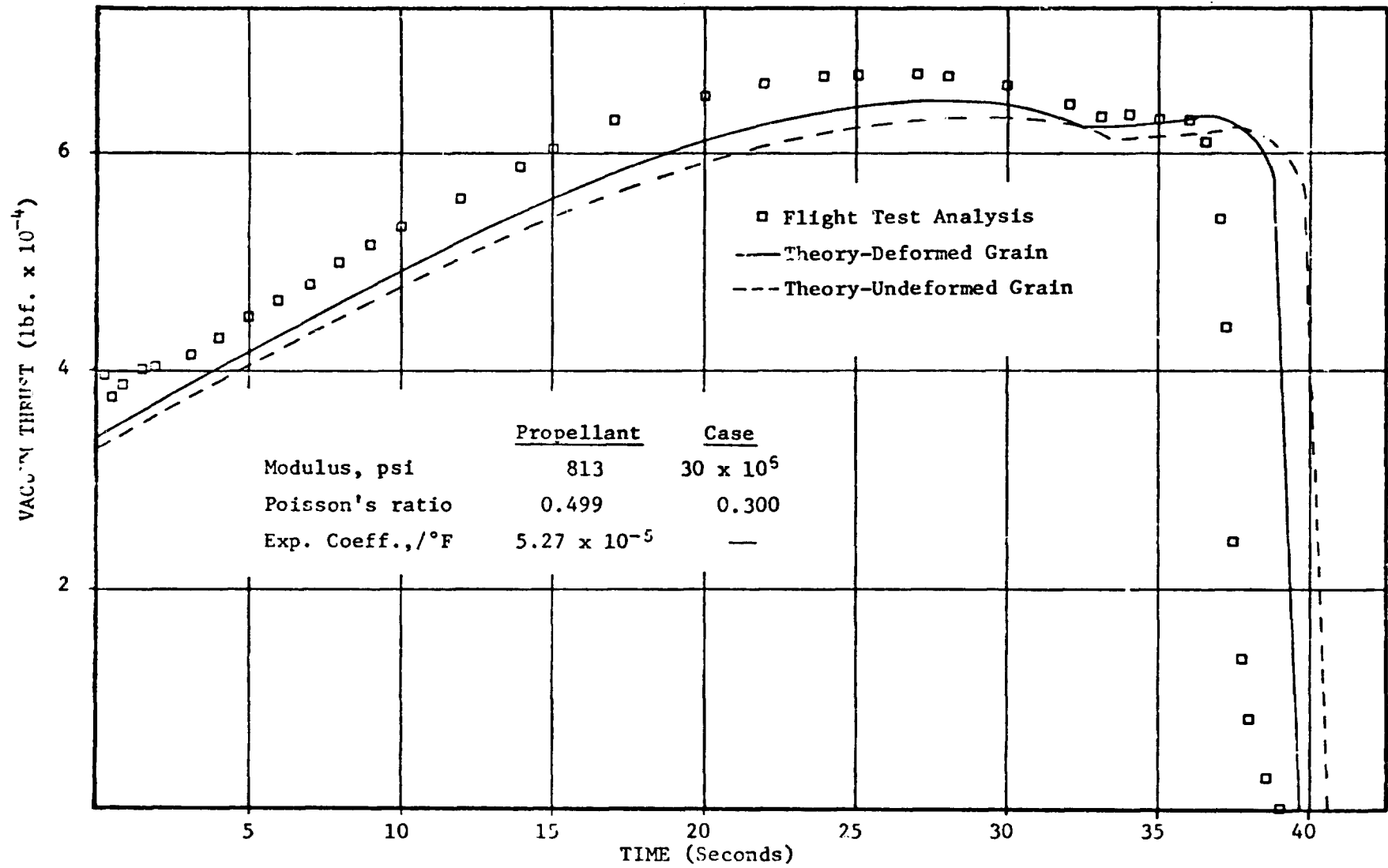


Figure III-5. Comparison of theoretical and experimental results for a Castor TX 354-5 SRM with no scale factor on small ballistic test motor burning rate.

would not improve the area discrepancies and would mask the true throat erosion and/or buildup phenomena.

Variations in the propellant properties used in the deformed grain program can affect the results. Likewise variations between SRMs of a pair firing in parallel can contribute to thrust imbalance. As shown in Ref. 4, the effect of propellant modulus is especially important. However, additional confirmation of the deformed grain model, preferably including direct experimental verification, should be obtained before the effect is incorporated into the Monte Carlo program.

Equations III-3 and III-7 which give the basic burning rate theory of the model may also be coupled to more rigorous descriptions of the grain deformation and/or more rigorous models of the other aspects of internal ballistics than those used in the modified design analysis program.

#### IV. THERMOELASTIC ANALYSIS

The problem to be discussed in this section is the effect on the solid propellant burning rate produced when heat is generated by mechanical deformations of the solid propellant. The basic theory and the numerical solution procedure used in the thermoelastic analysis as well as the results which have been obtained are presented.

The basic formulations and concepts associated with the coupling between thermal and mechanical loadings can be traced to the work of Duhamel (Ref. 13). Other early investigators include Lord Kelvin (Ref. 14) and Joule (Ref. 15). It was Duhamel who developed the relationships used to express the distribution of strain in a body subjected to differential heating.

##### Basic Theory

Consider a small element of an isotropic elastic solid subjected to an arbitrary stress which is removed from its surroundings and subjected to a temperature change,  $\Delta T$ . The additional strain in the element is given by the tensor  $\beta \Delta T \delta_{ij}/3$ , where  $\beta$  is the coefficient of volumetric expansion and  $\delta_{ij}$  is the Kronecker delta. From this it follows that if the strain tensor is originally given by  $e_{ij}$ , then the new strain tensor would be  $e_{ij} - \beta \Delta T \delta_{ij}/3$  and this would be the strain used in the constitutive relation. The effect of a nonuniform temperature distribution becomes equivalent to that of a body force per unit volume, given by  $-(\beta/\eta)\nabla(\Delta T)$ ,  $\eta$  being the compressibility and  $\nabla$  the gradient operator. Thus, once  $\Delta T$  is known from the solution of the heat conduction problem, the system of equations for the displacement field is fully defined. As can be seen, this approach postulates the effect of the temperature gradients on the state of strain, but assumes that the heat transfer is totally unaffected by the state of strain. This result is upheld rigorously when the medium is in mechanical and thermal equilibrium, but its application to time dependent problems is not satisfactory. However, Duhamel and Neumann do suggest that a term proportional to  $\partial \epsilon_{kk}/\partial t$ , the rate of change of dilatation, be included in the heat conduction analysis. The present work investigates this term's effect on a thermoelastic analysis, and in turn, on the propellant burning rate.

Much effort has been expended in recent years to obtain solutions for problems involving thermomechanical coupling. This has been due, at least in part, to the necessity for structural analysis of bodies subjected to a nonisothermal, transient temperature distribution. One of the better examples of a body subjected to this type of loading is the solid-propellant rocket motor. The general analytical formulation of the problem is well known and can be found in various publications, of which Ref. 16 is typical. The problem to date has been obtaining solutions for problems whose geometry and loading conditions, both thermal and mechanical, are sufficiently general to be of practical interest.

Several approaches appear to be suitable for analyzing problems involving thermomechanical coupling. The first possibility is that of obtaining analytical solutions of the governing equations. There have been several such solutions in the literature in recent years. However, the approach to now has been severely limited as to choice of geometry, loading and boundary conditions. The second possibility utilizes the finite element method and entails the approximation of the full set of the governing, coupled, nonlinear partial differential equations by a set of nonlinear algebraic equations which are then solved numerically. This finite element method is considerably more flexible than the first approach with regard to the variety of geometries, loading and boundary conditions which can be treated and has been applied to several classes of problems. However, this nonlinear finite element method also appears to be somewhat limited due to the complexity of solving large numbers of simultaneous nonlinear algebraic equations. Also added complexity is introduced if it is desired to investigate the effect of nonlinear material properties (except for materials which obey relatively simple mathematical laws), arbitrary loadings, and boundary conditions.

A third possibility is to approximate the transient nonlinear solution by a series of linear solutions. In this approach the variable, time, is included in what basically can be described as a time stepping procedure. At each time step, the initial thermal and mechanical states are established based on the conditions which are specified either by a direct input or by the conditions which existed at the end of the preceding time step. The solution then proceeds by obtaining the temperature distribution in the body for the given thermal loading. The thermal load may include applied temperature distributions on the external boundaries and/or at points within the body, heat flux through the boundaries, and convective heat sources (or sinks) distributed throughout the body. The internal heat sources are particularly important since they are used to account for the coupling phenomena. The solution then proceeds by using the computed temperature distribution as an input to the stress analysis portion of the computational procedure. Determination of the deformations, strains and stresses due to the combined loading is then made. Once this is done for a particular time interval, the coupling term, which is a function of the material properties (which may be functions of temperature), the local temperature, and the local strain rate, can be evaluated. With this information the computation then proceeds to the next time step where the coupling term is included as an internal heat source in the heat transfer analysis.

This third approach, the one used in this research, appears to eliminate most of the problems associated with arbitrary time dependent loadings, temperature dependent material properties, and also some of the numerical computational problems associated with the nonlinear finite element method described above. This reduces the numerical computation difficulty because the problem is now formulated as a set of linear algebraic equations. The main objection to this approach is obviously the linear modeling of a nonlinear problem. However, if the mathematical modeling of the geometry,

the loading, the material properties, and the time step is done carefully, this method is sufficiently reliable for the solution of a considerably larger group of problems than was heretofore practical.

The work presented here is restricted to axisymmetric bodies. This does not imply a restriction of the method, but is made because of the applicability to the problem at hand.

Problems in thermoelasticity require not only the solution of the equations of elasticity, but in addition those equations necessary to describe the thermal state of the body being analyzed. In many problems the thermal state can be sufficiently defined by determining the distribution of temperature throughout the body and also any changes in this distribution with respect to time. Quite often as in the present work it is convenient to obtain the temperature distribution from the conservation of energy equation. The discussion which follows will be primarily concerned with the energy equation since it is the equation which will be used to determine the influence of the thermoelastic coupling on the propellant burning rate. The elasticity equations are not presented because they are used in a more or less classical manner.

As in Ref. 2, the conservation of energy equation for a control volume moving with a velocity  $r(t)$  with respect to an observer situated on the boundary ( $x=0$ ) of the control volume and modified to account for volumetric heat release or absorption within the solid phase is

$$\partial T / \partial t = r(t) \partial T / \partial x + (\lambda / \rho c) \nabla^2 T - T \alpha E \dot{\epsilon} / [\rho c (1 - 2\nu)] \quad (IV-1)$$

where  $x$  is measured radially outward from the surface,  $\dot{\epsilon}$  represents the sum of three translational strain components at the point under consideration, and the entire last term represents the heat dissipated by elastic deformations.

The two terms which are of particular interest in the present analysis are the first and last terms on the right-hand side of Eq. IV-1. As mentioned above, the last term represents the contribution of heat from the elastic deformation of the body and can be calculated directly if the instantaneous local temperature is known as well as the time rate of change of the translational strain components. Once the initial temperature and strains are prescribed, the temperature at any point within the control volume at any time is obtained from the solution of Eq. (IV-1). The strain rates can then be calculated at any instant of time once the mechanical load is prescribed as a function of time. Hence, with regard to its calculation, the thermoelastic coupling term offers very little difficulty.

On the other hand the first term on the right-hand side of Eq. IV-1 requires that the instantaneous value of burning rate be calculated. One might initially propose that the burning rate  $r(t)$  could be easily obtained

from the pressure  $P(t)$  which is required for the thermoelastic term by extending the "standard" burning rate law for steady-state burning to the transient problem as

$$r(t) = a P(t)^n \quad (\text{IV-2})$$

However, as pointed out in Ref. 5, the instantaneous burning rate  $r(t)$  may differ greatly from that obtained from a steady-state analysis due to a highly complex heat feedback mechanism between the various regions in and near the combustion zone. Therefore, it is necessary to construct a model to account for this thermal feedback mechanism in order to properly evaluate  $r(t)$ .

One such model for determining the transient burning rate developed by Zeldovich and Novozhilov, referred to as the Z-N model, is described in Ref. 5. The present work uses this model to evaluate  $r(t)$  which is then incorporated into the conservation of energy equation. As in Ref. 5, the Z-N method uses measured steady-state burning rates as a function of pressure and ambient temperature. This data is then used to construct the heat feedback function from the gas to the solid in the proper instantaneous form to be used to study transient burning problems. The assumption which is made to allow use of steady state data is that the rate processes in the gas phase and at the propellant surface can be considered quasi-steady in the sense that their characteristic times are short compared to the pressure transient. The validity of this assumption is demonstrated in Ref. 5. What develops from this is that the steady state heat flux and the transient heat flux have the same functional form, which is written for the transient problem as

$$\lambda(\partial T/\partial x)_{\text{surface}} = r \rho c(T_s - T_o) \quad (\text{IV-3})$$

where  $T_s$  is the instantaneous solid surface temperature and  $T_o$  is a fictitious temperature which exists infinitely far from the solid surface. Now, assuming the pyrolysis law to be of the Arrhenius type

$$T_s = - E_s / [R \ln(r/A_s)] \quad (\text{IV-4})$$

and the empirical expression for  $r$  in terms of  $p$  and  $T_o$  to be given by

$$r = a p^n \exp[\sigma_p (T_o - T_{\text{ref}})] \quad (\text{IV-5})$$

where  $\sigma_p$  is the temperature sensitivity coefficient at constant pressure, which for this work is expressed as a linear function of pressure by

$$\sigma_p = 1.1 \times 10^{-6} P + 6.9 \times 10^{-4} \quad (\text{IV-6})$$

One can solve simultaneously Eqs. IV-1, 4, and 5 to obtain the unknowns  $r$ ,  $T_s$  and  $T_o$ .

#### Numerical Solution Procedure

The finite element method as used in this study is based on the work of Becker and Parr (Ref. 17). The basic program used for the finite element analysis is that of Brisbane (Ref. 9) and is primarily an extension of that given in Ref. 17. The method used is also quite similar to that given by Wilson and Nickell (Ref. 18).

The use of the finite element method involves the division of the region of interest into a number of subregions which normally have a relatively simple geometric shape. Usually a polygon is used for two-dimensional problems and quite often triangles are used. In this work the problem is axisymmetric and a circular ring element with a triangular cross-section is used. A typical element is shown in Fig. IV-1. The subregions, or elements, are connected at discrete points called nodal points. These nodal points are usually at the corners of the polygon as will be the case in the present work.

For the heat conduction problem a simple relationship for temperature and its first derivative as a function of position within the element is assumed. One of the more common assumptions and the one made here is that both temperature and its first derivative are linear functions of position within the element. Hence, for the axisymmetric problem the temperature and its gradient can be written as

$$T(x,z) = C_1 + C_2x + C_3z \quad (\text{IV-7})$$

and

$$\partial T(x,z)/\partial t = C_4 + C_5x + C_6z \quad (\text{IV-8})$$

It should be noted that  $T(x,z)$  and  $\partial T(x,z)/\partial t$  are considered to be evaluated at a particular time; e.g.,  $t = t^*$ , and hence, no explicit time dependence is expressed in the above equations.

Once this approximation has been made, it is substituted into the basic field equations which describe the heat transfer process. The result is a set of linear algebraic equations, the unknowns of which are the temperatures which exist at the nodal points.

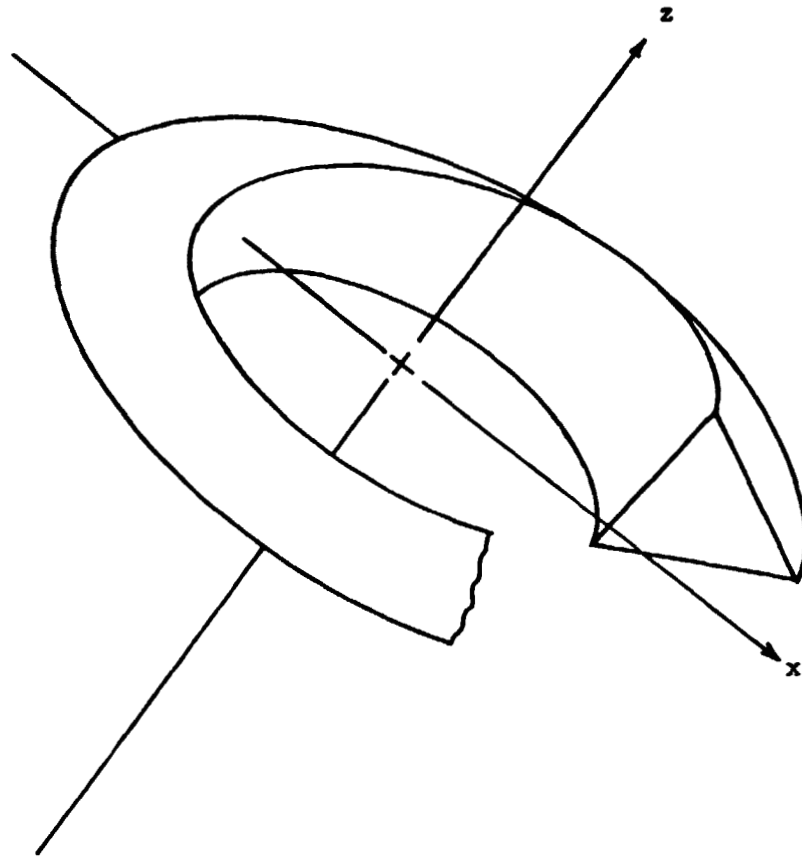


Figure IV-1. Typical finite element for axisymmetric problem.



Basically the same procedure is used for the elasticity problem except that the displacements are approximated instead of the temperature. Another linear approximation is used for the displacements. This approximation is then substituted into the field equations for the elasticity problem and a set of algebraic equations is obtained for the nodal point displacements. These nodal displacements are used to evaluate the constants in the linear displacement assumption which is then appropriately differentiated to obtain the strains at a particular time.

It is now appropriate to examine in more detail the computational procedure which is used and the manner in which the coupling between the thermal and mechanical loading as well as the burning rate term are introduced into the numerical computational process. The solution technique consists of solving separately the energy equation and the elasticity equations at each time step. Outputs from each are then used as inputs to the other, thereby forming a closed loop computational scheme. The calculation of the temperature dependent term which appears in the stress-strain relations is common to both the uncoupled and coupled solutions. It is calculated from the apparent element temperature which is obtained from a geometrical weighting of the four nodal point temperatures which are computed in the heat conduction part of the analysis.

The computation of the thermoelastic coupling term which appears in the energy equation, Eq. IV-1, requires some knowledge of the deformation history of the body in order to compute the strain rate. For the work presented here it is only necessary that the state of strain at time,  $t - \Delta t$ , and at time,  $t$ , be known, where  $\Delta t$  is the time increment between steps. This requires that the strain components for each element be retained at the end of each time step. The old values are then replaced by the new state of strain which is then used in the next time step. The initial strain has been taken to be zero, but no significant problems arise if a non-zero initial strain condition is used. For an isotropic body, the thermoelastic coupling term in Eq. IV-1 involves only the dilatational components of the strain tensor. The axisymmetric solution requires that three strain components be known for each element. However, the coupling term in Eq. IV-1 contains the sum of the three dilatational components so that only the trace of the strain tensor need be retained for each element. This results in a considerable saving of computer storage. The strain rate for each element can then be computed by taking the difference between the trace of the element strain tensor at time,  $t - \Delta t$ , and at time,  $t$ , and dividing by the increment  $\Delta t$ . The resulting linear approximation is then transferred to the heat conduction analysis. The remaining variables in the coupling term involve the temperature and material properties of the element. The temperature is known from the calculations described above and the material properties are either prescribed constants or are given in tabular form as a function of temperature. If the material properties are given as constants, a direct substitution is made and the coupling term is evaluated directly. If the material properties are given in tabular form, a linear interpolation routine is used to obtain values not given in the table.

The term containing the burning rate requires that the Z-N model be used to evaluate the instantaneous burning rate  $r(t)$  based on the existing surface temperature at the end of each time step. The burning rate term is then added to the heat balance for each element. The heat flux at the surface is computed using Eq. IV-3 and this becomes the heat flux boundary condition for the next time step.

The numerical example presented here is a simulated ignition of a large SRM. The motor is modeled as a straight circular perforated grain with an initial bore diameter of 60 inches and a web thickness of 40 inches. The grain is encased in a 0.5-inch thick steel case. The motor is subjected to a time dependent increase in pressure on the bore and end surfaces, but burning is allowed in a direction normal to the bore surface only. The variables in the analysis are assumed to be distributed symmetrically about the motor centerline.

#### Finite element model

It is well known that solid propellants are extremely good insulators and that the heat-affected zone of a burning propellant is of the order of about 10 mils. The finite element model is constructed to analyze this region with reasonable accuracy. A schematic of the finite element model is shown in Fig. IV-2. Finite elements with a radial thickness of 1 mil are used for the first 20 mils of the propellant web (Steady state temperature profiles show that this will more than adequately cover the heat-affected zone under most normal operating conditions). The remaining web is modeled using finite elements which have a radial thickness of approximately 10 inches. The steel case is modeled by two elements 0.25 inches thick. The vertical dimension of each element is 10 inches. The coarseness of the grid in the vertical direction is justified because the variables under consideration (i.e., temperature, displacements, strains, etc.) do not have gradients in the vertical direction. To further refine the numerical calculations, each rectangular cross section element described above is subdivided into four triangular elements of the type illustrated in Figure IV-1.

As the propellant regresses, a new finite element grid is constructed at each time step. The first 20 mils of the propellant is always modeled by elements of the size described above. The remaining elements, except those associated with the steel case, become decreasingly small as the web thickness diminishes. This is done to assure that the same degree of accuracy is maintained with regard to the propellant in or near the heat-affected zone.

#### Initial conditions

- 1) no initial strains exist;
- 2) an initial uniform pressure exists over the entire propellant surface;
- 3) the initial temperature distribution corresponds to that which would

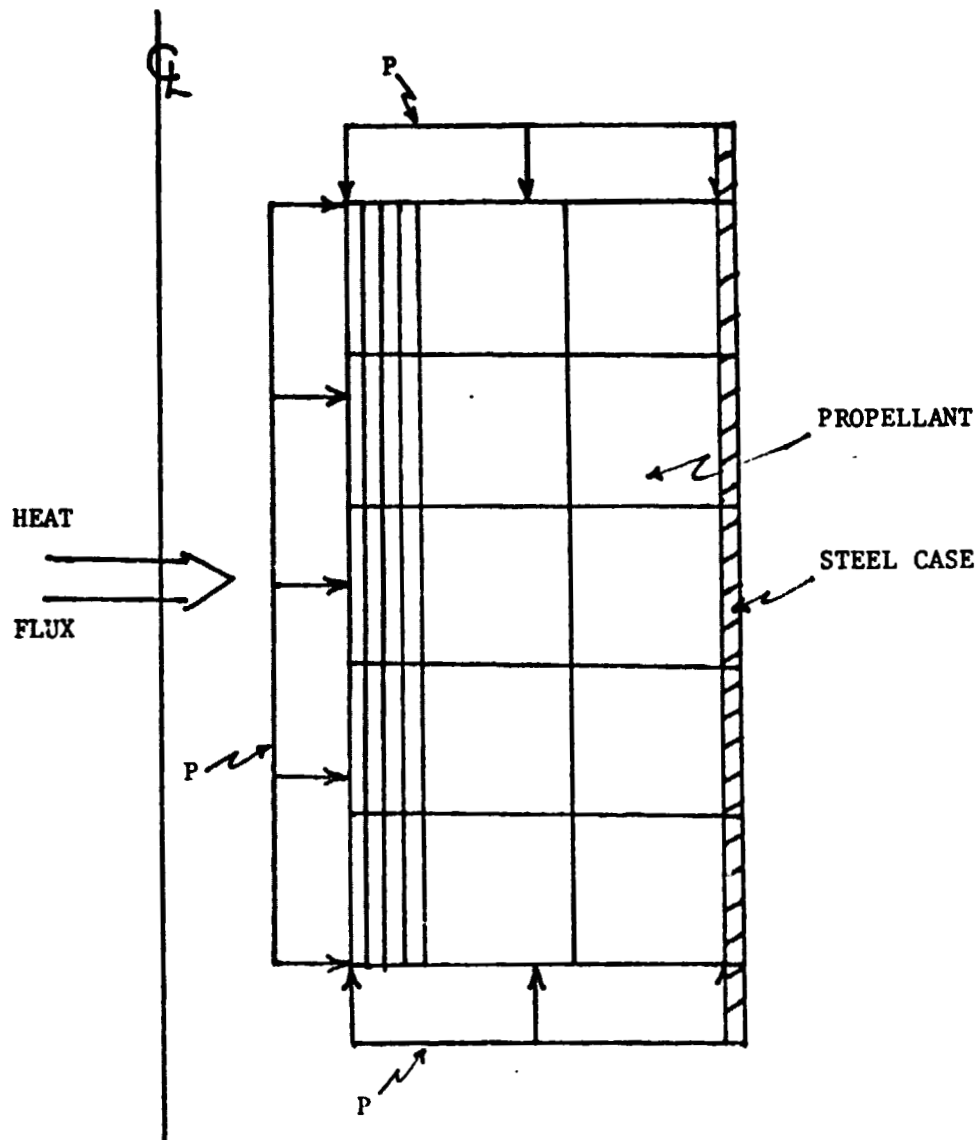


Figure IV-2. Schematic of finite element model (no scale).

exist if the propellant were burning under steady state conditions at the existing pressure. The equation for this distribution is

$$T(x) = [T_s(p_i, T_0) - T_0] \exp[-(x\rho c r/\lambda)] + T_0 \quad (\text{IV-9})$$

where  $T_0$  is taken to be the initial propellant bulk temperature; 4) the initial heat flux at the burning surface is obtained using steady state values in Eq. IV-9.

#### Boundary conditions

The boundary conditions are: 1) The propellant and case remain bonded together, but the propellant-case assemblage is unconstrained; 2) the temperature of the bore surface at any instant of time is uniformly distributed; 3) only the bore surface is subjected to the heat flux calculated from Equation IV-3 (i.e., the ends of the propellant are assumed to be insulated); 4) the pressure at any instant of time is uniformly distributed over both the bore surface and the ends of the propellant. The pressure increases exponentially according to the relation

$$P = P_{\max} - (P_{\max} - P_i) \exp[-\dot{P}_{it}/(P_{\max} - P_i)] \quad (\text{IV-10})$$

#### Numerical Results and Discussion

The numerical results presented here show how the propellant burning rate is affected by thermoelastic coupling and also how these effects are modified when certain parameters are varied. The results do not represent a detailed parametric study but are presented to show the general influence of certain parameters.

For comparison purposes, a "baseline" case was established as a reference for making comparisons. Table IV-1 shows the basic data used for the baseline analysis. The results obtained for the baseline example are shown in Table IV-2 for 50 milliseconds. The time period chosen is sufficiently long to allow the dynamic effect on burning rate to decrease to within a few percent of the quasi-steady state rate and, as can be seen in Table IV-2, the influence of thermoelastic coupling on the dynamic rate has practically vanished. The notation for burning rate in Table IV-2 and in later tables,  $r_{ss}$ ,  $r_t)_{w/o}$  and  $r_t)_w$  represent the quasi-steady state rate, transient rate without thermoelastic coupling and transient rate with thermoelastic coupling, respectively. This table indicates that the influence of thermoelastic coupling is present but that its significance with regard to burning rate decreases very rapidly with time.

Table IV-1. Baseline example data.

Burning rate coefficient (a)	.03783 in/sec-psi <sup>n</sup>
Burning rate exponent (n)	.35
Pyrolysis law (Eq. IV-4) constant (A <sub>g</sub> )	882.28 in/sec
Activation energy (E <sub>g</sub> )	28800 BTU/lb-mole
Thermal conductivity (λ)	5.1 x 10 <sup>-6</sup> BTU/sec-in-°R
Density (ρ)	.063657 lbm/in <sup>3</sup>
Specific heat a constant volume (c)	.24 BTU/lbm-°R
Modulus of elasticity (E)	550 psi
Linear coefficient of thermal expansion (α)	5.27 x 10 <sup>-5</sup> /°R
Poisson's ratio (ν)	.499
Initial pressurization rate ( $\dot{P}_i$ )	14000 psi/sec
Initial ambient pressure (P <sub>i</sub> )	14.7 psi
Maximum chamber pressure (P <sub>max</sub> )	1000 psi

The first parameter to be varied is the pressurization rate. This is done by changing the initial pressurization rate used in Eq. IV-10 from 14,000 to 28,000 psi/sec. The results obtained for this example are shown in Table IV-3.

The effect on the significance of the thermoelastic coupling produced by changing the pressurization rate can be seen in Fig. IV-3. This figure shows the logarithm (base 10) of the absolute value of the percent difference between the transient rate without thermoelastic coupling and the transient rate with thermoelastic coupling for both the increased pressurization rate and baseline examples as a function of time. As can be seen, increasing the pressurization rate has a significant effect on the thermoelastic phenomena. This result is consistent since the thermoelastic term in Eq. IV-1 has a strain rate factor which is proportional to the pressurization rate.

The second parameter altered was the elastic modulus of the propellant. Not only does the elastic modulus affect the strain and hence the strain rate, but it is also a multiplying factor in the thermoelastic term of Eq. IV-1. The elastic modulus was changed from 550 to 2,000 psi. This change is somewhat arbitrary, but it is known that a propellant does exhibit a considerably higher effective elastic modulus under rapid loading conditions. The results obtained for this example are shown in Table IV-4. Note that  $r_{SS}$  and  $r_t)_{w/o}$  are the same as in Table IV-2, since these values are not affected by the elastic modulus.

The effect of this change on the thermoelastic coupling is shown in Fig. IV-4. which is again presented as the logarithm (base 10) of the absolute value of the percent difference between the

Table IV-2. Results for baseline example

Time (msec)	$r_{ss}$ (in/sec)	$r_t)_{w/o}$ (in/sec)	$r_t)_{w}$ (in/sec)
1	.1223	.1122	.1122
2	.1403	.1430	.1398
3	.1546	.1820	.1795
4	.1666	.2153	.2140
5	.1770	.2386	.2379
6	.1864	.2563	.2559
7	.1948	.2703	.2706
8	.2024	.2813	.2812
9	.2095	.2900	.2900
10	.2160	.2969	.2969
11	.2222	.3023	.3023
12	.2279	.3065	.3066
13	.2333	.3098	.3100
14	.2384	.3125	.3127
15	.2433	.3146	.3156
20	.2643	.3214	.3224
25	.2815	.3259	.3268
30	.2959	.3304	.3311
35	.3082	.3350	.3357
40	.3189	.3399	.3404
45	.3283	.3449	.3453
50	.3367	.3449	.3503

Table IV-3. Results for modified pressurization rate example.

Time (msec)	$r_{ss}$ (in/sec)	$r_t$ w/o (in/sec)	$r_t$ w (in/sec)
1	.1403	.1122	.1122
2	.1666	.1625	.1510
3	.1864	.2452	.2270
4	.2024	.3004	.2946
5	.2160	.3271	.3249
6	.2279	.3493	.3479
7	.2384	.3631	.3629
8	.2479	.3724	.3729
9	.2565	.3779	.3789
10	.2643	.3808	.3822
11	.2716	.3821	.3837
12	.2783	.3823	.3840
13	.2846	.3819	.3837
14	.2904	.3813	.3830
15	.2959	.3807	.3823
20	.3189	.3787	.3800
25	.3367	.3790	.3800
30	.3508	.3810	.3818
35	.3622	.3840	.3847
40	.3716	.3875	.3881
45	.3794	.3913	.3918
50	.3859	.3952	.3957

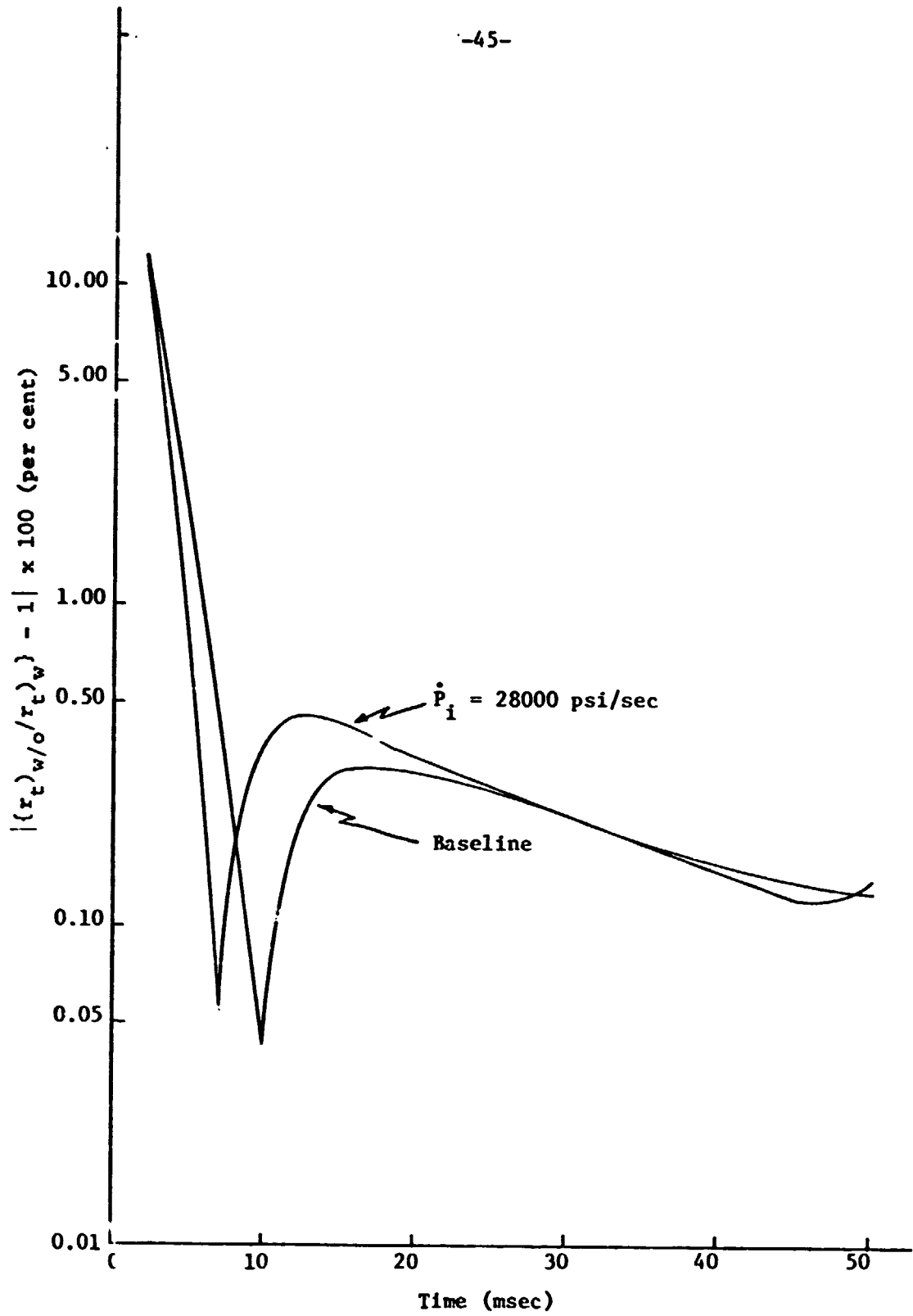


Figure IV-3. Comparison of results with increased pressurization rate to baseline example.



Table IV-4. Results for modified elastic modulus example

Time (msec)	$r_{ss}$ (in/sec)	$r_t)_{w/0}$ (in/sec)	$r_t)_{w}$ (in/sec)
1	.1223	.1122	.1122
2	.1403	.1430	.0930
3	.1546	.1820	.1308
4	.1666	.2153	.1777
5	.1770	.2386	.2211
6	.1864	.2563	.2424
7	.1948	.2703	.2650
8	.2024	.2813	.2785
9	.2095	.2900	.2890
10	.2160	.2969	.2972
11	.2222	.3023	.3036
12	.2279	.3065	.3086
13	.2333	.3098	.3125
14	.2384	.3125	.3156
15	.2433	.3146	.3180
20	.2643	.3214	.3249
25	.2815	.3259	.3290
30	.2959	.3304	.3329
35	.3082	.3350	.3371
40	.3189	.3399	.3416
45	.3283	.3449	.3463
50	.3367	.3499	.3510

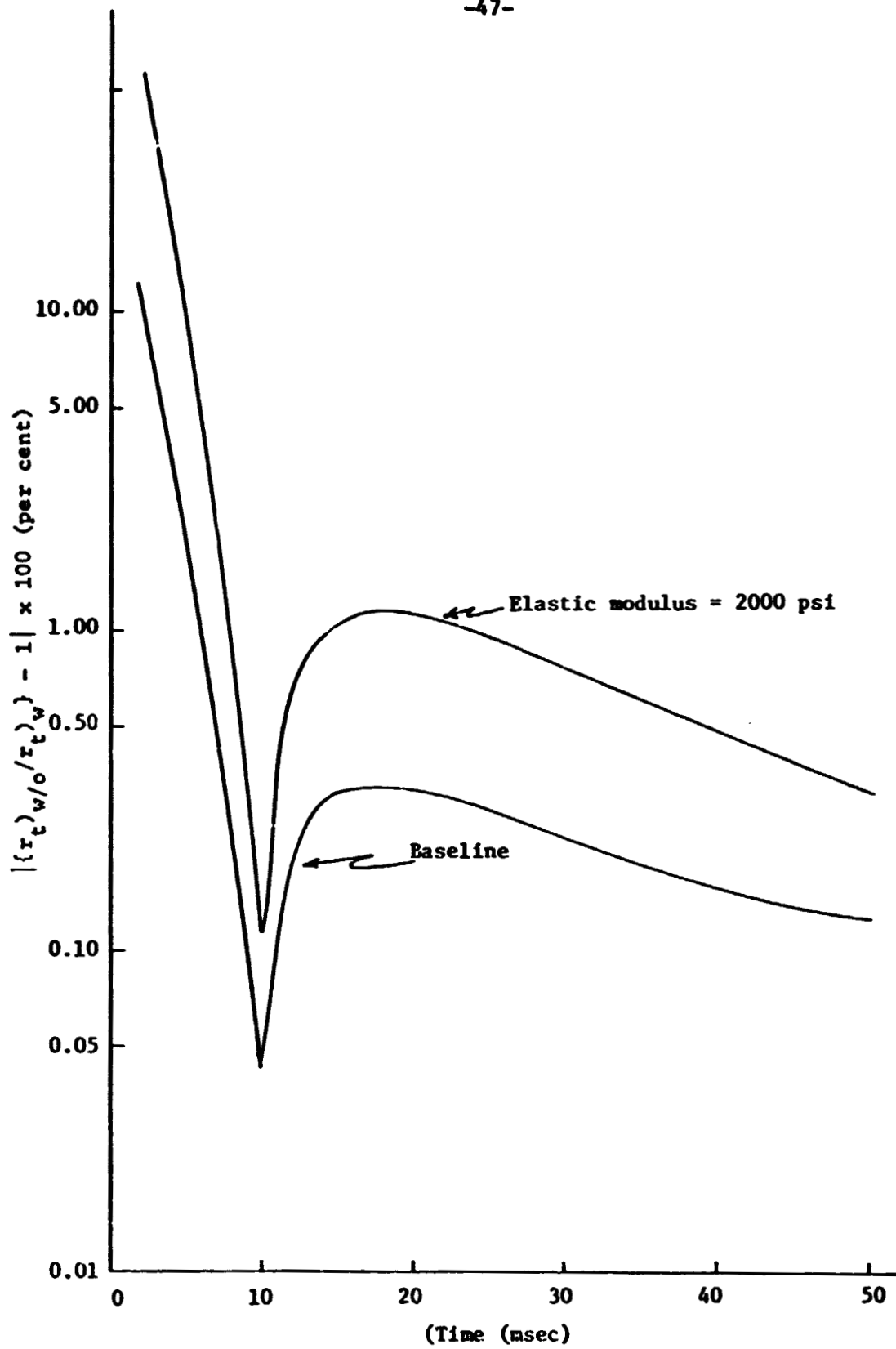


Figure IV-4. Comparison of results with increased elastic modulus to baseline solution.

transient rates with and without coupling for both the baseline and modified elastic modulus examples. The effect of a larger modulus is very similar to that of an increase in pressurization rate. For this example, the effect is significantly larger than for the increased pressurization rate. This should not be taken to mean that the influence of the elastic modulus is more significant than that of the pressurization rate. A much more detailed study would be required to draw any conclusion with regard to the relative importance of these two parameters.

Indeed, many other parameters which affect both the burning rate and the thermoelastic coupling should be subjects of future parametric studies. Among these would be the constants in the burning rate law and the application of the burning rate law over a wide range of temperatures. The coefficient of thermal expansion is also subject to the local temperature and state of strain. The experimental data required regarding the variation in the coefficient of thermal expansion under the conditions which exist during the firing of a solid rocket motor has not been found. Two other parameters which deserve consideration are the thermal conductivity and Poisson's ratio. The conductivity influences the depth of the heat-affected zone and hence the heat transfer feedback mechanism. Poisson's ratio could significantly affect the state of strain if it were much less than 0.5.

Many of the parameters discussed above would require a considerable experimental effort to determine the behavior of these variables under the conditions experienced during the firing of a rocket motor. However, considerable data is available for the elastic modulus with regard to thermal and mechanical loading conditions. Hence, future efforts should first be directed toward incorporating a more rigorous model of the modulus including the influence of both the thermal state and loading rate.

In summary, a model has been constructed to analyze the influence of thermoelastic coupling on propellant burning rate during transient operating conditions. The analysis utilizes a model of the combustion process which is derived from steady state burning rate data and which is more readily applied than some other models considered such as presented in Ref. 19 which require a more detailed model of the flame structure. Examples have been presented which show that the thermoelastic coupling does produce a small, but significant, effect during the initial portion of an ignition process. The results show that increasing the rate of pressurization and/or increasing the elastic modulus increases the thermoelastic effect. Several variables are mentioned as possible candidates for a rigorous parametric study and/or experimental research; in particular, the propellant modulus.

## V. PERFORMANCE PREDICTABILITY INVESTIGATION

In designing an SRM it is important to establish the limits within which the performance of the SRM may be expected to be at all points in its operating time. These limits will be more narrow when the quality of the prediction is higher. Poor predictability yields broad limits which in turn lead to conservatism and inefficient, uneconomical designs. The problem addressed here is how to assess the degree of predictability so that limits can be set with confidence.

The quality of a ballistic prediction is degraded by two general failings: 1) model inadequacies and 2) uncertainties of basic materials and dimensional characteristics used to evaluate the model. Examples of model inadequacy include inability to model exactly ignition transients and even equilibrium burning rate as a function of all pertinent variables. Likewise, for non-homogeneity of chemical species and, to a lesser extent, grain temperature. Even the dimensional specifications are often not portrayed precisely; e.g., the ovality of a nominally c.p. grain and the eccentricity of the grain bore with respect to the motor centerline. Although the modeling is constantly being improved, it must be admitted that all ballistic models leave much to be desired.

For examples of the second general shortcoming of ballistic analysis which degrades predictability, uncertainties of basic material and dimensional characteristics, we have only to consider such parameters as burning rate, throat erosion, propellant density and again, mandrel ovality and misalignment. These and many other parameters are subject to processing and manufacturing variations. Now, although the statistical variation of these variables about some mean value may generally be deduced from previous motors, for any particular design the mean value itself is a matter of some uncertainty until a number of motors have been built and tested. The uncertainty in general decreases with each additional firing. This explains why the predictability limits become narrower with additional motors tested. The problem here is to identify quantitatively the degree of predictability for all points in time in the development program. Perhaps the predictability of the first motor should be stressed; however, because it influences the basic design which may be impractical to change later.

Application of arbitrary safety margins to allow for deviation from predicted performance could, of course, lead to either overly conservative or unsafe designs either of which is undesirable. The Monte Carlo program, on the other hand, provides an approach for establishing limits on performance on a logical probability basis.

Reference 2 shows how the Monte Carlo program can be adapted to permit statistical variation in mean values from motor to motor as well as statistical variation about the mean value. To evaluate the effect of the uncertainties on the limits of performance, it is only necessary to ascribe to

each variable a variability (e.g., a standard deviation for a normal distributed population) of its mean value corresponding to that deduced from experience on other programs. This variability will identify the uncertainty of the corresponding variable. Each variable may also be assigned distributions corresponding to more or less well established variations about the shifting (uncertain) mean values. After evaluation of a large number of motors selected on a probability basis in the manner of the Monte Carlo program, the performance limits versus time are established. The uncertainties can be adjusted to obtain predictability limits at various times in the development program as more information of the mean values is obtained. Also, both pair and individual motor population performance variations may be determined.

It is customary in ballistic predictions to adjust the constants in the burning rate relation used to obtain improved predictability as data from firings is obtained. The improvement is often dramatic. The improvement may actually be due to adjustment for inadequacies of the burning rate coefficient. This suggests that model inadequacies may at least partially be treated as uncertainties in the approach outlined here. Care must be taken, however, in deducing values for uncertainty from previous programs to segregate those that are due to actual variation in input parameters from those that are due to model inadequacies.

Unfortunately, it now appears impractical to obtain the data necessary to establish uncertainties of any type as our queries of industry and government sources and survey of the literature reveals. It is most difficult to recover documentation on what values of a specific variable were used in an original design calculation versus those that were later established to be more valid in various stages of the development and production programs. This is the type of information required for the suggested predictability assessment.

So our efforts to find a better way to establish predictability limits have proved somewhat abortive. Nevertheless, we have recorded the basic approach in the hope that it gives impetus to acquisition and documentation of more detailed statistical data on design and manufacturing variables.

## VI. CHANGES TO PREVIOUS COMPUTER PROGRAMS

In this section, changes to the two computer programs listed in the Appendices to Ref. 2 are given. Each change is listed separately and identified with a page and line number counted from the top of the page. Brief explanations of the reason for each set of changes are also given. The changes are for the most part refinements in analysis or program logic. A few minor errors in the design analysis program have been found and are corrected herein. The most extensive change is the improvement of the use of tabular values of burning surface area during tailoff in the Monte Carlo program. This was accomplished earlier for the design analysis program.

The specific modifications are given in the form of new or revised cards. The cards should be punched beginning with column 7 except that statement numbers are punched to end in column 5 or unless otherwise noted. The card numbers given are for reference to the MSFC and Auburn University program listings only. Numbers for cards that have been deleted are marked with an asterisk. Modifications Nos. 1 through 15 apply to the Monte Carlo program and Nos. 16 through 22 to the design analysis program.

### Modification No. 1 - Card No. 00087050

Purpose: To eliminate statistical analysis for single motors.

Add card between lines 6 and 7 p. 89:

```
IF(NRUNS.EQ.1) STOP
```

### Modification No. 2 - Card Nos. 00169800 & 00170000

Purpose: To permit use of fractional number of slots.

Change line 24 p. 106 to:

```
501 FORMAT(6X,F10.3,3X,F10.2)
```

Change line 26, p. 106 beginning in card column 6 to:

```
1.3,/,13X,'XTZO= ',F7.3,/,13X,'S= ',F6.2,/,13X,'THETAG= ',F8.5,/,13
```

### Modification No. 3 - Card Nos. 00077400\* & 00077500\*

Purpose: To eliminate instability in mass balance iteration during tailoff near transition pressure (PTRAN).

Delete lines 6 and 7 p. 87

Modification No. 4 - Card Nos. 00069900 & 00070000

Purpose: To eliminate occasional instability in mass balance iteration caused by too small a distance burned increment at web time

Change line 27 p. 85 to:

IF(Y.GE.ANS.AND KOUNT.EQ.0) DELY=ANS-YLED+0.05\*DELTAY

Change line 28 p.85 to:

IF(Y.GE.ANS.AND.KOUNT.EQ.0)Y=ANS+0.05\*DELTAY

Modification No. 5 - Card Nos. 00004400, 00174400, 00005100, 00045800\*, 00045900\*, 00046000\*, 00084750

Purpose: To improve accuracy of calculation of action time; i.e. time at which specified low thrust level is reached during tailoff.

Add to line 28 p. 107 and line 44 p. 71:

,FPLOT

Add to line 3 p. 72

,FPLOT(999)

Delete lines 26, 27 and 28 p.80.

Insert between lines 31 and 32 p. 88:

CALL INTRP1(TPLOT,FPLOT,IPT,ATF,ATFAT,1)

Modification No. 6 - Card Nos. 00061950, 00061951, 00061952, 00062000

Purpose: To eliminate unnecessary calculations when there is no erosive burning.

Add 3 cards between lines 43 and 44 p. 83:

3 IF(ALPHA) 131, 132, 131

132 RNOZ=Q\*PNOZ\*\*N

GO TO 4

Change statement number on line 44 p. 83 from 3 to 131:

Modification No. 7 - Card Nos. 00002600, 00106800, 00044651, 00075000,  
00075300, 00075301, 00075900, 00075901, 00115850,  
00115851, 00115900, 00114150, 00114151, 00114200,  
00163150, 00164000, 00075600

**Purpose:** To improve logic of the use of tabular values of burning surface area during tailoff.

Add to lines 26 p. 71 and 18 p. 93:

,ABTT

Add between lines 14 and 15 p. 80:

ABTT=0.0

Change line 30 p. 86 to:

SUMAB=ABMAIN+ABTT

Change line 33 p. 86 (continuation card required) to:

SUMAB=(1.+SUMDY/ZW-DELYW/(2.\*ZW))\*ABTO-(SUMDY/ZW-DELYW/(2.\*ZW))\*ABMAIN+ABTT-ABDIF1

Change line 39 p.86 (continuation card required) to:

SUMAB=(1.-SUMDY/ZW+DELYW/(2.\*ZW))\*ABMAIN+(SUMDY/ZW-DELYW/(2.\*ZW))\*ABTO+ABTT-ABDIF1

Insert 2 lines between lines 12 & 13 p. 95:

YB=Y

IF(K.EQ.1)Y=YB-SUMDY/2.

Prefix line 13 p. 95 with statement number: 91

Insert 2 lines between lines 43 and 44 p. 94:

IF(K.EQ.2) GO TO 91

IF(K.EQ.1) Y=YB

Change line 44 p. 94 to:

IF(YT.LE.Y) GO TO 8

Insert between lines 5 and 6 p. 105:

ABTT=ABPT+ABST+ABNT



Add to lines 14 and 18 p. 105:

-ABTT

Change line 36 p. 86 to:

SUMAB=ABTO+ABTT

Modification No. 8 - Card Nos. 00081450, 00081550, 00104950, & 00104951.

Purpose: To provide printout to indicate DPOUT and XOUT limits have been exceeded if appropriate.

Insert between lines 46 and 47 p. 87:

IF(ABS(DPCDY).GE.DPOUT) WRITE (6,1890)

Insert between lines 47 and 48 p. 87:

IF(Y.GE.XOUT) WRITE(6,1891)

Insert 2 lines between lines 41 and 42 p. 92:

1890 FORMAT (' DPOUT LIMIT EXCEEDED')

1891 FORMAT (' XOUT LIMIT EXCEEDED')

Modification No. 9 - Card Nos. 00185151, 00185152, 00191651, 00191652,  
00196550, 00196551

Purpose: To output imbalance data to tape (see Section II).

Insert 2 lines between lines 39 and 40 p. 109 and 8 and 9 p. 111:

WRITE(8,99999) NX

WRITE(8,99998) (TPLOT(I),FDIFF(I),IDIFF(I),IADIFF(I),I=1,NX)

Insert 2 lines between lines 9 and 10 p. 112

99998 FORMAT(4E16.9)

99999 FORMAT(I10)

Modification No. 10 - Card Nos. 00007402, 00014002, 00015202, 00015951,  
00030700, 00030800

Purpose: To allow card input of radial grain temperature gradient.

Insert between lines 26 and 27 p. 72:

IREAD=3

Insert between lines 44 and 45 p. 73 beginning in card column 1:

C \* 2 FOR CARD INPUT OF TEMPERATURE GRADIENTS \*

Insert between lines 8 and 9 p. 74:

IF(ITEMP.EQ. 2)IREAD = 5

Insert between lines 15 and 16 p. 74:

IF(ITEMP.EQ. 2) ITEMP = 0

Change lines 19 and 20 p. 77 to:

READ (IREAD, 3700) TUBULKO, TBULKE

2700 READ (IREAD, 3700) (YTAB(ITAB),TTABA(ITAB),TTABB(ITAB),  
TTABC(ITAB),

Modification No. 11 - Card Nos. 00031300, 00031500, 00032800, 00036950,  
00039500, 00077100, 00098900, 00099700, 00099701

Purpose: To permit user to specify the extinguishment chamber pressure (PEXT) and the grain reference temperature (TREF). See also Modification No. 13 for other necessary changes for TREF.

Add to lines 25, 27 and 40 p. 77 and line 11 p. 79:

,PEXT,TREF

Insert between lines 33 and 34 p. 78:

C \* PEXT IS THE PRESSURE AT WHICH THE PROPELLANT  
EXTINGLISHES \*

Change line 3 p. 87 to:

IF(PONoz.LE.PEXT) GO TO 25

Add to line 29 p. 91 inside closing parenthesis:

,6X,F10.2,6X,F10.2

Add to line 36 p. 91 inside closing parenthesis (additional continuation card required):

,/,13X,'PEXT= ',F6.2,/,13X,'TREF= ',F6.2

Modification No. 12 - Card Nos. 00077000, 00077010, 00077020, 00079100

Purpose: To improve logic of mass balance iteration during tailoff

Change line 2 p. 87 to:

22 IF(PBAR.LT.PTRAN) DPCDY = PBAR\*DADY/(1.-N1)/ABAVE

Insert 2 lines between lines 2 and 3 p. 87:

IF(PBAR.GE.PTRAN) DPCDY = PBAR\*DADY/(1.-N2)/ABAVE

PONoz = PONOJ+DPCDY\*DELY

Change line 23 p. 87 to:

4. CONTINUE

Modification No. 13 - Card Nos. 00036960, 00048300, 00046100, 00055000,  
00058200, 00060500, 00077600, 00048500, 00048700,  
00048800, 00048900, 00049000, 00049600, 00049700,  
00055200, 00055300, 00055400, 00055500, 00055900,  
00056000, 00058400, 00058500, 00058600, 00058700,  
00059100, 00059200, 00060700, 00060800, 00060900,  
00061000, 00061400, 00061500, 00077800, 00077900,  
00078000, 00078100, 00078500, 00078600

Purpose: To allow user to specify a grain reference temperature (TREF)  
See also Modification No. 11.

Insert between lines 33 and 34 p. 78:

C \* TREF IS THE DESIGN TEMPERATURE OF THE GRAIN \*

Change 00.0 in the following places to TREF:

Line 3, p. 81; line 29 p. 80; line 22 p. 82; line 6 p. 83; line 29  
p. 83; line 8 p. 87; line 5 p. 81; lines 7, 8, 9, 10,  
16 and 17 p. 81; lines 24, 25, 26, 27, 31 and 32 p. 82;  
lines 8, 9, 10, 11, 15 and 16 p. 83; lines 31, 32, 33, 34,  
38, and 39 p. 33; lines 10, 11, 12, 13, 17 and 18 p. 87.

Modification No. 14 - Card Nos. 00179500, 00179520, 00179540, 00196553

**Purpose:** To create a tape containing the thrust versus time data for each SRM. The data is written on unit 9 and the appropriate job control cards must be provided for this unit. This modification was accomplished to obtain nominal trace characteristics for statistical correlation of thrust imbalance with nominal trace characteristics (See Section II).

Change line 31 p. 108 to:

2 WRITE(9,99999) NP

Insert 2 lines between lines 31 and 32 p. 108:

WRITE(9,99997) (TPlot(I),FPlot(I),I=1,NP)

NP=NP+2

Insert between lines 9 and 10 p. 112 after Modification 7 insertion:

99997 FORMAT(2E16.9)

Modification No. 15 - Card Nos. 00012200, 00012500, 00012600, 00012700, 00013900

**Purpose:** To improve clarity of option descriptions.

Insert line 26 p. 73 between OVALITY and ANALYSIS:

OR NON-AXISYMMETRIC THERMAL

Change description line 29 p. 73 to:

FOR PLOTS, TABULAR OUTPUT AND STATISTICAL ANALYSIS

Change description line 30 p. 73 to:

FOR TABULAR OUTPUT AND STATISTICAL ANALYSIS

Change description line 31 p. 73 to:

FOR PLOTS AND STATISTICAL ANALYSIS

Change description line 43 p. 73 to:

FOR TAPE INPUT OF TEMPERATURE GRADIENTS

See also Modification 10 (between lines 44 and 45 p. 73)

Modification No. 16 - Card Nos. 00030200\*, 00030300\*, 00020451, 00020452,  
00020651, 00020652, 00020653, 00020700

Purpose: To correct error in calculation of burning rate coefficients Q1 and Q2 which occurs with input of grain temperature gradients.

Remove Q1 and Q2 equations, lines 15 and 16 p. 158, and insert same between lines 13 and 14 p. 156.

Insert 3 lines between lines 15 and 16 p. 156:

```
IF(ITEMP) 10005, 10006, 10005
```

```
10005 Q1=A1*EXP(PIPK*(1.-N1)*(TGR-TREF))
```

```
Q2=A2*EXP(PIPK*(1.-N2)*TGR-TREF))
```

Change line 16 p. 156 to:

```
10006 IF(XT.LE.0.0)GO TO 40
```

Modification No. 17 - Card Nos. 00032151, 00032152, 00032153, 00033154,  
00032200

Purpose: To eliminate iteration for burning rate when there is no erosive burning.

Insert 4 lines between lines 34 and 35 p. 158:

```
3 IF(ALPHA) 131,132,131
```

```
132 IF(PNOZ.LE.PTRAN) RNOZ = Q1*PNOZ**N1
```

```
IF(PNOZ.GT.PTRAN) RNOZ = Q2*PNOZ**N2
```

```
GO TO 4
```

Change statement number on line 35 p. 158 from 3 to 131

Modification No. 18 - Card Nos. 00037300 & 00037400

Purpose: To eliminate occasional instability in mass balance iteration at web time which occurs when y (DELY) increment just prior to beginning of tailoff is too small.

Add to lines 38 and 39 p. 159:

```
+0.05*DELTAY
```

Modification No. 19 - Card No. 00045100\*

**Purpose:** To eliminate instability in mass balance iteration during tailoff when the chamber pressure crosses the transition pressure PTRAN.

Delete line 20 p. 161.

Modification No. 20 - Card Nos. 00045000, 00045010, 00045020

**Purpose:** To correct error in selection of N2 and N1 when PTRAN is crossed during tailoff

Change line 19 p. 161 to:

IF(PONoz.LE.PTRAN) Q2=Q1

Insert 2 lines between lines 19 and 20 p. 161:

IF(PONoz.LE.PTRAN) N2=N1

RNOZ=Q2\*PONoz\*\*N2

Modification No. 21 - Card Nos. 00124800, 00124900, 00125000

**Purpose:** To allow the plotting of additional data points so that the user may use smaller y increments.

Change 200 to 999 throughout lines 6, 7, and 8 p. 178.

Modification No. 22 - Card Nos. 00019810, and 00020600

**Purpose:** To correct an error in the place of calculation of the characteristic velocity. This error would occur when  $TGR \neq TREF$  and  $CSTART \neq 0.0$ . causing a small accumulative error in CSTAR over the operating time.

Insert between lines 14 and 15 p. 156:

CSTARN=CSTAR

Change line 15 p. 156 to:

10003 CSTAR=CSTARN\*(1.+CSTART\*(TGR-TREF))

## VII. CONCLUDING REMARKS

The continued research in internal ballistics performance variation has produced considerable improvement in the flexibility of the Monte Carlo and design analysis computer programs. In addition to a large number of minor improvements in both programs, two new computer program codes now permit more detailed examination of the thrust imbalance characteristics defined by the Monte Carlo program. Sample evaluations for the Titan IIIC and comparisons with flight test data show good agreement throughout the operating time of the motors and thus provide additional confirmation of the Monte Carlo method. Statistical correlation studies of the sample results suggest several new and possibly important approaches to predicting thrust imbalance.

Design analysis program modifications now permit evaluation of the internal ballistic effect of general deformation of circular-perforated grains. Although additional validation of the model is needed, application of the method to two different SRMs indicates that the deformation may account for a substantial portion of the so-called "scale factor" on burning rates.

The research in the thermoelastic coupling of propellant strain rate with grain temperature and burning rate has culminated in an apparently successful method for theoretical evaluation of the phenomenon. Assessment of the influence of thermoelastic coupling indicates a small but definite effect which warrants further investigation.

## REFERENCES

1. Sforzini, R. H., and Foster, W. A., Jr., "Monte Carlo Investigation of Thrust Imbalance of Solid Rocket Motor Pairs," Journal of Spacecraft and Rockets, Vol. 13, No. 14, April 1976, pp. 198-202.
2. Sforzini, R. H., and Foster, W. A., Jr., "Solid-Propellant Rocket Motor Ballistic Performance Variation Analyses," Final Report, NASA Contractor Report CR-144264, Engineering Experiment Station, Auburn University, September 1975.
3. Sforzini, R. H., Foster, W. A., Jr., and Johnson, J. S., Jr., "A Monte Carlo Investigation of Thrust Imbalance of Solid Rocket Motor Pairs," Final Report, NASA Contractor Report CR-120700, Auburn University, November 1974.
4. Smith, D. F., "Solid Propellant General Deformations and Their Effect on Motor Performance," Master of Science Thesis, Auburn University, Scheduled for Submission in October 1976.
5. Summerfield, M., Caveny, L. H., et al, "Theory of Dynamic Extinguishment of Solid Propellants with Special Reference to Nonsteady Heat Feedback Law," AIAA Journal, Vol. 8, No. 3, March 1971, pp. 251-258.
6. Foster, W. A., Jr., "A Method for the Transient Nonlinear Coupled Thermoelastic Analysis of Axisymmetric Bodies Using Finite Elements," Ph.D. Dissertation, Auburn University, Auburn, Alabama, 1974.
7. Baker, J. S., "Equilibrium Thrust Imbalance Analysis for TC-227A-75," Memorandum transmitted to K. W. Jones, MSFC, by L. G. Bailey, Wasatch Division, Thiokol Chemical Corporation, Letter No. 7010/LB-75-547, 13 November 1975.
8. Barrère, M., Jaumotte, A., Fraejis, De Vaubeke, B., and Vandekerckhove, J., Rocket Propulsion, Elsevier, Amsterdam, 1960, pp. 277-281.
9. Brisbane, J. J., "Heat Conduction and Stress Analysis of Solid-Propellant Rocket Motor Nozzles," Technical Report S-198, U.S. Army Missile Command, Redstone Arsenal, Alabama, 1969.
10. "Propellant Burning Rate Investigation," Final Report, UTC 4310-73-51, to Space and Missile System Organization, USAF Systems Command, United Technology Center, Sunnyvale, Calif., Oct. 31, 1973, p. 3-27 and p. 4-5.



11. "Technical Description of the TX 354-5 Rocket Motor," Huntsville Division, Thiokol Chemical Corporation, Control No. U-67-1005A, May 9, 1967.
12. Sforzini, R. H., "Design and Performance Analysis of Solid-Propellant Rocket Motors Using a Simplified Computer Program, Final Report, NASA Contractor Report CR-129025, October 1972.
13. Duhamel, J. N. C., "Second Mémoire sur les Phénomènes Thermomécaniques," J. de l'Ecole Polytechnique, Vol. 15, 1837.
14. Kelvin, Lord (Sir William Thompson), Mathematical and Physical Papers, Vol. 3, Cambridge University, Press Warehouse, London, 1890, pp. 1-260.
15. Joule, J. P., The Scientific Papers of James Prescott Joule, Vol. 1, The Physical Society of London, 1887, pp. 413-473.
16. Hermann, G., "On Variational Principles in Thermoelasticity and Heat Conduction," Quart-Appl. Math., Vol. 21, No. 2, 1963.
17. Becker, E. B., and Parr, C. H., "Application of the Finite Element Method to Heat Conduction in Solids," Technical Report S-117, U.S. Army Missile Command, Redstone Arsenal, Alabama, 1967.
18. Wilson, E. L., and Nickell, R. E., "Application of the Finite Element Method to Heat Conduction Analysis," Nuclear Engineering and Design, Vol. 4, No. 3, 1966.
19. Krier, H., et al, "Nonsteady Burning Phenomena of Solid Propellants: Theory and Experiments," AIAA Journal, Vol. 6, No. 2, February 1968. pp. 278-285.

## **APPENDICES**

### **COMPUTER PROGRAMS**

- A. Analysis of SRM Pair Imbalance Data during Specified Time Intervals**
- B. Analysis of SRM Pair Imbalance Data at Specified Times during Operation**
- C. SRM Design Analysis with Option Permitting Evaluation of Grain Deformation Effects**

## APPENDIX A

### A COMPUTER PROGRAM FOR ANALYSIS OF SRM PAIR IMBALANCE DATA DURING SPECIFIED TIME INTERVALS

The computer program listed in this appendix is used to analyze a data tape containing motor pair data which is generated by the Monte Carlo performance analysis program described in Refs. 2 and 3. This program analyzes the data for a prescribed number of time intervals. The variables investigated are the absolute values of thrust imbalance and its first time derivative, the impulse imbalance and the absolute impulse imbalance. For each variable the program calculates the maximum value for each pair during the time interval, the maximum value occurring in all time intervals for all pairs, the mean value for each time interval and the standard deviation for each time interval. The program also determines the mean value and standard deviation of the time at which the maximum value of the variable occurs within the time interval.

#### Input Data

The discussion below gives the general purpose, order and FORTRAN coding information for the input data.

Card 1 Number of time intervals to be analyzed (I10)

Col. 1-10 Number of time intervals (NSETS)

Card 2 Time interval data (I10, 2F10.4)(one card for each time interval)

Col. 1-10 Number of motor pairs to be analyzed (NAMAX)

11-20 Beginning time of interval (ATMIN)

21-30 Ending time of interval (ATMAX)

#### Program Listing

The program listing is presented in Table A-1.

#### Output

The output of the program is discussed in Section II of the main report where a sample output illustration is also given.

Table A-1. Computer program for analysis of SRM pair imbalance data during specified time intervals.

```

DIMENSION FDIFF(1000),TPL0T(1000),DFDUT(1000)
DIMENSION NAMAX(50),ATMIN(50),ATMAX(50)
CALL GSIZE(500.,11.,1121)
READ(5,101) NSETS
DO 7000 IPLT=1,3
REWIND 8
DO 6000 L=1,NSETS
IF(IPLT.EQ.2.AND.L.EQ.1) CALL PLOT(24.,0.,-3)
IF(IPLT.EQ.2.AND.L.GT.1) CALL PLOT(9.,0.,-3)
IF(IPLT.EQ.3) CALL PLOT(9.,0.,-3)
XMAX=0.0
TMAX=0.0
XDMAX=0.0
TDMAX=0.0
REWIND 8
IF(L.GT.1.AND.IPLT.EQ.1) CALL PLOT(24.,0.,-3)
IF(IPLT.EQ.1) READ(5,101) NAMAX(L),ATMIN(L),ATMAX(L)
NMAX=NAMAX(L)
TMIN=ATMIN(L)
TMAX=ATMAX(L)
WRITE(6,103) L,NMAX,TMIN,TMAX
DO 1000 N=1,NMAX
DFMAX=0.0
TDFMAX=0.0
READ(8,101) NX
KUUNT=0
K=0
IC=0
DO 4000 J=1,NX
CALL INPUT(T,F,IPLT)
IF(T.LT.TMIN) K=J
IF(T.LT.TMIN) GO TO 4000
I=J-K
IF(T.GT.TMAX.AND.KUUNT.EQ.0) KUUNT=I-1
IF(KUUNT) 11,11,4000
11 TPL0T(I)=T
FDIFF(I)=F
AF=ABS(F)
IF( AF.GT.DFMAX) TDFMAX=T
IF( AF.GT.DFMAX) DFMAX=AF
IF(DFMAX.GT.XMAX) TMAX=TDFMAX
IF(DFMAX.GT.XMAX) XMAX=DFMAX
IF(T.LT.TMAX.AND.J.GE.NX) IC=I
4000 CONTINUE
GO TO (87,88,89),IPLT
87 WRITE(6,107) N,DFMAX
GO TO 90
88 WRITE(6,1071) N,DFMAX

```

Table A-1 (Cont'd)

```

GO TO 90
89 WRITE(6,1072) N,DFMAX
90 WRITE(6,106) TDFMAX
   CALL SIGBAR(DFMAX,S1,S2,XMAXS,XMAXM,N,NMAX)
   CALL SIGBAR(TDFMAX,S3,S4,TMXXS,TMXXM,N,NMAX)
   IF(KOUNT.NE.0) NX=KOUNT
   IF(IC.NE.0) NX=IC
   IF(N-1) 14,14,16
14 CALL SCALE(FDIFF,8.0,NX,1)
   IF(FDIFF(NX+1).LT.0.0.AND.8.0*FDIFF(NX+2)+FDIFF(NX+1).LE.0.0)
   2FIRSTV=FDIFF(NX+1)*2.
   IF(FDIFF(NX+1).LT.0.0.AND.8.0*FDIFF(NX+2)+FDIFF(NX+1).GT.0.0)
   2FIRSTV=-ABS(8.*FDIFF(NX+2))
   IF(FDIFF(NX+1).GE.0.0) FIRSTV=-(FDIFF(NX+1)+8.0*FDIFF(NX+2))*2.
   DELTAV=-FIRSTV/4.0
16 CONTINUE
   FDIFF(NX+1)=FIRSTV
   FDIFF(NX+2)=DELTAV
   TPL0T(NX+1)=TMIN
   TPL0T(NX+2)=(TMAX-TMIN)/5.0
   IF(N.EQ.1.AND.L.EQ.1.AND.IPLT.EQ.1) CALL PLOT(4.0,1.5,-3)
   IF(N.NE.1) GO TO 999
   GO TO (1,2,3),IPLT
1 CALL AXIS(0.0,0.0,'THRUST IMBALANCE (LBF)',22,8.0,90.0,
2FIRSTV,DELTAV)
   GO TO 4
2 CALL AXIS(0.0,0.0,'IMPULSE IMBALANCE (LBF-SECS)',28,8.0,90.0,
2FIRSTV,DELTAV)
   GO TO 4
3 CALL AXIS(0.0,0.0,'ABSOLUTE IMPULSE IMBALANCE (LBF-SECS)',
237,8.0,90.0,
2FIRSTV,DELTAV)
4 CALL AXIS(0.0,4.0,'TIME (SECS)',-11,5.0,0.0,TPL0T(NX+1)
2,TPL0T(NX+2))
999 CALL PLOT(0.,4.,3)
   CALL LINE(TPL0T,FDIFF,NX,1,0,1)
1000 CONTINUE
   GO TO (5,6,7),IPLT
5 WRITE(6,104) XMAX
   WRITE(6,106) TMXX
   WRITE(6,109)
   WRITE(6,104) XMAXM
   WRITE(6,111)
   WRITE(6,104) XMAXS
   WRITE(6,110) TMXXM
   WRITE(6,112) TMXXS
   GO TO 8
6 WRITE(6,1041) XMAX

```

Table A-1 (Cont'd)

```

WRITE(6,106) TMXX
WRITE(6,109)
WRITE(6,1041) XMAXM
WRITE(6,111)
WRITE(6,1041) XMAXS
WRITE(6,110) TMXXM
WRITE(6,112) TMXXS
GO TO 8
7 WRITE(6,1042) XMAX
WRITE(6,106) TMXX
WRITE(6,109)
WRITE(6,1042) XMAXM
WRITE(6,111)
WRITE(6,1041) XMAXS
WRITE(6,110) TMXXM
WRITE(6,112) TMXXS
8 IF(IPLT.NE.1) GO TO 6000
REWIND 8
DO 2000 N=1,NMAX
DFDMAX=0.0
TDFDMX=0.0
READ(8,101) NX
KOUNT=0
K=0
IC=0
DO 5000 J=1,NX
CALL INPUT(T,F,IPLT)
IF(T.LT.TMIN) K=J
IF(T.LT.TMIN) GO TO 5000
I=J-K
IF(T.GT.TMAX.AND.KOUNT.EQ.0) KOUNT=I-1
IF(KOUNT) 13,13,5000
13 TPLOT(I)=T
FDIFF(I)=F
IF(T.LT.TMAX.AND.J.GE.NX) IC=I
5000 CONTINUE
IF(KOUNT.NE.0) NX=KOUNT
IF(IC.NE.0) NX=IC
DFDOT(1)=FDIFF(1)/TPLOT(1)
DFDMAX=ABS(DFDOT(1))
TDFDMX=TPLOT(1)
DO 3000 J=2,NX
DFDOT(J)=(FDIFF(J)-FDIFF(J-1))/(TPLOT(J)-TPLOT(J-1))
AFD=ABS(DFDOT(J))
IF(          AFD.GT.DFDMAX) TDFDMX=TPLOT(J)
IF(          AFD.GT.DFDMAX) DFDMAX=ABS(DFDOT(J))
IF(DFDMAX.GT.XDMAX) TDMAX=TDFDMX
3000 IF(DFDMAX.GT.XDMAX) XDMAX=DFDMAX

```

Table A-1 (Cont'd)

```

WRITE(6,108) N,DFDMAX
WRITE(6,113) TDFDMX
CALL SIGBAR(DFDMAX,S5,S6,XDMAXS,XDMAXM,N,NMAX)
CALL SIGBAR(TDFDMX,S7,S8,TDMAXS,TDMAXM,N,NMAX)
IF(N-1) 15,15,17
15 CALL SCALE(DFDOT,8.0,NX,1)
   IF(DFDOT(NX+1).LT.0.0.AND.8.0*DFDOT(NX+2)+DFDOT(NX+1).LE.0.0)
   2FIRSTV=DFDOT(NX+1)*2.
   IF(DFDOT(NX+1).LT.0.0.AND.8.0*DFDOT(NX+2)+DFDOT(NX+1).GT.0.0)
   2FIRSTV=-ABS(8.*DFDOT(NX+2))
   IF(DFDOT(NX+1).GE.0.0) FIRSTV=-(DFDOT(NX+1)+8.0*DFDOT(NX+2))*2.
   DELTAV=-FIRSTV/4.0
17 CONTINUE
   DFDOT(NX+1)=FIRSTV
   DFDOT(NX+2)=DELTAV
   TPLLOT(NX+1)=TMIN
   TPLLOT(NX+2)=(TMAX-TMIN)/20.0
   IF(N.EQ.1.AND.IPLT.EQ.1) CALL PLOT(9.0,0.0,-3)
   IF(N.EQ.1) CALL AXIS(0.0,0.0,'THRUST IMBALANCE RATE (LBS/SEC)',31,
28.0,90.0,FIRSTV,DELTAV)
   IF(N.EQ.1)CALL AXIS(0.0,4.0,'TIME (SECS)',-11,20.,0.0,TPLOT(NX+1)
2,TPLOT(NX+2))
   CALL PLOT(0.0,4.0,3)
   CALL LINE(TPLOT,DFDOT,NX,1,0,1)
2000 CONTINUE
   WRITE(6,105) XDMAX
   WRITE(6,113) TDMAX
   WRITE(6,109)
   WRITE(6,105) XDMAXM
   WRITE(6,111)
   WRITE(6,105) XDMAXS
   WRITE(6,114) TDMAXM
   WRITE(6,115) TDMAXS
6000 CONTINUE
7000 CONTINUE
   CALL PLOT(0.0,0.0,999)
100 FORMAT(4E16.9)
101 FORMAT(110,2F10.4)
102 FORMAT(3(5X,E16.9))
103 FORMAT(1H1, 9X,'THIS IS TIME INTERVAL NUMBER',I4,/,10X,'THERE ARE
2 ',I4,' SETS OF DATA FOR THIS TIME INTERVAL',/,10X,'THIS TIME INT
2ERVAL BEGINS AT',F7.2,' SECS AND ENDS AT',F7.2,' SECS',/)
104 FORMAT(10X,'THE ABSOLUTE VALUE OF THE MAXIMUM THRUST IMBALANCE DUR
2ING THIS TIME INTERVAL IS ',1PE11.4,' LBF')
1041 FORMAT(10X,'THE ABSOLUTE VALUE OF THE MAXIMUM IMPULSE IMBALANCE DU
2RING THIS TIME INTERVAL IS ',1PE11.4,' LBF-SECS')
1042 FORMAT(10X,'THE MAXIMUM ABSOLUTE IMPULSE IMB
2ALANCE DURING THIS TIME INTERVAL IS ',1PE11.4,' LBF-SECS')

```

ORIGINAL PAGE IS  
OF POOR QUALITY

Table A-1 (Cont'd)

```

105 FORMAT(10X,'THE ABSOLUTE VALUE OF THE MAXIMUM THRUST IMBALANCE RATE
    DURING THIS TIME INTERVAL IS ',1PE11.4,' LBF/SEC')
106 FORMAT(10X,'THIS IMBALANCE OCCURS AT ',F7.2,' SECS',/)
107 FORMAT(10X,'THE ABSOLUTE VALUE OF THE MAXIMUM THRUST IMBALANCE FOR
    2 MOTOR PAIR NUMBER ',I4,' IS ',1PE11.4,' LBF')
1071 FORMAT(10X,'THE ABSOLUTE VALUE OF THE MAXIMUM IMPULSE IMBALANCE FOR
    2R MOTOR PAIR NUMBER ',I4,' IS ',1PE11.4,' LBF-SECS')
1072 FORMAT(10X,
    'THE MAXIMUM ABSOLUTE IMPULSE IMBALANCE FOR MOTOR PAIR NUMBER ',I4,' IS ',1PE11.4,' LBF-SECS')
108 FORMAT(10X,'THE ABSOLUTE VALUE OF THE MAXIMUM THRUST IMBALANCE RATE
    FOR MOTOR PAIR NUMBER ',I4,' IS ',1PE11.4,' LBF/SEC')
109 FORMAT(10X,'THE MEAN VALUE OF')
110 FORMAT(/,10X,'THE MEAN VALUE OF THE TIME FOR THIS IMBALANCE IS ',
    2F7.2,' SECS',/)
111 FORMAT(/,10X,'THE STANDARD DEVIATION OF')
112 FORMAT(10X,'THE STANDARD DEVIATION OF THE TIME FOR THIS IMBALANCE
    2IS ',F7.2,' SECS',/)
113 FORMAT(10X,'THIS IMBALANCE RATE OCCURS AT ',F7.2,' SECS',/)
114 FORMAT(/,10X,'THE MEAN VALUE OF THE TIME FOR THIS IMBALANCE RATE I
    2S ',F7.2,' SECS',/)
115 FORMAT(10X,'THE STANDARD DEVIATION OF THE TIME FOR THIS IMBALANCE
    2RATE IS ',F7.2,' SECS',/)
    STOP
    END

```

```

SUBROUTINE SIGBAR(X,XI,XI2,SIGX,BX,ICOUNT,N)
    XN=FLOAT(N)
    IF(ICOUNT.GT.1) GO TO 1
    XI2=0.0
    XI=0.0
1   XI2=XI2+X**2
    XI=XI+X
    BX=XI/XN
    XI2=XI2-XI**2
    ARG=(XI2/XN)-(BX**2)
    IF(ARG)2,2,3
2   SIGX=0.0
    GO TO 4
3   SIGX=SQRT(ARG)
4   RETURN
    END

```

```

SUBROUTINE INPUT(T,F,IPLT)
    GO TO (1,2,3),IPLT
1   READ(8,100) T,F,D1,D2
    GO TO 4
2   READ(8,100) T,D1,F,D2
    GO TO 4
3   READ(8,100) T,D1,D2,F
4   RETURN
100 FORMAT(4E10.9)
    END

```



## APPENDIX B

### A COMPUTER PROGRAM FOR ANALYSIS OF SRM PAIR IMBALANCE DATA AT SPECIFIED TIMES DURING OPERATION

The computer program listed in this appendix is used to analyze a data tape containing motor pair data which is generated by the Monte Carlo performance analysis program described in Refs. 2 and 3. This program analyzes the data at a prescribed number of discrete time slices and calculates the statistical tolerance limits about a zero mean value for the thrust imbalance, thrust imbalance rate and impulse imbalance. For the absolute impulse imbalance the statistical tolerance limits are computed about the true mean value.

#### Input Data

The discussion below gives the general purpose, order and FORTRAN coding information for the input data.

##### Card 1 (3F10.0)

- Col. 1-10 One sided K-factor (SIGK1)
- 11-20 Two sided K-factor (SIGK2)
- 21-30 Initial time point to be plotted (TMIN)

##### Card 2 (2I10)

- Col. 1-10 Number of time slices to be taken (N)
- 11-20 Number of motor pairs to be analyzed (NMAX)

##### Card 3 Time Slice Card (F10.0)(one card per time slice)

- Col. 1-10 Time at which analysis is to be made (TSL)

#### Program Listing

The program listing is presented in Table B-1.

#### Output

The output of the program is discussed in Section II of the main report where a sample output illustration is also given.

Table B-1. Computer program for analysis of SRM pair imbalance data at specified times during operation.

```

DIMENSION F(1000),FD(1000),T(1000),TSL(500),FDIS(500),FIS(500)
DIMENSION FI(500),FDI(500),FIM(500),FDIM(500),FISM(500)
DIMENSION S1(500),S2(500),S3(500),S4(500)
CALL GSIZE(500.,11.,1121)
READ(5,100) SIGK1,SIGK2,TMIN
READ(5,101) N,NMAX
WRITE(6,105) NMAX,SIGK1,SIGK2,N
101 FORMAT(2I10)
DO 4000 K=1,N
4000 READ(5,100) TSL(K)
100 FORMAT(8F10.0)
DO 99999 IPLT=1,3
REWIND 8
DO 3000 L=1,NMAX
CALL INPUT(T,F,NX,IPLT)
102 FORMAT(4E16.9)
FD(1)=F(1)/T(1)
DO 1000 J=2,NX
1000 F(J)=(F(J)-F(J-1))/(T(J)-T(J-1))
DO 3000 K=1,N
CALL INTRP1(F,T,NX,TSL(K),FI(K))
CALL INTRP1(FD,T,NX,TSL(K),FDI(K))
104 FORMAT(10X,3E16.9)
CALL SIGBAR(FI(K),S1(K),S2(K),FIS(K),FIM(K),L,NMAX,IPLT)
3000 CALL SIGBAR(FDI(K),S3(K),S4(K),FDIS(K),FDIM(K),L,NMAX,IPLT)
DO 1 I=1,N
FIS(I)=          SIGK2*FDIS(I)
IF(IPLT.EQ.3) GO TO 11
FIS(I)=          SIGK2*FIS(I)
GO TO 1
11 FISM(I)=FIM(I)-SIGK1*FIS(I)
IF(FISM(I).LE.0.0) FISM(I)=0.0
FIS(I)=FIM(I)+SIGK1*FIS(I)
1 CONTINUE
DO 4 I=1,N
WRITE(6,106) TSL(I)
IF(IPLT .NE.1) GO TO 30
WRITE(6,103) FIS(I),FDIS(I)
GO TO 4
30 IF(IPLT .NE.2) GO TO 40
WRITE(6,113) FIS(I)
GO TO 4
40 WRITE(6,132) FIM(I)
WRITE(6,123) FIS(I)
WRITE(6,133) FISM(I)
4 CONTINUE
IF(IPLT-1) 80,80,70
80 CALL PLOT(4.0,1.5,-3)

```

Table B-1 (Cont'd)

```

GO TO 90
70 CALL PLOT(9.0,0.0,-3)
90 CONTINUE
  CALL SCALE(FIS,8.0,N,1)
  IF(FIS(N+1).LT.0.0.AND.8.0*FIS(N+2)+FIS(N+1).LE.0.0)
2FIRSTV=FIS(N+1)*2.
  IF(FIS(N+1).LT.0.0.AND.8.0*FIS(N+2)+FIS(N+1).GT.0.0)
2FIRSTV=-ABS(8.*FIS(N+2))
  IF(FIS(N+1).GE.0.0) FIRSTV=-(FIS(N+1)+8.0*FIS(N+2))*2.
  DELTAV=-FIRSTV/4.0
  FIS(N+1)=FIRSTV
  FIS(N+2)=DELTAV
  TSL(N+1)=TMIN
  TSL(N+2)=(TSL(N)-TSL(N+1))/5.0
  IF(IPLT.NE.1) GO TO 10
  CALL AXIS(0.0,0.0,'THRUST IMBALANCE (LBF)',22,8.0,90.0,
2FIRSTV,DELTAV)
  GO TO 15
10 IF(IPLT.NE.2) GO TO 20
  CALL AXIS(0.0,0.0,'IMPULSE IMBALANCE (LBF-SECS)',28,0.0,90.0,
2FIRSTV,DELTAV)
  GO TO 15
20 CALL AXIS(0.0,0.0,'ABSOLUTE IMPULSE IMBALANCE (LBF-SECS)',37,8.0,
290.0,FIRSTV,DELTAV)
15 CALL AXIS(0.0,4.0,'TIME (SECS)',-11,5.0,0.0,TSL(N+1)
2,TSL(N+2))
  CALL PLOT(0.,4.,3)
  CALL LINE(TSL,FIS,N,1,0,1)
  DO 2 I=1,N
  FIS(I)=-FIS(I)
2 IF(IPLT.EQ.3) FIS(I)=FISM(I)
  CALL PLOT(0.,4.,3)
  CALL LINE(TSL,FIS,N,0,1)
  IF(IPLT.NE.1) GO TO 999
  CALL PLOT(9.0,0.0,-3)
  CALL SCALE(FDIS,8.0,N,1)
  IF(FDIS(N+1).LT.0.0.AND.8.0*FDIS(N+2)+FDIS(N+1).LE.0.0)
2FIRSTV=FDIS(N+1)*2.
  IF(FDIS(N+1).LT.0.0.AND.8.0*FDIS(N+2)+FDIS(N+1).GT.0.0)
2FIRSTV=-ABS(8.*FDIS(N+2))
  IF(FDIS(N+1).GE.0.0) FIRSTV=-(FDIS(N+1)+8.0*FDIS(N+2))*2.
  DELTAV=-FIRSTV/4.0
  FDIS(N+1)=FIRSTV
  FDIS(N+2)=DELTAV
  CALL AXIS(0.0,0.0,'THRUST IMBALANCE RATE (LBF/SEC)',31,
28.0,90.0,FIRSTV,DELTAV)
  CALL AXIS(0.0,4.0,'TIME (SECS)',-11,5.,0.0,TSL(N+1)
2,TSL(N+2))

```

Table B-1 (Cont'd)

```

CALL PLOT(0.0,4.0,3)
CALL LINE(TSL,FDIS,N,1,0,1)
DO 3 I=1,N
3 FDIS(I)=-FDIS(I)
CALL PLOT(0.0,4.0,3)
CALL LINE(TSL,FDIS,N,1,0,1)
99999 IF(IPLT.EQ.3) CALL PLOT(0.0,0.0,999)
RETURN
103 FORMAT(10X,
2'THE + OR - K2*SIGMA LIMIT ABOUT A ZERO MEAN FOR THE THRUST IMBALA
2NCE IS ',1PE11.4,' LBF',/,10X,'THE + OR - K2*SIGMA LIMIT ABOUT A Z
2ZERO MEAN FOR THE THRUST IMBALANCE RATE IS ',1PE11.4,' LBF/SEC',//)
105 FORMAT(1H1,9X,'THERE ARE ',14,' SETS OF MOTOR PAIR DATA',/,10X,'TH
2E ONE SIDED K FACTOR (K1) FOR THIS SAMPLE SIZE IS ',F7.3,/,
310X,'THE TWO SIDED K FACTOR (K2) FOR THIS SAMPLE SIZE IS ',F7.3,/
2,10X,'THE RESULTS ARE CALCULATED AT ',14,' TIME SLICES',//)
106 FORMAT(10X,'THIS TIME SLICE WAS TAKEN AT ',F7.2,' SECS')
113 FORMAT(10X,
2'THE + OR - K2*SIGMA LIMIT ABOUT A ZERO MEAN FOR THE IMPULSE IMBAL
2ANCE IS ',1PE11.4,' LBF-SECS',//)
123 FORMAT(10X,
2 'THE + K1*SIGMA LIMIT ABOUT THE MEAN FOR THE ABSOLUTE IMPULSE
2 IMBALANCE IS ',1PE11.4,' LBF-SEC')
133 FORMAT(10X,
2 'THE - K1*SIGMA LIMIT ABOUT THE MEAN FOR THE ABSOLUTE IMPULSE
2 IMBALANCE IS ',1PE11.4,' LBF-SEC',//)
132 FORMAT(10X,'THE MEAN VALUE OF THE ABSOLUTE IMPULSE IMBALANCE IS ',
21PE11.4,' LBF-SECS')
STOP
END

SUBROUTINE SIGBAR(X,XI,XI2,SIGX,BX,ICOUNT,N,IPLT)
XN=FLOAT(N)
IF(ICOUNT.GT.1) GO TO 1
XI2=0.0
XI=0.0
1 XI2=XI2+X**2
XI=XI+X
BX=XI/XN
XIS=XI**2
IF(IPLT-3) 2,3,2
2 ARG=(XI2/XN)
GO TO 4
3 ARG=(XI2/XN)-(XIS/XN**2)
IF(ARG.LE.0.0) ARG=0.0
4 SIGX=SQRT(ARG)
RETURN
END

```

Table B-1 (Cont'd)

```

SUBROUTINE INTRP1(Y,T,N,TT,DY)
DIMENSION Y(N),T(N)
N1=N-1
DY=0.0
DO 1 I=1,N1
IF(TT.GE.T(I).AND.TT.LT.T(I+1)) DY=((Y(I+1)-Y(I))/(T(I+1)-T(I)))
2*(TT-T(I))+Y(I)
IF(DY.NE.0.0. RETURN
1 CONTINUE
RETURN
END

SUBROUTINE INPUT(T,DX,NX,IPLT)
DIMENSION T(1000),DX(1000)
READ(8,100) NX
GO TO (1,2,3),IPLT
1 READ(8,200) (T(I),DX(I),D1,D2,I=1,NX)
GO TO 4
2 READ(8,200) (T(I),D1,DX(I),D2,I=1,NX)
GO TO 4
3 READ(8,200) (T(I),D1,D2,DX(I),I=1,NX)
4 RETURN
100 FORMAT(I10)
200 FURMAT(4E16.9)
END

```

## APPENDIX C

### THE SRM DESIGN ANALYSIS PROGRAM WITH OPTION PERMITTING EVALUATION OF GRAIN DEFORMATION EFFECTS

This appendix contains the instructions for the preparation and arrangement of the data cards. In addition, a complete listing of the program statements is given. The program was written for use on an IBM 370/155 computer and requires approximately 100K storage locations on that machine. The program also is designed to be used with a CALCOMP 663 drum plotter. The plotter requires one external storage device (magnetic tape or disk). However, only minor program modifications are required to eliminate the plotting capability of the program.

#### Input Data

The discussion below gives the general purpose, order and FORTRAN coding information for the input data. All of the data, except for the changes described herein, are identical to the input data described in Appendix B of Ref. 2.

Card 4A Replaces Card 4A of Ref. 2. Ignition, inert weight and grain deformation options (4X,11,9X,11,9X,11)

Col. 1-4 IGO =

5 { 0 For no ignition calculations  
1 For ignition calculations

6-14 IWO =

15 { 0 For no inert weight calculations  
1 For inert weight calculations

16-24 ISO =

25 { 0 For no grain deformation effects  
1 For grain deformation effects

Card 9 Replaces Card 9 of Ref. 2. Uniform temperature and grain deformation constants (3 cards).

Card 9A Uniform temperature card (input only if ITEMP=1) (5X,F10.0)

Col. 1-5 TGR =

6-15 Value of TGR

Card 9B Grain deformation constants (input only if ISO = 1)(7X,E12.4,  
10X,E12.4,9X,F8.5,9X,F8.5)

Col. 1-7 PMOD =  
8-19 Value of PMOD  
20-29 CMOD =  
30-41 Value of CMOD  
42-50 PMU =  
51-58 Value of PMU  
59-67 CMU =  
68-75 Value of CMU

Card 9C Grain deformation constants (input only if ISO=1)(10X,E12.4,  
10X,F8.5)

Col. 1-10 ALPTS =  
11-22 Value of ALPTS  
23-32 TAUC =  
33-40 Value of TAUC

Table C-1 represents an example set of data. Table C-2 is a sample computer printout obtained with this input data.

#### Program Listing

Table C-3 presents the complete program listing. The program has been designed to produce graphical representations of the computational results on the CALCOMP plotter. To delete the plotter compilation requirements, dummy subroutines may be substituted for the following subroutines: CSIZE, PLOT, LINE, AXIS, and SYMBOL.







Table C-2. Sample computer printout for design analysis program with grain deformation.

TABULAR VALUES FOR YT EQUAL ZERO READ IN  
 APFK= 0.0 ABSK= 0.0 ABNK= 1.2707E 03 APNK= 0.0 APNK= 0.0

VCIT= 1.9000E 03

.....

\*\*\*\*\*  
 \*\*\* EQUILIBRIUM BURNING \*\*\*  
 \*\*\*\*\*

INITIAL KEYWORDS NUMBER= 9.2779E 07

TIME= 0.0 Y= 0.0  
 RNCZ= 2.4740E-01 RHEAD= 2.7161E-01 PCNCZ= 3.8134E 02 PHEAD= 4.6915E 02  
 PTRZ= 1.0355E 00 MACZ= 4.8183E-01 SUMAR= 7.3843E 03 SG= 0.0  
 PATM= 1.4696E 01 CFVAC= 1.7266E 00 FVAC= 3.3876E 04 F= 2.7791E 04  
 ISP= 2.1675E 02 CF= 1.4333E 00 VC= 1.0827E 04 PCCT= 1.2708E 02  
 CFVOC= 1.6459E 00 ITCT= 0.0 ITVAC= 0.0 ISPVAC= 2.6658E 02  
 WP= 0.0 RADER= 1.2093E-37 EPS= 7.6640E 00 ALT= 0.0  
 CT= 8.2900E 00 APHEAD= 4.4179E 01 APNCZ= 5.9947E 01 CCF= 1.5771E 00  
 CFC= 1.3505E 00

ETHETA= 4.4762E-02 RHDS= 2.066E-03 RATP= 0.3871E-01 RATR2= 5.9605E-02 XETH= 1.0000E 00 YETA= 0.0

TABULAR VALUES FOR YT= 1.000 READ IN  
 APFK= 0.0 ABSK= 0.0 ABNK= 1.3270E 03 APNK= 0.0 APNK= 0.0

.....

TIME= 40.17 Y= 11.60  
 RNCZ= 0.0 RHEAD= 0.0 PCNCZ= 9.1370E-03 PHEAD= 9.137 E-03  
 PTRZ= 1.2803E 01 MACZ= 4.6514E-02 SUMAR= 8.9545E 03 SG= 0.0  
 PATM= 1.4696E 01 CFVAC= 1.7227E 00 FVAC= 8.6599E-01 F= 0.0  
 ISP= 0.0 CF= -1.1468E 04 VC= 1.3780E 05 PCCT= 3.2667E-03  
 CFVOC= 1.6357E 00 ITCT= 1.9446E 06 ITVAC= 2.1643E 06 ISPVAC= 2.651 E 02  
 WP= 8.2200E 03 RADER= 3.7500E-03 EPS= 7.1436E 00 ALT= 0.0  
 CT= 8.5867E 00 APHEAD= 7.2638E 02 APNCZ= 7.4119E 02 CCF= 1.5631E 00  
 CFC= -1.1489E 04

ETHETA= 2.0545E-03 RHDS= 2.0175E-03 RATP= 9.9997E-01 RATR2= 9.9178E-01 XETH= 1.0000E 00 YETA= 1.1374E 01

WP1= 8.2200E 03  
 WP2= 8.2146E 03  
 WP= 8.2200E 03  
 PPMAR= 6.5751E 02  
 ISP= 2.3657E 02  
 ISPVAC= 2.6574E 02  
 ITCT= 1.9446E 06  
 ITVAC= 2.1543E 06  
 F AV= 4.8407E 04  
 FVACAV= 5.4375E 04  
 PCAV= 5.9226E 02  
 VCI= 1.0827E 04  
 VCF= 1.3780E 05  
 LAMBDA= 9.2143E-01

ORIGINAL PAGE IS  
 OF POOR QUALITY

TABLE C-3

```

C *****
C *
C *          SRM DESIGN AND PERFORMANCE ANALYSIS          *
C *          PREPARED AT AUBURN UNIVERSITY                *
C *          UNDER MOD. NO. 14 TO COOPERATIVE AGREEMENT WITH *
C *          NASA MARSHALL SPACE FLIGHT CENTER            *
C *
C *
C *          BY
C *          R. H. SFORZINI AND W. A. FOSTER, JR.         *
C *          AEROSPACE ENGINEERING DEPARTMENT           *
C *          SEPTEMBER 1975                               *
C *
C *
C *          MODIFIED FOR GRAIN DEFORMATION INTERNAL BALLISTIC EFFECTS *
C *
C *          BY
C *          R. H. SFORZINI AND DAVID F. SMITH            *
C *          AEROSPACE ENGINEERING DEPARTMENT           *
C *          SEPTEMBER 1976                               *
C *****
C
C

```

```

INTEGER GRAIN
REAL MGEN,MDIS,MNOZ,MNI,JROCK,N,L,ME1,ME,ISP,ITOT,MU,MASS,ISPVAC
REAL N1,N2,NSEG,K1,K2,KEH,KEN,NS,LCC,LTAP
REAL M2,MDBAR,ISP2,ITVAC,KA,KB,LAMBDA,ITV
COMMON/CONST1/ZW,AE,AT,THETA,ALFAN
COMMON/CONST2/CAPGAM,ME,BUTE,ZETA,F,TB,HB,GAME,CGAME,TDPE,ZAPE
COMMON/CONST3/S,NS,GRAIN,NTABY,NCARD
COMMON/CONST4/DELDI,DO,ZO,DI
COMMON/VARIA1/Y,T,DELY,DELTAT,PONNOZ,PHEAD,RNOZ,RHEAD,SUMAB,PHMAX
COMMON/VARIA2/ABPORT,ABSLOT,ABNOZ,APHEAD,APNOZ,DADY,ABP2,ABN2,ABS2
COMMON/VARIA3/ITOT,ITVAC,JROCK,ISP,ISPVAC,MDIS,MNOZ,SG,SUMMT
COMMON/VARIA4/RNT,RHT,SUMZ,R1,R2,R3,RHAVE,RNAVE,RBAR,YB,KOUNT,TL
COMMON/VARIA5/ABMAIN,ABTO,SUMDY,VC1,ABTT,PTRAN
COMMON/VARIA6/WP2,CF,WP,RADER,EPS,VC,FLAST,TLAST,DT,PONTDT,WPI
COMMON/VARIA7/TIMX,FV,ITV,NX
COMMON/VARIA8/YDI
COMMON/VARIA9/EIETHETA,RHOS,RATP,PMCD,CMCD,PMU,CMU,ALPTS,RATR2
COMMON/VARIA10/YETA,XETH,ISO
COMMON/IGN1/KA,KB,UFS,RHO,L,PMIG,TI1,TI2,CSIG,Q1,N1,Q2,N2
COMMON/IGN2/ALPHA,BETA,PBIG,KRIG,DELTAIG,X,TOP,ZAP
COMMON/PLOTT/NUMPLI(16),IPO,NDUM,IPT,IGP
DIMENSION YTAB(30),ITAB(30)
DATA PI,G/3.14159,32.1725/
CALL GSIZE (416.,11.0,1100)
CALL PLOT(6.25,2.,-3)
IOP=0
READ(5,500) NRUNS

```

Table C-3 (Cont'd)

```

C *****
C * READ IN THE NUMBER OF CONFIGURATIONS TO BE TESTED *
C *****
      NTABY=0
      NCARD=0
      DO 901 I=1, NRUNS
      NEXTR=NTABY-NCARD
      IF(NEXTR)1901,1901,1902
1902 READ(5,1903) (D1,D2,D3,D4,D5,D6,IEX=1,NEXTR)
1901 WRITE(6,602) I
      READ(5,11111) NTAB,NTABY
      READ(5,499) SUNDY,ANS,ZH,Y,T,DELTAT,RNOZ,RHEAD,SUMAB,PHMAX,SUM2,IT
      10T,RHT,RNT,R1,R2,R3,RHAVE,RNAVE,RBAR,ITVAC,SUMMT,PONTOT
C *****
C * SET INITIAL VALUES OF SELECTED VARIABLES EQUAL TO ZERO *
C * ***NOTE*** THESE VALUES MUST BE ZEROED AT THE BEGINNING OF *
C * EACH CONFIGURATION RUN *
C *****
      READ (5,491) IGO,IWO,ISO
      READ(5,493) IPO,(NUMPLT(JJ),JJ=1,16),ITEMP
C *****
C * READ IN THE USER'S OPTIONS *
C * *
C * VALUES FOR IGO ARE *
C * 0 FOR NO IGNITION TRANSIENT CALCULATIONS *
C * 1 FOR IGNITION TRANSIENT CALCULATIONS *
C * VALUES FOR IWO ARE *
C * 0 FOR NO INERT WEIGHT CALCULATIONS *
C * 1 FOR INERT WEIGHT CALCULATIONS *
C * VALUES FOR ISO ARE *
C * 0 FOR NO GRAIN DEFORMATION EFFECTS *
C * 1 FOR GRAIN DEFORMATION BALLISTIC EFFECTS *
C * ***NOTE*** IF GRAIN=2(ALL STAR GRAIN), ISO MUST BE 0 *
C * VALUES FOR IPO ARE *
C * 0 FOR NO PLOTS *
C * 1 FOR PLOTS OF EQUILIBRIUM BURNING ONLY *
C * 2 FOR PLOTS OF IGNITION TRANSIENT ONLY *
C * 3 FOR PLOTS OF BOTH IGNITION TRANSIENT AND *
C * EQUILIBRIUM BURNING *
C * VALUES FOR NUMPLT(JJ) ARE (NOT REQUIRED FOR IPO=0) *
C * 0 IF SPECIFIC PLOT IS NOT DESIRED *
C * 1 IF SPECIFIC PLOT IS DESIRED *
C * ORDER OF SPECIFICATION OF NUMPLT(JJ) IS *
C * 1 PHEAD VS TIME *
C * 2 PONOZ VS TIME *
C * 3 PHEAD AND PONOZ VS TIME *
C * 4 RHEAD VS TIME *
C * 5 RNLZ VS TIME *

```

Table C-3 (Cont'd)

```

C *          6 RHEAD AND RNCZ VS TIME *
1000 CONTINUE
C *          7 SUMAB VS TIME *
C *          8 SG VS TIME *
C *          9 SUMAB AND SG VS TIME *
C *         10 F VS TIME *
C *         11 FVAC VS TIME *
C *         12 F AND FVAC VS TIME *
C *         13 VC VS TIME *
C *         14 SUMAB VS YB *
C *         15 SG VS YB *
C *         16 SUMAB AND SG VS YB *
C *   VALUES FOR ITEMP ARE *
C *       0 FOR TEMPERATURE GRADIENT *
C *       1 FOR UNIFORM TEMPERATURE *
C *   NTAB IS THE NUMBER OF Y STATIONS FOR WHICH TABULAR *
C *   TEMPERATURES ARE SPECIFIED *
C *   NTABY IS THE NUMBER OF Y STATIONS FOR WHICH TABULAR AREAS *
C *   ARE SPECIFIED *
C *****
C > WRITE (6,492) IGO,IWO,ISO
  WRITE(6,494) IPO,(NUMPLT(JJ),JJ=1,16),ITEMP
  WRITE(6,11112) NTAB,NTABY
  READ(5,501) RN2N1,RHO,A1,N1,ALPHA,BETA,MU,CSTAR
C *****
C *   READ IN BASIC PROPELLANT CHARACTERISTICS *
C * *
C****  MODIFICATION MADE 5/3/76
C *   RN2N1 IS THE RATIO OF THE NOMINAL VALUES OF THE BURNING RATE *
C *   EXPONENTS ABOVE AND BELOW THE TRANSITION PRESSURE *
C *   RHO IS THE DENSITY OF THE PROPELLANT IN LBM/IN**3 *
C *   A1 IS THE BURNING RATE COEFFICIENT BELOW THE TRANSITION *
C *   PRESSURE *
C *   N1 IS THE BURNING RATE EXPONENT BELOW THE TRANSITION PRESSURE *
C *   ALPHA AND BETA ARE THE CONSTANTS IN THE EROSION BURNING *
C *   RELATION OF ROBILLARD AND LENOIR *
C *   MU IS THE VISCOSITY OF THE PROPELLANT GASES *
C *   CSTAR IS THE CHARACTERISTIC EXHAUST VELOCITY IN FT/SEC *
C *****
  WRITE(6,603) RHO,A1,N1,ALPHA,BETA,MU,CSTAR,RN2N1
  RHO=RHO/32.174
  READ(5,502) L,TAU,DE,DTI,THETA,ALFAN,LTAP,XT,ZO,CSTART,PTRAN
C *****
C *   READ IN BASIC MOTOR DIMENSIONS *
C * *
C *   L IS THE TOTAL LENGTH OF THE GRAIN IN INCHES *
C *   TAU IS THE AVERAGE WEB THICKNESS OF THE CONTROLLING GRAIN *
C *   LENGTH IN INCHES *

```

Table C-3 (Cont'd)

```

C *   DE IS THE DIAMETER OF THE NOZZLE EXIT IN INCHES *
C *   DTI IS THE INITIAL DIAMETER OF THE NOZZLE THROAT IN INCHES *
C *   THETA IS THE CANT ANGLE OF THE NOZZLE WITH RESPECT TO THE *
C *   MOTOR AXIS IN DEGREES *
C *   ALFAN IS THE EXIT HALF ANGLE OF THE NOZZLE IN DEGREES *
C *   LTAP IS THE LENGTH OF THE GRAIN AT THE NOZZLE END HAVING *
C *   ADDITIONAL TAPER NOT REPRESENTED BY ZO IN INCHES *
C *   XT IS THE DIFFERENCE IN WEB THICKNESS ASSOCIATED WITH LTAP *
C *   ZO IS THE INITIAL DIFFERENCE BETWEEN WEB THICKNESSES AT THE *
C *   HEAD AND AFT ENDS OF THE CONTROLLING GRAIN LENGTH *
C *   CSTART IS THE TEMPERATURE SENSITIVITY OF CSTAR *
C *   AT CONSTANT PRESSURE *
C *   PTRAN IS THE PRESSURE ABOVE WHICH THE BURNING RATE EXPONENT *
C *   CHANGES *
C *****
N2=N1*RN2N1
A2=A1*PTRAN**(N1-N2)
WRITE(6,604) L,TAU,DE,DTI,THETA,ALFAN,LTAP,XT,ZO,CSTART,PTRAN,N2
THETA=THETA/57.29578
ALFAN=ALFAN/57.29578
READ(5,503) DELTAY,XOUT,DPOUT,ZETAF,TB,HB,GAM,ERREF,PREF,
1DTREF,PIPK,TREF,GAME,PEXT
IF(ITEMP.NE.0) GO TO 10000
READ(5,700) (YTAB(ITAB),TTAB(ITAB),ITAB=1,NTAB)
WRITE(6,701) (YTAB(ITAB),TTAB(ITAB),ITAB=1,NTAB)
GO TO 10004
10000 READ(5,10001) TGR
C *****
C *   READ IN BASIC PERFORMANCE CONSTANTS *
C * *
C *   DELTAY IS THE DESIRED BURN INCREMENT DURING TAILOFF IN INCHES *
C *   XOUT IS THE DISTANCE BURNED IN INCHES AT WHICH THE PROPELLANT *
C *   BREAKS UP *
C *   DPOUT IS THE DEPRESSURIZATION RATE IN LB/IN**3 AT WHICH THE *
C *   PROPELLANT IS EXTINGUISHED *
C *   ZETAF IS THE THRUST LOSS COEFFICIENT *
C *   TB IS THE ESTIMATED BURN TIME IN SECONDS *
C *   HB IS THE ESTIMATED BURNOUT ALTITUDE IN FEET *
C *   A2 IS THE BURNING RATE COEFFICIENT ABOVE THE TRANSITION *
C *   PRESSURE *
C *   GAM IS THE RATIO OF SPECIFIC HEATS FOR THE PROPELLANT GASES *
C *   ERREF IS THE REFERENCE THROAT EROSION RATE IN IN/SEC *
C *   TGR IS THE TEMPERATURE OF THE GRAIN IN DEGREES F *
C *   PREF IS THE REFERENCE NOZZLE STAGNATION PRESSURE IN LB/IN**2 *
C *   DTREF IS THE REFERENCE THROAT DIAMETER IN INCHES *
C *   PIPK IS THE TEMPERATURE SENSITIVITY COEFFICIENT OF PRESSURE *
C *   AT CONSTANT K PER DEGREE F *
C *   TREF IS THE DESIGN TEMPERATURE OF THE GRAIN IN DEGREES F *

```

Table C-3 (Cont'd)

```

C *      GAME IS THE EFFECTIVE GAMMA AT THE NOZZLE EXIT PLANE      *
C *      PEXT IS THE PRESSURE AT WHICH THE PROPELLANT EXTINGUISHES IN *
C *      LB/IN**2                                                  *
C *****
10004 WRITE(6,606)DELTAY,XOUT,DPOUT,ZETA,F,TB,HB,GAM,ERREF,PREF,DTREF
      1,PIPK,A2,TREF,GAME,PEXT
      IF(ITEMP.NE.0) WRITE(6,10002) TGR
      NCARD=0
      NDUM=0
      IPT=0
      MN1=.85
      Z=Z0
      S=0.0
      NS=0.0
      KOUNT=0
      ABMAIN=0.0
      ABTO=0.0
      ABTT=0.
      TLAST=1.
      DELY=DELTAY
      ▶ ETHETA=0.
      ▶ PMU=0.5
      ▶ ALPTS=0.
      ▶ YETA=0.
      ▶ DYETA=0.
      ▶ PMOD=10000.
      ▶ YE=0.0
      ▶ XETH=0.
      TOP=GAM+1.
      BOT=GAM-1.
      ZAP=TOP/(2.*BOT)
      CAPGAM=SQRT(GAM)*(2./TOP)**ZAP
      TOPE=GAME+1.
      BOTE=GAME-1.
      ZAPE=TOPE/(2.*BOTE)
      CGAME=SQRT(GAME)*(2./TOPE)**ZAPE
      AE=P[*DE*DE/4.
      CSTART=CSTAR
      1 IF(XT.LE.0.0) T1=0.0
      IF(ITEMP.NE.0) GO TO 10003
      CALL INTRP1(TTAB,YTAB,NTAB,Y,TGR,0)
      C****      MODIFICATION MADE 1/7/76
      Q1=A1*EXP(PIPK*(1.-N1)*(TGR-TREF))
      Q2=A2*EXP(PIPK*(1.-N2)*(TGR-TREF))
      WRITE(6,701) Y,TGR
10003 CSTAR=CSTAR*(1.+CSTART*(TGR-TREF))
      C****      MODIFICATION MADE 1/7/76
      IF(ITEMP)10005,10006,10005

```

Table C-3 (Cont'd)

```

10005 Q1=A1*EXP(PIPK*(1.-N1)*(TGR-TREF))
      Q2=A2*EXP(PIPK*(1.-N2)*(TGR-TREF))
10006 IF(XT.LE.0.0) GO TO 40
      TL=(Y-TAU+XT+Z/2.)*LTAP/XT
      IF(TL.LE.0.0) TL=0.0
      IF(TL.GE.LTAP) TL=LTAP
40 IF (T) 41,41,42
41 DT=DTI
   GO TO 43
42 RADER=ERREF*((PONOZ/PREF)**0.8)*[(DTREF/DT)**0.2]
   DT=DT+(2.0*RADER*DELTAT)
43 AT=PI*DT*DT/4.
   EPS=AE/AT
   IF(IGO.EQ.0.OR.Y.GT.0.0) GO TO 900
   READ(5,97) KA,KB,UFS,CSIG,PMIG,TI1,TI2,RRIG,DELTIG,PBIG
C *****
C *   READ IN VALUES REQUIRED FOR IGNITION CALCULATIONS *
C *   ***NOTE*** NOT REQUIRED IF IGO=0 *
C * * * * *
C *   KA AND KB DEFINE THE CHARACTERISTIC VELOCITY IN FT/SEC *
C *   CSTR = KA + KB * PRESSURE *
C *   UFS IS THE FLAME-SPREADING SPEED IN IN/SEC *
C *   CSIG IS THE CHARACTERISTIC VELOCITY OF THE IGNITER IN FT/SEC *
C *   PMIG IS THE MAXIMUM IGNITER PRESSURE IN LBS/IN**2 *
C *   TI1 IS THE TIME OF MAXIMUM IGNITER PRESSURE IN SECONDS *
C *   TI2 IS THE TIME (IN SECONDS) FOR THE IGNITER PRESSURE TO *
C *   DROP TO 10 PER CENT OF MAXIMUM VALUE (PMIG) *
C *   RRIG IS THE AVERAGE REGRESSION RATE OF THE FIRST HALF OF THE *
C *   IGNITER PRESSURE TIME TRACE IN LBS/IN**2/SEC *
C *   DELTIG IS THE TIME INCREMENT FOR IGNITION TRANSIENT *
C *   CALCULATIONS IN SECONDS *
C *   PBIG IS THE BLOWOUT PRESSURE OF THE MAIN MOTOR BLOWOUT PLUG *
C *   IN LBS/IN**2 *
C *****
      WRITE(6,842) KA,KB,UFS,CSIG,PMIG,TI1,TI2,RRIG,DELTIG,PBIG
900 IF(IWO.EQ.0.OR.Y.GT.0.0) GO TO 832
      READ(5,600) DTEMP,SIGMAP,SIGMAS,X1,X2,SYCNOM,DCC,PSIC,DELCL,LC
      IC,NSEG,HCN,SYNNOM,PSIS,PSIA,K1,K2,PSIINS,DELIINS,KEH,KEN,DLINER,TAU
      2L,WA
C *****
C *   READ IN BASIC PROPERTIES REQUIRED FOR WEIGHT CALCULATIONS *
C *   ***NOTE*** NOT REQUIRED IF IWO=0 *
C * * * * *
C *   DTEMP IS THE MAX EXPECTED INCREASE IN TEMPERATURE ABOVE *
C *   CONDITIONS UNDER WHICH MAIN TRACE WAS CALCULATED IN *
C *   DEGREES FAHRENHEIT *
C *   SIGMAP IS THE VARIATION IN PHMAX *
C *   SIGMAS IS THE VARIATION IN CASE MATERIAL YIELD STRENGTH *

```



Table C-3 (Cont'd)

```

C * X1 IS THE NUMBER OF STANDARD DEVIATIONS IN PHMAX TO BE USED *
C * AS A BASIS FOR DESIGN *
C * X2 IS THE NUMBER OF STANDARD DEVIATIONS IN SY TO BE USED AS *
C * A BASIS FOR DESIGN *
C * SYCNOM IS THE NOMINAL YIELD STRENGTH OF THE CASE MATERIAL *
C * IN LBS/INCH *
C * DCC IS THE ESTIMATED MEAN DIAMETER OF THE CASE IN INCHES *
C * PSIC IS THE SAFETY FACTOR ON THE CASE THICKNESS *
C * DELC IS THE SPECIFIC WEIGHT OF THE CASE MATERIAL IN LBS/IN**3 *
C * LCC IS THE LENGTH OF THE CYLINDRICAL PORTION OF THE CASE *
C * INCLUDING FORWARD AND AFT SEGMENTS IN INCHES *
C * NSEG IS THE NUMBER OF CASE SEGMENTS *
C * HCN IS THE AXIAL LENGTH OF THE NOZZLE CLOSURE IN INCHES *
C * SYNNOH IS THE NOMINAL YIELD STRENGTH OF THE NOZZLE MATERIAL *
C * IN LBS/INCH *
C * PSIS IS THE SAFETY FACTOR ON THE NOZZLE STRUCTURAL MATERIAL *
C * PSIA IS THE SAFETY FACTOR ON THE NOZZLE ABLATIVE MATERIAL *
C * K1 AND K2 ARE EMPIRICAL CONSTANTS IN THE NOZZLE WT. EQUATION *
C * PSIINS IS THE SAFETY FACTOR ON NOZZLE INSULATION *
C * DELINS IS THE SPECIFIC WEIGHT OF THE INSULATION IN LBS/IN**3 *
001 CONTINUE
C * KEH IS THE EROSION RATE OF INSULATION TAKEN CONSTANT *
C * EVERYWHERE EXCEPT AT THE NOZZLE CLOSURE IN IN/SEC *
C * KEN IS THE EROSION RATE OF INSULATION AT THE NOZZLE CLOSURE *
C * IN IN/SEC *
C * DLINER IS THE SPECIFIC WEIGHT OF THE LINER IN LBS/IN**3 *
C * TAUL IS THE THICKNESS OF THE LINER IN INCHES *
C * WA IS ANY ADDITIONAL WEIGHT NOT CONSIDERED ELSEWHERE IN LBS *
C *****
WRITE(6,610) DTEMP,SIGMAP,SIGMAS,X1,X2,SYCNOM,DCC,PSIC,DELC,L
1CC,NSEG,HCN,SYNNOH,PSIS,PSIA,K1,K2,PSIINS,DELINS,KEH,KEN,DLINER,TA
2UL,WA
832 CONTINUE
▶ IF(ISO.EQ.0 .OR. Y.GT. 0.0) GO TO 80
▶ READ(5,505) PMOD,CMOD,PMU,CMU,ALPTS,TAUC
▶C *****
▶C * READ IN THE CONSTANTS FOR GRAIN DEFORMATION *
▶C * ***NOTE*** NOT REQUIRED IF ISO=0 *
▶C * PMOD IS THE ELASTIC MODULUS OF THE PROPELLANT IN PSIA (AT THE *
▶C * TEMPERATURE TGR) *
▶C * CMOD IS THE ELASTIC MODULUS OF THE CASE (@ THE BULK TEMPERATURE *
▶C * OF THE GRAIN) IN LBS/IN**2 *
▶C * PMU IS POISSON'S RATIO FOR THE PROPELLANT (@ THE BULK TEMPERATURE *
▶C * OF THE GRAIN) *
▶C * CMU IS POISSON'S RATIO FOR THE CASE (@ THE BULK TEMPERATURE OF *
▶C * THE GRAIN) *
▶C * ALPTS IS THE LINEAR COEFFICIENT OF THERMAL EXPANSION OF THE *
▶C * PROPELLANT IN IN/IN *

```

Table C-3 (Cont'd)

```

>C * TAUC IS THE CASE THICKNESS IN INCHES *
>C *****
> WRITE(6,799) PMOD, CMOD, PMU, CMU, ALPTS, TALC
> 80 CONTINUE
    CALL AREAS
    IF(Y.LE.0.0) VC=VCI
    IF(ABS(ZM).GT.0.0) GO TO 20
    IF(SUMAB.LE.0.0) GO TO 31
    X=(ABPORT+ABSLOT)/SUMAB
90  VNOZ=AT*X/APNOZ*(2.*(1.+BOT/2.*MNI*MNI)/TOP)**ZAP
    IF(ABS(MNOZ-MNI).LE.0.002) GO TO 2
    MNI=MNOZ
    GO TO 90
    2 VNOZ=GAM*CSTAR*MNOZ*SQRT(((2./TOP)**(TOP/BOT))/(1.+BOT/2.*MNOZ*MNOZ
    1Z))
    PRAT=(1.+BOT/2.*MNOZ*MNOZ)**(-GAM/BOT)
    JROCK=AT/APNOZ
    SUMYA=DELY*(ABP2+ABN2+ABS2)
    IF(Y.EQ.0.0) SUMYA=0.0
    VC=VC+SUMYA
> IF(ISO.EQ.0) GO TO 9
> RATR=2.*I/DO + DI/DO
> RATR2=RATR**2
> RATP=(2.*RATR*(1.-PMU**2)/(1.-RATR2))/(PMOD*DO*(1.-PMU*CMU)/(CMOD
> 1*TAUC*2.)-PMU*(1.+PMU)+(1.-PMU**2)*(1.+RATR2)/(1.-RATR2))
> 9 CONTINUE
    IF(Y.GT.0.0) GO TO 11
C**** MODIFICATION MADE 1/7/76
    PONOZ=(Q1*RHO*CSTAR*SUMAB/AT)**(1./(1.-N1))*(1.+(CAPGAM*JROCK)**2/
    12.)*(N1/(1.-N1))
    IF(PONOZ.GT.PTRAN)PONOZ=(Q2*RHO*CSTAR*SUMAB/AT)**(1./(1.-N2))*(1.+
    1(CAPGAM*JROCK)**2/2.)*(N2/(1.-N2))
    MDIS=AT*PONOZ/CSTAR
    P2=PONOZ
    PONOZ2=PONOZ
    PNOZ=PRAT*PONOZ
    P4=2.*MDIS*VNOZ/(APHEAD+APNOZ)+PNOZ
    IF(GRAIN.EQ.3) P4=MDIS * VNOZ/APNOZ + PNCZ
5 PNOZ=PRAT*PONOZ
    PHEAD=2.*MDIS*VNOZ/(APHEAD+APNOZ)+PNOZ
    IF(GRAIN.EQ.3) PHEAD=MDIS * VNOZ/APNOZ + PNOZ
    IF(PHEAD.LE.PTRAN)RHEAD=Q1*PHEAD**N1
    IF(PHEAD.GT.PTRAN)RHEAD=Q2*PHEAD**N2
    ZIT=MDIS*X/APNOZ
    RN1=RHEAD
    PHEAD2=PHEAD
C**** MODIFICATION MADE 1/9/76
3 IF(ALPHA) 131,132,131

```

C-2

Table C-3 (Cont'd)

```

132 IF (PNOZ.LE.PTRAN) RNOZ=Q1*PNOZ**N1
    IF (PNOZ.GT.PTRAN) RNOZ=Q2*PNOZ**N2
    GO TO 4
131 IF (PNOZ.LE.PTRAN) RNOZ=RN1-((RN1-XQ*PNOZ**XN-ALPHA*ZIT**.8/(L**.2*E
    IXP(BETA*RN1*RHO/ZIT)))/(1.+ALPHA*ZIT**.8*BETA*RHO/ZIT/(L**.2*EXP(B
    ZETA*RN1*RHO/ZIT))))
    IF (PNOZ.GT.PTRAN) RNOZ=RN1-((RN1-Q2*PNOZ**N2-ALPHA*ZIT**.8/(L**.2*E
    IXP(BETA*RN1*RHO/ZIT)))/(1.+ALPHA*ZIT**.8*BETA*RHO/ZIT/(L**.2*EXP(B
    ZETA*RN1*RHO/ZIT))))
    IF (ABS(RN1-RNOZ).LE.0.002) GO TO 4
    RN1=RNOZ
    GO TO 3
4 AVE1=(RHEAD+RNOZ)/2.
  IF (ISO.EQ.1) GO TO 404
  RHO5=RHO
  ABPOR6=ABPORT
404 CONTINUE
  IF (Y.GT.0.0) GO TO 7
  RN2=RNOZ
  RH2=RHEAD
  PONJ=PONZ
  DPCDY=0.0
  AVE2=AVE1
7 RNAVE=(RNOZ+RN2)/2.
  RHAVE=(RHEAD+RH2)/2.
  IF (ISO.EQ.0) GO TO 8
401 CONTINUE
  ETHETA=(PONZ/PMOD)*(RATP*(2.*(PMU**2-1.)/(1.-RATR2)+PMU*CMU*PMOD*
  IDO/(2.*CMOD*TAUC))+(1.+RATR2+PMU*(1.-RATR2-2.*RATR2*PMU))/(1.-RATR
  22))
  RHO5=RHO/(((1.+ALPTS*(TGR-TREF))*(1.-PONZ*(1.-2.*PMU)/PMOD)))**3
  IF (KOUNT.GE.1) GO TO 405
  ABPOR6=ABPORT*(1.+ETHETA*XETH)
8 CONTINUE
  IF (PONZ.LE.PTRAN) MGEN=RHO5*(AVE1*(ABPOR6+ABSLOT)+Q1*PONZ**N1*ABN
  10Z)
  IF (PONZ.GT.PTRAN) MGEN=RHO5*(AVE1*(ABPOR6+ABSLOT)+Q2*PONZ**N2*ABN
  10Z)
  DRDY=(AVE1-AVE2)/DELY
  RBAR=(AVE1+AVE2)/2.
  GMAX=1.002*MDIS
  GMIN=0.9998*MDIS
  IF (Y.GT.0.0) GO TO 12
  GMAX=1.001*MDIS
  GMIN=0.999*MDIS
  IF (MGEN.GE.GMIN.AND.MGEN.LE.GMAX) GO TO 6
  MDIS=MGEN
  PONZ=MDIS*CSTAR/AT

```

Table C-3 (Cont'd)

```

GO TO 5
6 RE=2.*MDIS*X*L/((APNOZ+APHEAD)*MU)
  IF(IGO.NE.0.AND.Y.LE.0.0) CALL IGNITN
  IF(Y.LE.0.0) WRITE(6,101) RE
  PONJ=PONOZ
  CALL OUTPUT
10 IF(Y.LE..05*TAU) GO TO 16
  SINK1=VC/(CAPGAM*CSTAR)**2*RBAR*DPCDY/12.
  MASS=.01*MDIS
  ANS4=Y+10.0*DELTAY
  IF(KOUNT.GT.0) GO TO 16
  IF(ABS(SINK1).LE.MASS.AND.ANS4.LE.ANS-XT) GO TO 18
  GO TO 16
18 DELY=10.*DELTAY
  GO TO 55
16 DELY=DELTAY
55 YLED=Y
  Y=Y+DELY
  ANS=TAU-ABS(Z/2.)
C**** MODIFICATION MADE 1/9/76
  IF(Y.GE.ANS.AND.KOUNT.EQ.0) DELY=ANS-YLED+0.05*DELTAY
  IF(Y.GE.ANS.AND.KOUNT.EQ.0) Y=ANS+0.05*DELTAY
  DELTAT=2.*DELY/(RHAVE+RSAVE)
▶ DELTAT=DELTAT*((1.-PONOZ*(1.-2.*PMU)/PMOD)*(1.+ALPTS*(TGR-TREF)))*
▶ 1*3/(1.+ETHETA)
▶ DYETA=DELY*((1.+ALPTS*(TGR-TREF))*(1.-PONOZ*(1.-2.*PMU)/PMOD))**3/
▶ 1(1.+ETHETA)
▶ YETA=YETA+DYETA
▶ IF(ISO.EQ.0) YETA=Y
  SUM2=SUMAB
  RN2=RNOZ
  RH2=RHEAD
  AVE2=AVE1
  GO TO 1
11 MDIS=AT*PONOZ/CSTAR
  GO TO 5
12 DPCDY=(PHEAD2+PONOZ2)/(RSAVE+RHAVE)*DRDY+(PHEAD2+PONOZ2)/((ABP2+AB
  IN2+ABS2)*2.)*DAUY
  IF(ABS(DPCDY).GE.DPOUT.OR.Y.GE.XOUT) GO TO 25
  SINK1=VC/(CAPGAM*CSTAR)**2*RBAR*DPCDY/12.+(PHEAD2+PONOZ2)/2.*(RSAVE
  LE+RHAVE)/2.*(ABP2+ABN2+ABS2)/(12.*(CSTAR*CAPGAM)**2)
  STUFF=MGEN-SINK1
  MDIS=STUFF
  PONOZ=MDIS*CSTAR/AT
  IF(Y.GE.0.9*(ANS-XT))PONOZ=PONJ+DPCDY*DELY
  IF(STUFF.GE.GMIN.AND.STUFF.LE.GMAX) GO TO 14
  GO TO 5
14 P1=PONOZ

```

Table C-3 (Cont'd)

```

PONJ=PONQZ
PONOZ2=(P1+P2)/2.
P2=FONQZ
P3=PHEAD
PHEAD2=(P3+P4)/2.
P4=PHEAD
MDIS=AT*PONOZ/CSTAR
DELTAT=2.*DELY/(RHAVE+RNAVE)
▶ DELTAT=DELTAT*((1.-PONOZ*(1.-2.*PMU)/PMOD)*(1.+ALPTS*(TGR-TREF)))*
▶ 1*3/(1.+ETHETA)
Z=Z+DELTAT*(RNAVE-RHAVE)
T=T+DELTAT
IF(Y.LT.ANS) CALL OUTPUT
IF(Y.LT.ANS) GO TO 10
ZW=Z
SUMBA=SUMAB
P1=PONOZ
RH2=RHEAD
RN2=RNOZ
RAVE=AVE1
ABMAIN=SUMAB
ABTO=0.0
WRITE(6,51)
20 ANS2=TAU+ABS(ZW/2.)
KOUNT=KOUNT+1
IF(KOUNT.EQ.1) CALL OUTPUT
IF(KOUNT.EQ.1) GO TO 10
DELYW=DELTAY
DY2=DELYW
IF(ZW) 32,32,33
32 IF(Y.LT.ANS2.AND.ABS(ZW).GT.DY2) GO TO 211
SUMAB=ABMAIN+ABTT
GO TO 31
211 SUMDY=SUMDY+DELYW
SUMAB=(1.+SUMDY/ZW-DELYW/(2.*ZW))*ABTO-(SUMDY/ZW-DELYW/(2.*ZW))*AB
MAIN+ABTT
GO TO 31
33 IF(Y.LT.ANS2.AND.ZW.GT.DY2) GO TO 21
SUMAB=ABTO+ABTT
GO TO 31
21 SUMDY=SUMDY+DELYW
SUMAB=(1.-SUMDY/ZW+DELYW/(2.*ZW))*ABMAIN+(SUMDY/ZW-DELYW/(2.*ZW))*
1ABTO+ABTT
31 IF(SUMAB.LE.0.0) PONQZ=PONOZ/2.
IF(SUMAB.LE.0.0) GO TO 25
MDIS=AT*PONQZ/CSTAR
ABAVE=(SUMAB+SUMBA)/2.
SUMYA=DELY*ABAVE

```

Table C-3 (Cont'd)

```

VC=VC+SUMYA
DADY=(SUMAB-SUMBA)/DELY
PBAR=(P1+PONOZ)/2.
SUMBA=SUMAB
22 IF(PBAR.LE.PTRAN)DPCDY=PBAR*DADY/(1.-N1)/ABAVE
IF(PBAR.GT.PTRAN)DPCDY=PBAR*DADY/(1.-N2)/ABAVE
PONOZ=PONJ+DPCDY*DELY
IF(PONOZ.LE.0.0) PONOZ=0.0
IF(PONOZ.LE.PEXT) GO TO 25
C**** MODIFICATION MADE 5/3/76
IF(PONOZ.LE.PTRAN) Q2=Q1
IF(PONOZ.LE.PTRAN) N2=N1
RNOZ=Q2*PONOZ**N2
C**** MODIFICATION MADE 1/9/76
RHEAD=RNOZ
RBAR=(RHEAD+RAVE)/2.
▶ IF(ISO.EQ.0) GO TO 405
▶ GO TO 401
▶ 405 CONTINUE
▶ MGEN=RHO5*(RNOZ+RHEAD)/2.*SUMAB
▶ IF(ISO.EQ.1) MGEN1=MGEN*(1.+ETHETA*XETH)
▶ IF(ISO.EQ.0) MGEN1=MGEN
GMAX=1.0002*MDIS
GMIN=0.9998*MDIS
SINK1=VC/(CAPGAM*CSTAR)**2*RBAR*DPCDY/12.+PBAR*ABAVE/(12.*(CAPGAM*
1CSTAR)**2)*RBAR
STUFF=MGEN1-SINK1
MDIS=STUFF
IF(STUFF.GE.GMIN.AND.STUFF.LE.GMAX) GO TO 23
PBAR=(P1+PONOZ)/2.
GO TO 22
23 RHAVE=(RH2+RHEAD)/2.
RSAVE=(RN2+RNOZ)/2.
RH2=RHEAD
RN2=RNOZ
PHEAD=PONOZ
RAVE=RHEAD
P1=PONOZ
PONJ=PONOZ
MDIS=AT*PONOZ/CSTAR
IF(ABS(DPCDY).GE.DPOUT) GO TO 25
IF(Y.GE.XOUT) GO TO 25
DELTAT=2.*DELY/(RHAVE+RSAVE)
▶ DELTAT=DELTAT*(1.-PONOZ*(1.-2.*PMU)/PMO)*((1.+ALPTS*(TGR-TREF)))*
▶ 1*3/(1.+ETHETA)
Z=Z+DELTAT*(RSAVE-RHAVE)
T=T+DELTAT
CALL OUTPUT

```

Table C-3 (Cont'd)

```

GO TO 10
25 RHEAD=0.0
   RNOZ=RHEAD
   PHEAD=PONOZ
   MDIS=AT*PONOZ/CSTAR
   WRITE(6,318)
   DELTAT=2.*DELY/(RHAVE+RNAVE)
▶   DELTAT=DELTAT*((1.-PONOZ*(1.-2.*PMU)/PMOD)*(1.+ALPTS*(TGR-TREF)))*
▶   1*3/(1.+ETHETA)
   T=T+DELTAT
   CALL OUTPUT
   TIME=T
   DELTAT=.5
   TIM=TIME+5.
   PHT=PHEAD
   SG=0.0
29 T=T+DELTAT
   PHEAD=PHT/EXP(CAPGAM**2*AT*CSTAR/VC*(T-TIME)*12.)
   PONOZ=PHEAD
   MDIS=PONOZ*AT/CSTAR
   Y=Y+.5*RHEAD
   CALL OUTPUT
   IF(T.LT.TIM.AND.PHEAD.GE.0.04)GO TO 29
   WP1=G*SUMMT
   WP2=RHO*(VC-VC I)*G
   WP=(WP1+WP2)/2.
▶   IF(ISO.EQ.1) WP=WP1
   ISP=ITOT/WP
   ISPVAC=ITVAC/WP
   FAV=ITOT/T
   FVACAV=ITVAC/T
   PONAV=PONTOT/T
   LAMBDA=(VC-VC I)/VC
   WRITE(6,102) WP1,WP2,WP,PHMAX,ISP,ISPVAC,ITOT,ITVAC,FAV,FVACAV,PON
1AV,VC I,VC,LAMBDA
   IF(IWO.EQ.0) GO TO 903
   PMEOP=PHMAX*(1.+X1*SIGMAP)*EXP(PIPK*UTEMP)
   SYC=SYCNOM*(1.-X2*SIGMAS)
   TAUC=PSIC*PMEOP*DCC/(2.*SYC)
   WCC=PI*TAUC*DCC*DEL C*LCC*(1.+INSEG-1.)*(40.*TAUC/LCC)
   TAUCD=TAUC/2.
   WCH=2.5*PI/2.*DCC*DCC*TAUCD*DEL C
   WCN=4.5*PI/2.*DCC*HCN*TAUCD*DEL C
   WC=WCC+WCH+WCN
   EPSIL=AE/PI/DTI/DTI*4.
   WN=K1*DTI*DTI/(1.+5*SIN(ALFAN))*((EPSIL-SQRT(EPSIL))*PMEOP*DTI*PS
1IS/SYNNOM+K2*T*PSIA)
   WINS=T*PSIINS*DELINS*DCC*PI*(KEH*(DCC*.40+(S+NS)*TAU/2.+0.15/

```

Table C-3 (Cont'd)

```

IPSIINS*(LCC-TAU*(S+NS)))+KEN*.80*HCN)
WL=TAUL*DLINER*PI*DCC*(DCC/2.+LCC+HCN)
WI=WC+WN+WINS+WL+WA
WM=WI+WP
ZETAM=WP/WM
RATIO=ITOT/WM
WRITE(6,605)
WRITE(6,601) PMEUP,TAUCC,WC,WN,WINS,WL,WI,WM,ZETAM,RATIO
903 CONTINUE
NDUM=1
IF(IPO.NE.0.AND.IPO.NE.2) CALL OUTPUT
901 CONTINUE
IF(IOP.NE.0) CALL PLOT(0.0,0.0,999)
STOP
500 FORMAT(42X,I2)
1903 FORMAT(6X,F6.2,10X,E11.4,10X,E11.4,8X,E11.4,/,22X,E11.4,9X,E11.4)
11111 FORMAT(6X,I3,7X,I3)
602 FORMAT(1H1,42X,21HCONFIGURATION NUMBER ,I3)
499 FORMAT(23F3.1)
▶ 491 FORMAT(4X,I1,9X,I1,9X,I1)
493 FORMAT(4X,I1,15X,16I1,/,7X,I1)
▶ 492 FORMAT(/,20X,7HOPTIONS,/,13X,5HIGO= ,I1,/,13X,5HIWO= ,I1,/,13X,5H
▶ $ISO= ,I1)
494 FORMAT(13X,5HIPO= ,I1,/,13X,12HNUMPLT(JJ)= ,I1,15(1H,,I2),
2/,13X,'ITEMP= ',I2)
11112 FORMAT(13X,'NTAB= ',I3,/,13X,'NTABY= ',I3)
▶ 505 FORMAT(7X,E12.4,10X,E12.4,9X,F8.5,9X,F8.5,/,10X,E12.4,10X,F8.5)
▶ 799 FORMAT(/,15X,27HGRAIN DEFORMATION CONSTANTS,/,13X,6HPMOD= ,E15.4
▶ 1,/,13X,6HCMOD= ,E15.4,/,13X,5HPMU= ,F8.4,/,13X,5HCMU= ,F8.4,/,13X,
▶ 27HALPTS= ,E15.4,/,13X,6HTAUC= ,F8.4)
501 FORMAT(7X,F10.0,/,
2 4X,F9.6,3X,F7.5,3X,F6.3,6X,F5.2,5X,F6.2,4X,E11.4,/,
26X,F6.0)
603 FORMAT( //,20X,26HPROPELLANT CHARACTERISTICS,/,13X,5HRHU= ,F9.6,/,
13X,3HAI= ,F9.6,/,13X,3HNI= ,F6.3,/,13X,7HALPHA= ,F6.2,/,13X,6HBETA=
2 ,F6.2,/,13X,3HMU= ,1PE11.4,/,13X,7HCSTAR= ,1PE11.4,/,13X,'RN2N1=
2',1PE11.4)
502 FORMAT(2X,F8.2,5X,F6.2,4X,F7.2,5X,F6.3,7X,F8.5,7X,F8.5,/,10X,
1 F7.2,4X,F6.2,4X,F6.2,8X,F10.7,6X,F8.2)
604 FORMAT(/,20X,22HBASIC MOTOR DIMENSIONS,/,13X,3HL= ,F8.2,/,13X,5HT
1AU= ,F6.2,/,13X,4HDE=
2 1PE11.4,/,13X,5HDTI= ,1PE11.4,/,13X,7HTHETA= ,1PE11.4,/,13X,7HALP
3HAN= ,1PE11.4,/,13X,6HHTAP= ,1PE11.4,/,13X,4HXT= ,1PE11.4,/,13X,4HZ
40= ,1PE11.4,/,13X,8HCSTART= ,1PE11.4,/,13X,7HPTRAN= ,1PE11.4,/,13X
5,4HN2= ,1PE11.4)
10001 FORMAT(5X,F10.0)
700 FORMAT(2F10.4)
701 FORMAT(20X,'Y= ',1PE11.4,10X,'TGR= ',1PE11.4)

```



Table C-3 (Cont'd)

```

503 FORMAT(7X,F6.3,5X,F7.2,7X,F7.2,7X,F5.4,3X,F6.2,3X,F8.0,/,
15X,F7.4,8X,F8.5,5X,F8.2,7X,F7.3,5X,F7.5,/,5X,F7.3,5X,F7.4,
25X,F6.1)
1002 FORMAT(13X,'TGR= ',1PE11.4)
606 FORMAT(/,15X,27HBASIC PERFORMANCE CONSTANTS,/,13X,8HDELTAY= ,F6.3
1,/,13X,6HXOUT= ,F8.2,/,13X,7HDPOUT= ,F8.1,/,13X,7HZETAF= ,F7.4,/,1
23X,4HTB= ,F6.1,/,13X,4HHB= ,F8.0,/,13X,5HGAM= ,F7.4,/,13X,7HERREF=
3 ,F8.5,/,13X,6HPREF= ,F8.2,/,13X,7HDTREF= ,F7.3
4,/,13X,6HPIPK= ,F8.5,/,13X,4HA2= ,F8.5,/,13X,6HTREF= ,F7.3,/,13X,6
5HGAME= ,F7.4,/,13X,6HPEXT= ,F6.1)
97 FORMAT(3X,F7.1,5X,F6.4,6X,F8.1,7X,F7.1,7X,F7.1,6X,F5.3,/,4X,F5.2,
1 7X,F7.1,9X,F5.3,7X,F7.3)
842 FORMAT(20X,18HIGNITION CUNSTANTS,/,13X,4HKA= ,F7.1,/,13X,4HK8= ,
1 F7.4,/,13X,5HUF5= ,F8.1,/,13X,6HCSIG= ,F7.1,/,13X,6HPMIG= ,
2 F7.1,/,13X,5HTI1= ,F6.3,/,13X,5HTI2= ,F5.2,/,13X,6HRRIG= ,
3 F8.1,/,13X,8HDELTIG= ,F6.3,/,13X,6HPBIG= ,F7.3,/)
600 FORMAT(
21X,F6.2,10X,F6.3,10X,F6.3,6X,F5.2,/,5X,F5.2,10X,F10
1.2,7X,F7.2,9X,F5.2,8X,F6.3,/,6X,F8.2,8X,F4.0,7X,F7.2,10X,F10.2,8X,
2F5.2,/,7X,F5.2,6X,F7.4,6X,F7.4,10X,F5.2,10X,F7.4,/,6X,F7.4,7X,F7.4
3,10X,F7.4,8X,F7.4,6X,F9.2)
610 FORMAT(
20X,19HINERT WEIGHT INPUTS,/,13X,
17HDTEMP= ,1PE11.4,/,13X,8HSIGMAP= ,1PE11.4,/,13X,8HSIGMAS= ,1PE11.
24,/,13X,4HX1= ,1PE11.4,/,13X,4HX2= ,1PE11.4,/,13X,8HSYCNOM= ,1PE11
3.4,/,13X,5HDCC= ,1PE11.4,/,13X,6HPSIC= ,1PE11.4,/,13X,6HDELC= ,1PE
411.4,/,13X,5HLCC= ,1PE11.4,/,13X,6HNSEG= ,1PE11.4,/,13X,5HHCN= ,1P
5E11.4,/,13X,8HSYNNUM= ,1PE11.4,/,13X,6HPSIS= ,1PE11.4,/,13X,6HPSIA
6= ,1PE11.4,/,13X,4HK1= ,1PE11.4,/,13X,4HK2= ,1PE11.4,/,13X,8HPSIIN
7S= ,1PE11.4,/,13X,8HDELINS= ,1PE11.4,/,13X,5HKEH= ,1PE11.4,/,13X,5
8HKEN= ,1PE11.4,/,13X,8HDLINER= ,1PE11.4,/,13X,6HTAUL= ,1PE11.4,/,1
93X,4HWA= ,1PE11.4)
101 FORMAT(/,33X,29H*****EQUILIBRIUM BURNING ***,/,33X,29H*****EQUI
LIBRIUM BURNING ***,/,33X,29H*****EQUILIBRIUM BURNING ***,/,30X,
225HINITIAL REYNOLDS NUMBER= ,1PE11.4)
51 FORMAT(37X,23H*****TAIL OFF BEGINS
1****,/,37X,23H*****TAIL OFF BEGINS
1****,/)
318 FORMAT(37X,23H*****BEGIN HALF SECOND T
RACE,/,37X,23H*****BEGIN HALF SECOND T
RACE,/)
102 FORMAT(13X,5HWPI= ,1PE11.4,/,13X,5HWPI= ,1PE11.4,/,13X,4HWP= ,1PE1
11.4,/,13X,7HPHMAX= ,1PE11.4,/,13X,5HISP= ,1PE11.4,/,13X,8HISPVAC=
2,1PE11.4,/,13X,6HITUT= ,1PE11.4,/,13X,7HITVAC= ,1PE11.4,/,13X,5HF
3AV= ,1PE11.4,/,13X,8HFVACAV= ,1PE11.4,/,13X,8HPONAV= ,1PE11.4,/,1
43X,5HVC1= ,1PE11.4,/,13X,5HVCF= ,1PE11.4,/,13X,8HLAMBDA= ,1PE11.4)
605 FORMAT(/,42X25HMOTOR WEIGHT CALCULATIONS)
601 FORMAT(13X,23HMAX EXPECTED PRESSURE= ,1PE11.4,/,13X,28HCYLINDRICAL
1 CASE THICKNESS= ,1PE11.4,/,13X,9HCASE WT= ,1PE11.4,/,13X,11HNOZZL
2E WT= ,1PE11.4,/,13X,15HINSULATION WT= ,1PE11.4,/,13X,10HLINER WT=
3 ,1PE11.4,/,13X,16HTOTAL INERT WT= ,1PE11.4,/,13X,20HTOTAL MOTOR W
4EIGHT= ,1PE11.4,/,13X,7HZETAM= ,1PE11.4,/,13X,21HRATIO OF ITOT TO
5WM= ,1PE11.4)
END

```

Table C-3 (Cont'd)

```

SUBROUTINE AREAS
C *****
C * SUBROUTINE AREAS CALCULATES BURNING AREAS AND PORT AREAS FOR *
C * CIRCULAR PERFORATED (C.P.) GRAINS AND STAR GRAINS OR FOR A *
C * COMBINATION OF C.P. AND STAR GRAINS *
C *****
      INTEGER STAR, GRAIN, ORDER, COP
      REAL MGEN, MDIS, MNOZ, MN1, JROCK, N, L, ME1, ME, ISP, ITOT, MU, MASS, ISPVAC
      REAL LGCI, LGNI, NS, NN, NP, LGSI, NT, LTP, LGC, LS, LF
      REAL M2, MDBAR, ISP2, ITVAC, L1, L2, LFW, LFWSQD
      COMMON/CONST1/ZW, AE, AT, THETA, ALFAN
      COMMON/CONST3/S, NS, GRAIN, NTA8Y, NCARD
      COMMON/CONST4/DELDI, DO, ZO, DI
      COMMON/VARIA1/Y, T, DELY, DELTAT, PNOZ, PHEAD, RNOZ, RHEAD, SUMAB, PHMAX
      COMMON/VARIA2/ABPORT, ABSLOT, ABNOZ, APHEAD, APNOZ, DADY, ABP2, ABN2, ABS2
      COMMON/VARIA3/ITOT, ITVAC, JROCK, ISP, ISPVAC, MDIS, MNOZ, SG, SUMMT
      COMMON/VARIA4/RNT, RHT, SUM2, R1, R2, R3, RHAVE, RHAVE, RBAK, YB, KOUNT, TL
      COMMON/VARIA5/ABMAIN, ABTO, SUMDY, VCI, ABTT, PTRAN
      COMMON/VARIA8/YDI
      COMMON/VARI20/YETA, XETH, ISO
      DATA PI/3.14159/
      ABPC=0.0
      ABNC=0.0
      ABSC=0.0
      ABPS=0.0
      ABNS=0.0
      ABSS=0.0
      DABT=0.0
      SG=0.0
      VCIT=0.0
      ANUM=PI/4.
      PID2=PI/2.
      RNT=RNT+RNOZ*DELTAT
      RHT=RHT+RHEAD*DELTAT
      IF(Y.LE.0.0) AGS=0.0
      K=0
      IF(ABS(ZW).GT.0.0) K=1
      YB=Y
      IF(K.EQ.1) Y=YB-SUMDY/2.
      2 IF(K.EQ.2) Y=YB+ABS(ZW)/2.-SUMDY/2.
      IF(ISO.EQ.0) YETA=Y
      IF(Y.LE.0.0) READ(5,500) INPUT, GRAIN, STAR, NT, ORDER, COP
C *****
C * READ THE TYPE OF INPUT FOR THE PROGRAM AND THE BASIC GRAIN *
C * CONFIGURATION AND ARRANGEMENT *
C * VALUES FOR INPUT ARE *
C * 1 FOR ONLY TABULAR INPUT *
C * 2 FOR ONLY EQUATION INPUTS (EQUATIONS ARE BUILT *

```

Table C-3 (Cont'd)

```

C *          INTO THE SUBROUTINE) *
C *          3 FOR A COMBINATION OF 1 AND 2 *
C *    VALUES FOR GRAIN ARE *
C *          1 FOR STRAIGHT C.P. GRAIN *
C *          2 FOR STRAIGHT STAR GRAIN *
C *          3 FOR COMBINATION OF C.P. AND STAR GRAINS *
C *    VALUES FOR STAR ARE (WAGON WHEEL IS CONSIDERED A TYPE OF *
C *    STAR GRAIN IN THIS PROGRAM) *
C *          0 FOR STRAIGHT C.P. GRAIN *
C *          1 FOR STANDARD STAR *
C *          2 FOR TRUNCATED STAR *
C *          3 FOR WAGON WHEEL *
C *    VALUES FOR NT ARE *
C *          0 IF THERE ARE NO TERMINATION PORTS *
C *          X WHERE X IS THE NUMBER OF TERMINATION PORTS *
C *    VALUES OF ORDER ESTABLISH HOW A COMBINATION C.P. AND STAR *
C *    GRAIN IS ARRANGED *
C *          1 IF DESIGN IS STAR AT HEAD END AND C.P. AT NOZZLE *
C *          2 IF DESIGN IS C.P. AT HEAD END AND C.P. AT NOZZLE *
C *          3 IF DESIGN IS C.P. AT HEAD END AND STAR AT NOZZLE *
C *          4 IF DESIGN IS STAR AT HEAD END AND STAR AT NOZZLE *
C *    ***NOTE*** IF GRAIN=1, VALUE OF ORDER MUST BE 2 *
1000 CONTINUE
C *    ***NOTE*** IF GRAIN=2, VALUE OF ORDER MUST BE 4 *
C *    VALUES FOR COP ARE (APPLICABLE TO C.P. GRAINS ONLY) *
C *          0 IF BOTH ENDS ARE CONICAL OR FLAT *
C *          1 IF HEAD END IS CONICAL OR FLAT AND AFT END IS *
C *            HEMISPHERICAL *
C *          2 IF BOTH ENDS ARE HEMISPHERICAL *
C *          3 IF HEAD END IS HEMISPHERICAL AND AFT END IS *
C *            CONICAL OR FLAT *
C *    *****
C *    IF(Y.LE.0.0) WRITE(6,607)
C *    IF(Y.LE.0.0) WRITE(6,600) INPUT,GRAIN,STAR,NT,ORDER,COP
C *    IF(INPUT.EQ.2) GO TO 12
C *    IF(Y.LE.0.0) GO TO 6
C *    IF(K.EQ.2) GO TO 91
C *    IF(K.EQ.1)Y=YB
C *    IF(YT.LE.Y) GO TO 8
9 DENOM=YT-YT2
SLOPE1=(ABPK-ABPK2)/DENOM
SLOPE2=(ABSK-ABSK2)/DENOM
SLOPE3=(ABNK-ABNK2)/DENOM
SLOPE4=(APHK-APHK2)/DENOM
SLOPE5=(APNK-APNK2)/DENOM
B1=ABPK-SLOPE1*YT
B2=ABSK-SLOPE2*YT
B3=ABNK-SLOPE3*YT

```

Table C-3 (Cont'd)

```

B4=APHK-SLOPE4*YT
B5=APNK-SLOPE5*YT
ABPT=SLOPE1*Y+B1
ABST=SLOPE2*Y+B2
ABNT=SLOPE3*Y+B3
APHT=SLOPE4*Y+B4
APNT=SLOPE5*Y+B5
YB=Y
IF(K.EQ.1) Y=YB-SUMDY/2.
91 IF(INPUT.EQ.3) GO TO 3
GO TO 52
6 READ(5,507) YT,ABPK,ABSK,ABNK,APHK,APNK,VCIT
NCARD=NCARD+1
C *****
C * READ IN TABULAR VALUES FOR Y=0.0 (NOT REQUIRED IF INPUT=2) *
C *
C * ABPK IS THE BURNING AREA IN THE PORT IN IN**2 *
C * ABSK IS THE BURNING AREA IN THE SLOTS IN IN**2 *
C * ABNK IS THE BURNING AREA IN THE NOZZLE END IN IN**2 *
C * APHK IS THE PORT AREA AT THE HEAD END IN IN**2 *
C * APNK IS THE PORT AREA AT THE NOZZLE END IN IN**2 *
C * VCIT IS THE INITIAL VOLUME OF CHAMBER GASES ASSOCIATED WITH *
C * TABULAR INPUT IN IN**3 *
C *****
WRITE(6,610)
WRITE(6,583) ABPK,ABSK,ABNK,APHK,APNK
WRITE(6,584)VCIT
ABPT=ABPK
ABST=ABSK
ABNT=ABNK
APHT=APHK
APNT=APNK
YT2=YT
IF(INPUT.EQ.3) GO TO 3
VC1=VCIT
GO TO 52
8 YT2=YT
ABPK2=ABPK
ABNK2=ABNK
ABSK2=ABSK
APHK2=APHK
APNK2=APNK
READ(5,505) YT,ABPK,ABSK,ABNK,APHK,APNK
NCARD=NCARD+1
C *****
C * READ IN TABULAR VALUES FOR Y=Y (NOT REQUIRED FOR INPUT=2) *
C * (NOTE THAT TABULAR VALUE CARDS FOR Y GT 0 DO NOT IMMEDIATELY *
C * FOLLOW THOSE FOR Y EQ 0 IN THE DATA DECK) *

```

Table C-3 (Cont'd)

```

C *****
  WRITE(6,611) YT
  WRITE(6,583) ABPK,ABSK,ABNK,APHK,APNK
  GO TO 9
12 ABPT=0.0
  ABNT=0.0
  ABST=0.0
  3 IF(GRAIN.NE.2) GO TO 4
  ABPC=0.0
  ABNC=0.0
  ABSC=0.0
  GO TO 7
  4 IF(Y.LE.0.0) READ(5,501) DO,DI,DELDI,S,THETAG,LGCI,LGNI,THETCN,THE
  TCH
C *****
C *   READ IN BASIC GEOMETRY FOR C.P. GRAIN (NOT REQUIRED FOR *
C *   STRAIGHT STAR GRAIN) *
C *   DO IS THE AVERAGE OUTSIDE INITIAL GRAIN DIAMETER IN INCHES *
C *   DI IS THE AVERAGE INITIAL INTERNAL GRAIN DIAMETER IN INCHES *
C *   DELDI IS THE DIFFERENCE BETWEEN THE INITIAL INTERNAL GRAIN *
C *   DIAMETER AT THE NOZZLE END OF LGCI AND DI IN INCHES *
C *   S IS THE NUMBER OF FLAT BURNING SLOT SIDES (NOT INCLUDING *
C *   THE NOZZLE END) *
C *   THETAG IS THE ANGLE THE NOZZLE END OF THE GRAIN MAKES WITH *
C *   THE MOTOR AXIS IN DEGREES *
C *   LGCI IS THE INITIAL TOTAL LENGTH OF THE CIRCULAR PERFORATION *
C *   IN INCHES *
C *   LGNI IS THE INITIAL SLANT LENGTH OF THE BURNING CONICAL *
C *   GRAIN AT THE NOZZLE END IN INCHES *
C *   THETCN IS THE CONTRACTION ANGLE OF THE BONDED GRAIN IN DEG. *
C *   THETCH IS THE CONTRACTION ANGLE AT THE HEAD END IN DEGREES *
C *****
  IF(Y.LE.0.0) WRITE(6,601) DO,DI,DELDI,S,THETAG,LGCI,LGNI,THETCN,TH
  TCH
  IF (Y.LE.0.0) THETAG=THETAG/57.29578
  IF (Y.LE.0.0) THETCN=THETCN/57.29578
  IF (Y.LE.0.0) THETCH=THETCH/57.29578
  DOSQD=DO*DO
  DISQD=DI*DI
  BNUM=ANUM*DOSQD
  TLL=TL
  IF(ORDER.GE.3) TLL=0.0
  YDI=2.*Y+DI
  YDISQD=YDI*YDI
  ABSC=S*ANUM*(DOSQD-YDISQD)
  IF(ABSC.LE.0.0) ABSC=0.0
  IF(YDI.GT.DO) GO TO 100
  IF(THETAG.GT.0.08727) GO TO 101

```

Table C-3 (Cont'd)

```

IF(COP.EQ.0) GO TO 700
IF(COP.EQ.1) GO TO 701
IF(COP.EQ.2) GO TO 702
CHK1=DOSQD-YDISQD
IF(CHCK1.LT.0.0) CHCK1=0.0
LGC=LGCI-(SQRT(DOSQD-DISQD)-SQRT(CHCK1))/2.-Y*COTAN(THETCN)
GO TO 710
702 CHCK1=DOSQD-YDISQD
IF(CHCK1.LT.0.0) CHCK1=0.0
IF(CHCK1.LT.0.0) CHCK1=0.0
LGC=LGCI-(SQRT(DOSQD-DISQD)-SQRT(CHCK1))
GO TO 710
701 CHCK2=DOSQD-(YDI+DELDI)**2
IF(CHCK2.LT.0.0) CHCK2=0.0
LGC=LGCI-(SQRT(DOSQD-(DI+DELDI)**2)-SQRT(CHCK2))/2.
1-Y*COTAN(THETCH)
GO TO 710
700 LGC=LGCI-Y*(COTAN(THETCN)+COTAN(THETCH))
▶ 710 ABPC=PI*YDI*(LGC-TLL-S*YETA)
ABNC=0.0
GO TO 732
101 CONTINUE
IF(COP.EQ.0.OR.COP.EQ.1) GO TO 720
CHK1=DOSQD-YDISQD
IF(CHCK1.LT.0.0) CHCK1=0.0
ABPC=PI*YDI*(LGCI-(SQRT(DOSQD-DISQD)-SQRT(CHCK1)))/2.-TLL
▶ 2-(S+TAN(THETAG/2.))*YETA)
GO TO 730
▶ 720 ABPC=PI*YDI*(LGCI-Y*COTAN(THETCH)-TLL-(S+TAN(THETAG/2.))*YETA)
730 IF(COP.EQ.1.OR.COP.EQ.2) GO TO 731
ABNC=PI*(LGNI-Y*COTAN(THETAG+THETCN)-Y*TAN(THETAG/2.))*(DI+
1 DELDI+Y+LGNI*SIN(THETAG)+Y*SIN(THETCN)/SIN(THETAG+THETCN))
GO TO 732
731 IF(Y.LE.0.0) GO TO 7311
GO TO 7312
7311 R7=((DI+DELDI)/2.+LGNI*SIN(THETAG))*COS(THETAG)-SIN(THETAG)*
1 SQRT(((DO/2.)**2-((DI+DELDI)/2.+LGNI*SIN(THETAG))**2)
7312 IF(R7+Y.LT.(DO/2.)*COS(THETAG)) GO TO 11111
ABNC=PI*(LGNI+(1./SIN(THETAG))*((DO/2.)-LGNI*SIN(THETAG)
1-(DI+DELDI)/2.))-Y*COTAN(THETAG)-Y*TAN(THETAG/2.))*((DI+DELDI)
2/2.+Y+DO/2.)
GO TO 22222
11111 RPR=SQRT(((DO/2.)**2)-R7**2)-SQRT(((DO/2.)**2)-(R7+Y)**2)
ABNC=PI*(LGNI-RPR-Y*TAN(THETAG/2.))*((DI+DELDI)/2.+SQRT((DO/
1 2.)**2-(R7+Y)**2)*SIN(THETAG)+Y+(R7+Y)*COS(THETAG))
22222 CONTINUE
732 IF(ABPC.LE.0.0) ABPC=0.0
IF(ABNC.LE.0.0) ABNC=0.0

```

Table C-3 (Cont'd)

```

GO TO 5
100 ABNC=0.0
    ABPC=0.0
    5 DH=DI-ZO
      APHT=ANUM*(DH+2.*RHT)**2
      IF(APHT.GE.BNUM) APHT=BNUM
      IF(K.LT.2) APHT1=APHT
      APNT=ANUM*(DI+DELDI+2.*RNT)**2
      IF(APNT.GE.BNUM) APNT=BNUM
      IF(GRAIN.NE.1) GO TO 7
      ABPS=0.0
      ABSS=0.0
      ABNS=0.0
      GO TO 50
    7 IF(Y.LE.0.0) READ(5,502) NS,LGSI,NP,RC,FILL,NN
C *****
C *   READ IN BASIC GEOMETRY FOR STAR GRAIN (NOT REQUIRED FOR *
C *   STRAIGHT C.P. GRAIN) *
C *   NS IS THE NUMBER OF FLAT BURNING SLOT SIDES (NOT INCLUDING *
C *   THE NOZZLE END) *
C *   LGSI IS THE INITIAL TOTAL LENGTH OF THE STAR SHAPED *
C *   PERFORATED GRAIN IN INCHES *
C *   NP IS THE NUMBER OF STAR POINTS *
C *   RC IS THE AVERAGE STAR GRAIN OUTSIDE RADIUS IN INCHES *
C *   FILL IS THE FILLET RADIUS IN INCHES *
C *   NN IS THE NUMBER OF STAR NOZZLE END BURNING SURFACES *
C *****
      IF(Y.LE.0.0) WRITE(6,602) NS,LGSI,NP,RC,FILL,NN
      PIDNP=PI/NP
      RCSQD=RC*RC
      IF(ISO.EQ.1) YE=Y
      IF(ISO.EQ.1) Y=YETA
      FY=FILL+Y
      FYSQD=FY*FY
      IF(STAR.EQ.1) GO TO 20
      IF(STAR.EQ.2) GO TO 201
      IF(Y.GT.0.0) GO TO 179
      AD(5,421) TAUWW,L1,L2,ALPHA1,ALPHA2,HW
C *****
C *   READ IN GEOMETRY FOR WAGON WHEEL (NOT REQUIRED FOR STANDARD *
C *   OR TRUNCATED STAR GRAINS) *
C *   TAUWW IS THE THICKNESS OF THE PROPELLANT WEB IN INCHES *
C *   L1 AND L2 ARE THE LENGTHS OF THE TWO PARALLEL SIDES OF THE *
C *   TWO SET OF STAR POINTS IN INCHES *
C *   ALPHA1 AND ALPHA2 ARE THE ANGLES BETWEEN THE SLANT SIDES OF *
C *   THE STAR POINTS CORRESPONDING TO L1 AND L2, RESPECTIVELY, *
C *   AND THE CENTER LINES OF THE POINTS IN DEGREES *
C *   HW IS HALF THE WIDTH OF THE STAR POINTS IN INCHES *

```

Table C-3 (Cont'd)

```

C *****
WRITE(6,422) TAUWW,L1,L2,ALPHA1,ALPHA2,Hw
ALPHA1=ALPHA1/57.29578
ALPHA2=ALPHA2/57.29578
ALP2=ALPHA2
XL2=L2
LFW=RC-TAUWW-FILL
LFWSQD=LFW*LFW
THETFW=ARCSIN((HW+FILL)/LFW)
SLFW=LFW*SIN(THETFW)
179 KKK=0
SG=0.0
ENUM=(RCSQD-LFWSQD-FYSQD)/(2.*LFW*FY)
ALPHA2=ALP2
L2=XL2
190 YTAN=Y*TAN(ALPHA2/2.)
COSALP=COS(ALPHA2)
SINALP=SIN(ALPHA2)
IF(YTAN.GT.L2) GO TO 182
IF(FY.GT.SLFW) GO TO 181
SGW=NP*(L2-2.*YTAN+(SLFW-FILL)/SINALP-Y*COTAN(ALPHA2)+FY*
1 (PID2+THETFW)+(LFW+FY)*(PIDNP-THETFW))
GO TO 183
181 IF(Y.GT.TAUWW) GO TO 184
SGW=NP*(FY*(PIDNP+ARCSIN(SLFW/FY))+iPIDNP-THETFW)*LFW)
GO TO 183
184 SGW=NP*FY*(THETFW+ARCSIN(SLFW/FY)-ARCCOS(ENUM))
GO TO 183
182 YPO=-SLFW
IF(ALPHA2.GE.PID2) GO TO 222
Q=-FILL+L2*TAN(ALPHA2)-Y/COSALP
XPI=(-Q*TAN(ALPHA2)-SQRT(-Q*Q+FYSQD/COSALP*COSALP))*COSALP*COSALP
YPI=XPI*TAN(ALPHA2)+Q
XPO=(YPO-Q)*COTAN(ALPHA2)
GO TO 223
222 XPI=Y-L2
YPI=-SQRT(FYSQD-XPI*XPI)
XPO=XPI
223 FYLS=SQRT(SLFW*SLFW+XPI*XPI)
XPI02=(XPI-XPO)*(XPI-XPO)
YPI02=(YPI-YPO)*(YPI-YPO)
IF(FY.GT.FYLS) GO TO 186
IF(Y.GE.TAUWW) GO TO 185
SGW=NP*(SQRT(XPI02+YPI02)+FY*(PID2+THETFW-ARCSIN(XPI/FY)))+(LFW+FY)*
1 (PIDNP-THETFW))
GO TO 183
185 SGW=NP*(SQRT(XPI02+YPI02)+FY*(PID2-ARCSIN(XPI/FY)-ARCCOS(ENUM)))
GO TO 183

```



Table C-3 (Cont'd)

```

186 IF(Y.GT.TAUWH) GO TO 187
    SGW=NP*(FY*(PIDNP+ARSIN(SLFW/FY))+(PIDNP-THETFW)*LFW)
    GO TO 183
187 SGW=NP*FY*(THETFW+ARSIN(SLFW/FY)-ARCOS(ENUM))
183 IF(SGW.LE.0.0) SGW=0.0
    IF(Y.GT.0.0) GO TO 188
    AGS2=.5*(PI*RC SQD-NP*LFW*SLFW*(COS(THETFW)-SIN(THETFW)*COTAN(ALPHA
1 2)-2.*(L2+FILL*TAN(ALPHA2/2.))/LFW)-(PI-THETFW*NP)*LFW SQD-2.*NP*F
2 ILL*(L2+SLFW/SINALP+LFW*(PIDNP-THETFW)+(PIDNP+PID2-L./SINALP)*
3 FILL/2.))
    AGS=AGS+AGS2
188 CONTINUE
    SG=SG+SGW
    IF(KKK.EQ.1) GO TO 24
    L2=L1
    ALPHA2=ALPHA1
    KKK=1
    GO TO 190
201 IF(Y.LE.0.0) READ(5,503) RP,TAUS
C *****
C *   READ IN GEOMETRY FOR TRUNCATED STAR (NOT REQUIRED FOR *
C *   STANDARD STAR OR WAGON WHEEL) *
C *   RP IS THE INITIAL RADIUS OF THE TRUNCATION IN INCHES *
C *   TAUS IS THE THICKNESS OF THE PROPELLANT WEB AT THE BOTTOM *
C *   OF THE SLOTS IN INCHES *
C *****
    IF(Y.LE.0.0) WRITE(6,603) RP,TAUS
    THETAS=PIDNP
    RPY=RP+Y
    LS=RC-TAUS-FILL-RP
    RPL=RP+LS
    THETS1=THETAS-ARSIN(FY/RPY)
    IF(THETS1.LE.0.0) GO TO 110
    IF(Y.LE.TAUS) GO TO 103
    THETAC=ARSIN((RCSQD-RPL*RPL-FYSQD)/(2.*FY*RPL))
    IF(THETAC.GE.0.0) GO TO 104
    IF(Y.LT.RC-RP) GO TO 105
    SG=0.0
    GO TO 14
103 SG=2.*NP*(RPY*THETS1+LS-(RPY*COS(THETAS-THETS1)-KP)+PI D2*FY)
    GO TO 14
104 SG=2.*NP*(RPY*THETS1+LS-(RPY*COS(THETAS-THETS1)-RP)+FY*THETAC)
    GO TO 14
105 SG=2.*NP*(RPY*THETS1+SQRT(RC SQD-FYSQD)-SQRT(RPY*RPY-FYSQD))
    14 IF(Y.LE.0.0) AGS=PI*(RCSQD-RP*RP)-NP*(PI*FILL*FILL/2.+2.*LS*FILL)
    GO TO 31
110 THETA F=THETAS
    THETA P=2.*THETAS

```

Table C-3 (Cont'd)

```

    TAUWS=TAUS
    GO TO 111
20 IF(Y.GT.0.0) GO TO 1791
    READ(5,504) THETA F,THETA P,TAUWS
C *****
C *   READ IN GEOMETRY FOR STANDARD STAR (NOT REQUIRED FOR *
C *   TRUNCATED STAR OR WAGON WHEEL) *
C *   THETA F IS THE ANGLE LOCATION OF THE FILLET CENTER IN DEGREES *
C *   THETA P IS THE ANGLE OF THE STAR POINT IN DEGREES *
C *   TAUWS IS THE WEB THICKNESS OF THE GRAIN IN INCHES *
C *****
    WRITE(6,604) THETA F,THETA P,TAUWS
    THETA F=THETA F/57.29578
    THETA P=THETA P/57.29578
    THETA S=PI/NP
    THETA S1=1.00
111 LF=RC-TAUWS-FILL
1791 CNUM=(Y+FILL)/LF
    DNUM=SIN(THETA F)/SIN(THETA P/2.)
    ENUM=(RCSQD-LF*LF-FYSQD)/(2.*LF*FY)
    FNUM=SIN(THETA F)/CCS(THETA P/2.)
    IF(CNUM.LE.FNUM) GO TO 106
    IF(Y.LE.TAUWS) GO TO 107
    SG=2.*NP*FY*(THETA F+ARSIN(SIN(THETA F)/CNUM)-ARCOS(ENUM))
    GO TO 23
106 IF(Y.LE.TAUWS) SG=2.*NP*LF*(DNUM+CNUM*(PID2+THETA S-THETA P/2.
1-COTAN(THETA P/2.))+THETA S-THETA F)
    IF(Y.LE.TAUWS) GO TO 23
    SG=2.*NP*(FY*(ARSIN(ENUM)+THETA F-THETA P/2.))+LF*DNUM-FY*COTAN(THETA
1P/2.))
    GO TO 23
107 SG=2.*NP*LF*(CNUM*(THETA S+ARSIN(SIN(THETA F)/CNUM))+THETA S-THETA F)
23 IF(THETA S1.LE.0.0) GO TO 14
    IF(Y.LE.0.0) AGS=PI*RC**2-NP*LF*LF*(SIN(THETA F)*(COS(THETA F)-
1SIN(THETA F)*COTAN(THETA P/2.))+THETA S-THETA F+2.*FILL/LF*(SIN(THETA F
2)/SIN(THETA P/2.))+THETA S-THETA F+FILL/(2.*LF)*(PID2+THETA S-THE
3TAP/2.-COTAN(THETA P/2.)))
24 CONTINUE
31 IF(SG.LE.0.0) SG=0.0
    IF(K.EQ.0.OR.K.EQ.2) SGN=SG
    IF(K.LE.1) SGH=SG
    IF(Y.LE.0.0) SG2=SG
    IF(K.EQ.2) GO TO 37
    RAVEDT=R1+(SG+SG2)/2.*RBAR*DELTAT
    RNDT=R2+(SG+SG2)/2.*RSAVE*DELTAT
    RHDT=R3+(SG+SG2)/2.*RHAVE*DELTAT
    R1=RAVEDT
    R2=RNDT

```

Table C-3 (Cont'd)

```

R3=RHDT
SG2=SG
GO TO 38
37 IF(KOUNT.NE.1) GO TO 39
SG3=SG
R4=R1
R5=R2
R6=R3
39 RAVEDT=R4+(SG+SG3)/2.*RBAR*DELTAT
RNDT=R5+(SG+SG3)/2.*RNAVE*DELTAT
RHDT=R6+(SG+SG3)/2.*RHAVE*DELTAT
R4=RAVEDT
R5=RNDT
R6=RHDT
SG3=SG
38 ABSS=(AGS-RAVEDT)*NS
IF(ABSS.LE.0.0.OR.SG.LE.0.0) ABSS=0.0
ABNS=(AGS-RNDT)*NN
IF(ABNS.LE.0.0.OR.SG.LE.0.0) ABNS=0.0
IF(ORDER.LE.2) ABPS=(LGS1-Y*(NS+NN))*SG
IF(ORDER.LE.2) GO TO 36
ABPS=(LGS1-TL-Y*(NS+NN))*SG
36 PIRCRC=PI*RCSQD
APHS=PIRCRC-AGS+RHDT
IF(APHS.GE.PIRCRC.OR.SG.LE.0.0) APHS=PIRCRC
APNS=PIRCRC-AGS+RNDT
IF(K.LT.2) APHS1=APHS
IF(APNS.GE.PIRCRC) APNS=PIRCRC
IF(ISO.EQ.1) Y=YE
50 IF(NT.EQ.0.0) GO TO 371
IF(Y.LE.0.0) READ(5,506) LTP,DTP,THETTP,TAUEFF
C *****
C * READ IN GEOMETRY ASSOCIATED WITH TERMINATION PORTS (NOT *
C * REQUIRED IF NT=0) *
C * LTP IS THE INITIAL LENGTH OF THE TERMINATION PASSAGES *
C * IN INCHES *
C * DTP IS THE INITIAL DIAMETER OF THE TERMINATION PASSAGE *
C * IN INCHES *
C * THETTP IS THE ACUTE ANGLE BETWEEN THE AXIS OF THE PASSAGE *
C * AND THE MOTOR AXIS IN DEGREES *
C * TAUEFF IS THE ESTIMATED EFFECTIVE WEB THICKNESS AT THE *
C * TERMINATION PORT IN INCHES *
C *****
IF(Y.LE.0.0) WRITE(6,606) LTP,DTP,THETTP,TAUEFF
THETTP=THETTP/57.29578
DABT=NT*3.14159*((DTP+2.*Y)*(LTP-Y/SIN(THETTP))-(DTP+2.*Y)**2/4.+
1(Y+DTP/2.)*(DTP/2.)*(1.-1./SIN(THETTP)))
IF(Y.GE.TAUEFF) DABT=0.0

```

Table C-3 (Cont'd)

```

371 IF(Y.GT.0.0) GO TO 52
    IF(NT.NE.0.0) GO TO 45
    LTP=0.0
    DTP=0.0
45 IF(GRAIN.NE.2) GO TO 49
    LGCI=0.0
    LGNI=0.0
    DISQD=0.0
    DOSQD=4.*RCSQD
49 IF(GRAIN.EQ.1) LGS1=0.0
    VCI=1.1*(ANUM*DISQD*(LGCI+LGNI)+(ANUM*DOSQD-AGS)*
1  LGS1+NT*LTP*ANUM*DTP*DTP)+VCIT
52 BBP=0.0
    BBS=0.0
    BBN=0.0
    ABPORT=ABPT+ABPC+ABPS+DABT+BBP
▶ IF(K.LT.2) XETH=ABPC/(ABPORT+1.E-20)
    ABSLOT=ABST+ABSC+ABSS+BBS
    ABNOZ=ABNT+ABNC+ABNS+BBN
    ABTT=ABPT+ABST+ABNT
    IF(K.GE.2) GO TO 5555
    SUMAB=ABPORT+ABSLOT+ABNOZ
5555 CONTINUE
    IF(K.EQ.0) GO TO 99
    IF(K.EQ.1) ABMAIN=ABPORT+ABSLOT+ABNOZ-ABTT
    K=K+1
    IF(K.GT.2) GO TO 69
    GO TO 2
69 ABTO=ABPORT+ABSLOT+ABNOZ-ABTT
99 CONTINUE
    IF(Y.GT.0.0) GO TO 70
    ABP1=ABPORT
    ABN1=ABNOZ
    ABS1=ABSLOT
70 ABP2=(ABP1+ABPORT)/2.
    ABN2=(ABN1+ABNOZ)/2.
    ABS2=(ABS1+ABSLOT)/2.
    IF(INPUT.EQ.1) GO TO 76
    GO TO (71,72,73,74),ORDER
71 APHEAD=APHS1
    APNOZ=APNT
    SG=SGH
    GO TO 75
72 APHEAD=APHT1
    APNOZ=APNT
    SG=0.0
    IF(GRAIN.EQ.3) SG=(SGH+SGN)/2.
    GO TO 75

```

Table C-3 (Cont'd)

```

73 APHEAD=APHT1
   APNOZ=APNS
   SG=SGN
   GO TO 75
74 APHEAD=APHS1
   APNOZ=APNS
   SG=SGN
   GO TO 75
76 APHEAD=APHT
   APNOZ=APNT
75 Y=YB
   DIFF=SUMAB-SUM2
   DADY=DIFF/DELY
   ABP1=ABPORT
   ABN1=ABNOZ
   ABS1=ABSLOT
   IF(ZW.GE.0.0) GO TO 77
   ABM1=ABMAIN
   ABMAIN=ABTO
   ABTO=ABM1
77 RETURN
500 FORMAT(9X,I2,9X,I2,8X,I2,6X,F4.0,9X,I2,7X,I2)
607 FORMAT(//,20X,19HGRAIN CONFIGURATION)
600 FORMAT(13X,7HINPUT= ,I2,/,13X,7HGRAIN= ,I2,/,13X,6HSTAR= ,I2,/,13X
1,4HNT= ,F4.0,/,13X,7HORDER= ,I2,/,13X,5HCOP= ,I2,/)
507 FORMAT(
6X,F6.2,10X,E11.4,10X,E11.4,8X,E11.4,/,22X,E11.4,
19X,E11.4,8X,E11.4)
610 FORMAT (/13X,40HTABULAR VALUES FOR YT EQUAL ZERO READ IN)
583 FORMAT(13X,5HABPK=,1PE11.4,5X,5HABSK=,1PE11.4,5X,5HABNK=,1PE11.4,
1 5X,5HAPHK=,1PE11.4,5X,5HAPNK=,1PE11.4,/)
584 FORMAT(13X,5HVCIT=,1PE11.4,/)
505 FORMAT(6X,F7.3,9X,E11.4,10X,E11.4,8X,E11.4,/,22X,E11.4,9X,E11.4)
611 FORMAT (/13X,23HTABULAR VALUES FOR YT= ,F7.3,9H READ IN)
501 FORMAT(5X,F8.2,6X,F7.3,9X,F7.3,5X,F6.2,9X,F8.5,/,7X,F8.2,7X,F7.2,9
1X,F8.5,9X,F8.5)
601 FORMAT(20X,19HC.P. GRAIN GEOMETRY,/,13X,4HDO= ,F8.2,/,13X,4HDI= ,F
17.3,/,13X,7HDELDI= ,F7.3,/,13X,3HS= ,F6.2,/,13X,8HTHETAG= ,F9.5,/,
213X,6HLGCI= ,F8.2,/,13X,6HLGNI= ,F7.2,/,13X,8HTHETCN= ,F9.5,/,13X,
38HTHETCH= ,F9.5,/)
502 FURMAT(5X,F6.2,7X,F8.2,5X,F4.0,5X,F8.3,9X,F7.3,5X,F4.0)
602 FORMAT(15X,19HBASIC STAR GEOMETRY,/,13X,4HNS= ,F6.2,/,13X,6HLGSI=
1,F8.2,/,13X,4HNP= ,F5.0,/,13X,4HRC= ,F8.3,/,13X,6HFILL= ,F7.3,/,13
2X,4HNN= ,F4.0,/)
421 FORMAT(3(6X,F5.2),2(10X,F7.5),6X,F5.2)
422 FORMAT(20X,20HWAGON WHEEL GEOMETRY,/,13X,7HTAUWW= ,F6.2,/,13X,
1 4HL1= ,F6.2,/,13X,4HL2= ,F6.2,/,13X,8HALPHA1= ,F9.5,/,13X,
2 8HALPHA2= ,F9.5,/,13X,4HHW= ,F6.2,/)
503 FORMAT(5X,F7.3,7X,F7.3)

```

Table C-3 (Cont'd)

```
603 FORMAT(20X,23HTRUNCATED STAR GEOMETRY,/,13X,4HRP= ,F7.3,/,13X,6HTA  
1US= ,F7.3,//)  
504 FORMAT(9X,F8.5,9X,F8.4,8X,F7.3)  
604 FORMAT(20X,22HSTANDARD STAR GEOMETRY,/,13X,8HTHETAF= ,F9.5,/,13X,8  
1HTHETAP= ,F9.4,/,13X,7HTAUWS= ,F7.3,//)  
506 FORMAT(7X,F7.2,7X,F6.2,10X,F8.5,10X,F7.3)  
606 FORMAT(20X,25HTERMINATION PORT GEOMETRY,/,13X,5HLTP= ,F7.2,/,13X,5  
1HDTP= ,F6.2,/,13X,2HTHETTP= ,F8.5,/,13X,6HTAUEFF= ,F7.3,//)  
END
```

Table C-3 (Cont'd)

SUBROUTINE OUTPUT

```

C *****
C * SUBROUTINE OUTPUT CALCULATES BASIC PERFORMANCE PARAMETERS *
C * AND PRINTS THEM OUT AS A FUNCTION OF DISTANCE BURNED *
C * (WEIGHT CALCULATIONS ARE PERFORMED IN THE MAIN PROGRAM) *
C * T IS THE TIME IN SECS *
C * Y IS THE DISTANCE BURNED IN INCHES *
C * RNOZ IS THE NOZZLE END BURNING RATE IN INCHES/SEC *
C * RHEAD IS THE HEAD END BURNING RATE IN INCHES/SEC *
C * PNOZ IS THE STAGNATION PRESSURE AT THE NOZZLE END IN PSIA *
C * PHEAD IS THE PRESSURE AT THE HEAD END OF THE GRAIN IN PSIA *
C * PTAR IS THE PORT TO THROAT AREA RATIO *
C * MNOZ IS THE MACH NUMBER AT THE NOZZLE END OF THE GRAIN *
C * SUMAB IS THE TOTAL BURNING AREA OF PROPELLANT IN IN**2 *
C * SG IS THE BURNING PERIMETER IN INCHES OF THE STAR SEGMENT *
C * (IF ANY) *
C * PATM IS THE ATMOSPHERIC PRESSURE AT ALTITUDE IN PSIA *
C * CFVAC IS THE THEORETICAL VACUUM THRUST COEFFICIENT *
C * FVAC IS THE VACUUM THRUST IN LBS *
C * F IS THE THRUST IN LBS AT AMBIENT PRESSURE *
C * ISP IS THE DELIVERED SPECIFIC IMPULSE IN SEC AT AMBIENT *
C * PRESSURE *
C * CF IS THE THEORETICAL THRUST COEFFICIENT AT AMBIENT PRESSURE *
C * VC IS THE VOLUME OF CHAMBER GASES IN IN**3 *
C * MDOT IS THE WEIGHT FLOWRATE IN LB/SEC *
C * CFVD IS THE DELIVERED VACUUM THRUST COEFFICIENT *
C * ITOT IS THE ACCUMULATED IMPULSE IN LB-SEC OVER THE *
C * TRAJECTORY *
C * ITVAC IS THE ACCUMULATED VACUUM IMPULSE IN LB-SEC *
C * ISPVAC IS THE DELIVERED VACUUM SPECIFIC IMPULSE IN SEC *
1000 CONTINUE
C * WP IS THE EXPENDED PROPELLANT WEIGHT IN LB *
C * RADER IS THE NOZZLE THROAT EROSION RATE IN IN/SEC *
C * EPS IS THE NOZZLE EXPANSION RATIO *
C * ALT IS THE ALTITUDE IN FT *
C * DT IS THE NOZZLE THROAT DIAMETER IN IN *
C * APHEAD IS THE HEAD END PORT AREA IN IN**2 *
C * APNOZ IS THE NOZZLE END PORT AREA IN IN**2 *
C * COF IS THE CHARACTERISTIC THRUST COEFFICIENT *
C * CFD IS THE DELIVERED THRUST COEFFICIENT AT AMBIENT PRESSURE *
C * ETHETA IS THE TANGENTIAL STRAIN OF THE C.P. GRAIN AT THE BORE *
C * RH05 IS THE DENSITY OF THE PROPELLANT IN SLUGS/IN**3 AT THE *
C * CHAMBER PRESSURE AND TEMPERATURE TGR *
C * RATP IS THE RATIO OF EXTERNAL TO INTERNAL PRESSURES ON THE *
C * C.P. GRAIN *
C * RATR2 IS THE SQUARE OF THE RATIO OF BORE RADIUS TO OUTSIDE *
C * RADIUS OF THE C.P. GRAIN *
C * XETH IS THE FRACTION OF THE TOTAL BURNING BORE SURFACE *

```

Table C-3 (Cont'd)

```

▶ C *          ASSOCIATED WITH THE C.P. GRAIN *
▶ C *          YETA IS THE DISTANCE BURNED IN INCHES FOR THE ENTIRE STAR *
▶ C *          GRAIN AND THE C.P. GRAIN ENDS WHEN THE GRAIN DEFORMATION *
▶ C *          MODIFICATION IS IN USE *
C *****
REAL MGEN,MDIS,MNOZ,MN1,JROCK,N,L,ME1,ME,ISP,ITOT,MU,MASS,ISPVAC
REAL M2,MDBAR,ISP2,ITVAC,MDUT,ISPV
COMMON/CONST1/ZW,AE,AT,THETA,ALFAN
COMMON/CONST2/CAPGAM,ME,BOTE,ZETA,F,TB,HB,GAME,CGAME,TOPE,ZAPE
COMMON/VARIA1/Y,T,DELY,DELTAT,PONUZ,PHEAD,RNOZ,RHEAD,SUMAB,PHMAX
COMMON/VARIA2/ABPORT,ABSLOT,ABNOZ,APHEAD,APNOZ,DACY,ABP2,ABN2,ABS2
COMMON/VARIA3/ITOT,ITVAC,JROCK,ISP,ISPVAC,MDIS,MNOZ,SG,SUMMT
COMMON/VARIA5/ABMAIN,ABTO,SUMDY,VC1,ABTT,PTRAN
COMMON/VARIA6/WP2,CF,WP,RADER,EPS,VC,FLAST,TLAST,DT,PONTOT,WPI
COMMON/VARIA7/TIME,FV,ISPV,NX
▶ COMMON/VARIA9/ETHETA,RHO5,RATP,PMOD,CMOD,PMU,CMU,ALPTS,RATR2
▶ COMMON/VARI20/YETA,XETH,ISO
COMMON/IGN1/KA,KB,UFS,RHO,L,PMIG,TI1,TI2,CSIG,Q1,N1,Q2,N2
COMMON/PLOTT/NUMPLT(16),IPU,NDUM,NP,IOP
DIMENSION TPLT(200),PNPLOT(200),PHPLOT(200),FPLT(200),FVPLT(200),
1) ,RNPLT(200),RHPLT(200),YBPLT(200),ABPLOT(200),SGPLOT(200),VCPL
20T(200)
DATA G/32.1725/
IF(NDUM.EQ.1) GO TO 2
ME1=7.0
NP=NP+1
YB=Y
VCX=VC
IF(Y.LE.0.0) M2=MDIS
MDBAR=(M2+MDIS)/2.
SUMMT=SUMMT+MDBAR*DELTAT
WPI=G*SUMMT
WP2=RHO*(VC-VC1)*G
WP=(WPI+WP2)/2.
▶ IF(ISO.EQ.1) WP=WPI
PTAR=1./JROCK
17 ME=SQRT(2./BOTE*(TOPE/2.*(AE*ME1/AT)**(1./ZAPE)-1.))
IF(ABS(ME-ME1).LE.0.002) GO TO 9
ME1=ME
GO TO 17
9 CONTINUE
PRES=(1.+BOTE/2.*ME*ME)**(-GAME/BOTE)
ALT=HB*(T/TB)**(7./3.)
PATM=14.696/EXP(0.43103E-04*ALT)
IF(MDIS.LE.0.0.OR.PONUZ.LE.0.0)GO TO 45
COF=CGAME*SQRT(2.*GAME/BOTE*(1.-PRES**(BOTE/GAME)))
CF=COF+AE/AT*(PRES-PATM/PONUZ)
CFVAC=CF+AE/AT*PATM/PONUZ

```



Table C-3 (Cont'd)

```

CFD=(COF*(1.+COS(ALFAN))/2.+EPS*PRES)*ZETA- EPS*PATM/PONOZ
CFVD=CFD+EPS*PATM/PONOZ
F=COS(THETA)*PONOZ*AT*CFD
IF(F.LE.0.0) F=0.0
IF(Y.LE.0.0) F2=F
FBAR=(F+F2)/2.
FVAC=COS(THETA)*PONOZ*AT*CFVD
IF(Y.LE.0.0) FV2=FVAC
FVBAR=(FV2+FVAC)/2.
MDOT=MDIS*G
ISP=F/MDOT
ISPVAC=FVAC/MDOT
ITOT=ITOT+FBAR*DELTAT
ITVAC=ITVAC+FVBAR*DELTAT
IF(Y.LE.0.0) PON2=PONOZ
PONBAR=(PON2+PONOZ)/2.
PONTOT=PONTOT+PONBAR*DELTAT
PON2=PONOZ
M2=MDIS
F2=F
FV2=FVAC
IF(PHEAD.GT.PHMAX) PHMAX=PHEAD
GO TO 47
45 CFVAC=0.0
FVAC=0.0
F=0.0
47 WRITE(6,1) T,YB,RNOZ,RHEAD,PCNOZ,PHEAD,PTAR,MNGZ,SUMAB,SG,PATM,CFV
1AC,FVAC,F,ISP,CF,VCX,MDOT,CFVD,ITOT,ITVAC,ISPVAC,WP,RADER,EPS,ALT
2,DT,APHEAD,APNOZ,COF,CFD
IF(ISO.EQ.0) GO TO 200
WRITE(6,5) ETHETA,RHO5,RATP,RATR2,XETH,YETA
200 CONTINUE
IF(IPO.EQ.0) RETURN
TPLOT(NP)=T
PNPLOT(NP)=PONOZ
PHPLOT(NP)=PHEAD
FPLOT(NP)=F
FVPLOT(NP)=FVAC
RNPLOT(NP)=RNOZ
RHPLOT(NP)=RHEAD
YBPLOT(NP)=YB
ABPLOT(NP)=SUMAB
SGPLOT(NP)=SG
VCPLOT(NP)=VC
RETURN
2 NP=NP+2
IOP=1
DO 1004 I=1,16

```

Table C-3 (Cont'd)

```

IF(NUMPLT(1).EQ.1) GO TO 1003
GO TO 1004
1003 GO TO (10,20,30,40,50,55,60,70,75,80,90,95,97,100,110,115),1
10 CALL PLOTIT(TPLOT,'TIME (SECS)',11,PHPLCT,'PHEAD (PSIA)',12,
1 PNPLOT,'PONOZ',5,NP,1,'DUMMY',5)
GO TO 1004
20 CALL PLOTIT(TPLOT,'TIME (SECS)',11,PNPLOT,'PONOZ (PSIA)',12,PHPLOT
1,'PHEAD (PSIA)',12,NP,1,'DUMMY',5)
GO TO 1004
30 CALL PLOTIT(TPLOT,'TIME (SECS)',11,PHPLOT,'PHEAD',5,PNPLOT
1,'PONOZ',5,NP,3,'PRESSURE (PSIA)',15)
GO TO 1004
40 CALL PLOTIT(TPLOT,'TIME (SECS)',11,RHPLOT,'RHEAD (IN PER SEC)',18,
1PHPLOT,'PHEAD (PSIA)',12,NP,1,'DUMMY',5)
GO TO 1004
50 CALL PLOTIT(TPLOT,'TIME (SECS)',11,RNPLOT,'RNOZ (IN PER SEC)',17,
1PNPLOT,'PONOZ (PSIA)',12,NP,1,'DUMMY',5)
GO TO 1004
55 CALL PLOTIT(TPLOT,'TIME (SECS)',11,RHPLOT,'RHEAD',5,RNPLOT,
1 'RNOZ',4,NP,3,'BURNING RATE (IN PER SEC)',25)
GO TO 1004
60 CALL PLOTIT(TPLOT,'TIME (SECS)',11,ABPLCT,'TOTAL BURNING AREA (SQ
1IN)',26,PNPLOT,'PONOZ',5,NP,1,'DUMMY',5)
GO TO 1004
70 CALL PLOTIT(TPLOT,'TIME (SECS)',11,SGPLOT,'STAR PERIMETER (IN)',19
1,PNPLOT,'PONOZ',5,NP,1,'DUMMY',5)
GO TO 1004
75 CALL PLOTIT(TPLOT,'TIME (SECS)',11,ABPLCT,'TOTAL BURNING AREA (SQ
1IN)',26,SGPLOT,'STAR PERIMETER (IN)',19,NP,2,'DUMMY',5)
GO TO 1004
80 CALL PLOTIT(TPLOT,'TIME (SECS)',11,FPLOT,'THRUST (LBS)',12,PNPLOT,
1 'PONOZ',5,NP,1,'DUMMY',5)
GO TO 1004
90 CALL PLOTIT(TPLOT,'TIME (SECS)',11,FVPLLOT,'VACUUM THRUST (LBS)',19
1,PNPLOT,'PONOZ',5,NP,1,'DUMMY',5)
GO TO 1004
95 CALL PLOTIT(TPLOT,'TIME (SECS)',11,FPLOT,'THRUST',6,FVPLLOT,
1 'VACUUM THRUST',13,NP,3,'THRUST (LBS)',12)
GO TO 1004
97 CALL PLOTIT(TPLOT,'TIME (SECS)',11,VCPLLOT,'CHAMBER VOLUME (IN**3)'
1 ,22,PNPLOT,'PONOZ',5,NP,1,'DUMMY',5)
GO TO 1004
100 CALL PLOTIT(YBPLOT,'BURNED DISTANCE (IN)',20,ABPLOT,'TOTAL BURNING
1 AREA (SQ IN)',26,PNPLOT,'PONOZ',5,NP,1,'DUMMY',5)
GO TO 1004
110 CALL PLOTIT(YBPLOT,'BURNED DISTANCE (IN)',20,SGPLOT,'STAR PERIMETE
1R (IN)',19,PNPLOT,'PONOZ',5,NP,1,'DUMMY',5)
GO TO 1004

```

Table C-3 (Cont'd)

```

115 CALL PLOTIT(YBPLOT,'BURNED DISTANCE (IN)',20,ABPLOT,'TOTAL BURNING
1 AREA (SQ IN)',26,SGPLOT,'STAR PERIMETER (IN)',19,NP,2,'DUMMY',5)
1004 CONTINUE
RETURN
1 FORMAT(13X,6HTIME= ,F7.2,12X,3HY= ,F6.2,/,13X,6HRNOZ= ,1PE11.4,9H
1 RHEAD= ,1PE11.4,9H PONOZ= ,1PE11.4,9H PHEAD= ,1PE11.4,/,13X,6HP
2TAR= ,1PE11.4,9H MNOZ= ,1PE11.4,9H SUMAB= ,1PE11.4,9H SG= ,
31PE11.4,/,13X,6HPATM= ,1PE11.4,9H CFVAC= ,1PE11.4,9H FVAC= ,1PE
411.4,9H F= ,1PE11.4,/,13X,6H ISP= ,1PE11.4,9H CF= ,1PE11.
54,9H VC= ,1PE11.4,9H MCDT= ,1PE11.4,/,13X,6HCFVD= ,1PE11.4,9
6H ITOT= ,1PE11.4,9H ITVAC= ,1PE11.4,9H ISPVAC= ,1PE11.4,/,13X,6
7HWP= ,1PE11.4,9H RADER= ,1PE11.4,9H EPS= ,1PE11.4,9H ALT=
8 ,1PE11.4,/,13X,6HDT= ,1PE11.4,9H APHEAD= ,1PE11.4,9H APNOZ= ,1
9PE11.4,9H COF= ,1PE11.4,/,13X,6H CFD= ,1PE11.4,/)
5 FORMAT(13X,8HETHETA= ,1PE11.4,9H RHOS= ,1PE11.4,9H RATP= ,1PE1
11.4,9H RATR2= ,1PE11.4,9H XETH= ,1PE11.4,7H YETA= ,1PE11.4,/)
END

```

Table C-3 (Cont'd)

```

SUBROUTINE IGNITN
C *****
C * SUBROUTINE IGNITN CALCULATES THE PRESSURE RISE DURING *
C * THE IGNITION PERIOD *
C * ASIG IS THE IGNITER THROAT AREA IN IN**2 *
C * WIGTOT IS THE TOTAL WEIGHT OF THE IGNITER PROPELLANT IN LBS *
C * MIGAV IS THE IGNITER AVERAGE MASS FLOW RATE OVER THE FIRST *
C * HALF OF THE IGNITER BURNING TIME IN LBS/SEC *
C * PCIG IS THE IGNITER PRESSURE IN LBS/IN**2 *
C *****
REAL K(4),L,KA,KB,JROCK,J2,MIG,MIGAV,MSRM,ME,MDIS,MNOZ,MNOZI,MNI
REAL N1,N2,MIGAVE
COMMON/CONST1/ZW,AE,AT,THETA,ALFAN
COMMON/CONST2/CAPGAM,ME,BOTE,ZETAF,TB,HB,GAME,CGAME,TOPE,ZAPE
COMMON/VARIA1/Y,TIG,DELY,DELTAT,PCNOZ,PHEAD,RNOZ,RHEAD,SUMAB,PHMAX
COMMON/VARIA2/ABPORT,ABSLOT,ABNOZ,APHEAD,APNOZ,DADY,ABP2,ABN2,ABS2
COMMON/VARIA3/ITOT,ITVAC,JROCK,ISP,ISPVAC,MDIS,MNOZ,SG,SUMMT
COMMON/VARIA5/ABMAIN,ABTO,SUMDY,VCI,ABTT,PTRAN
COMMON/IGN1/KA,KB,UFS,RHO,L,PMIG,TI1,TI2,CSIG,Q1,N1,Q2,N2
COMMON/IGN2/ALPHA,BETA,PBIG,RRIG,DELTIG,X,TOP,ZAP
COMMON/PLOTT/NUMPLT(16),IPO,NDUM,IPT,ICP
DIMENSION B(9)
DATA A1,A2,A3,A4/.17476,-.551481,1.205536,.171165/
DATA B(1),B(2),B(3),B(4),B(5)/0.,.4,.455737,1.,.296978/
DATA B(6),B(7),B(8),B(9)/.15876,.2181,-3.050965,3.832864/
C *****
C * THE A'S AND B'S ARE CONSTANTS FOR THE RUNGE-KUTTA INTEGRATION *
C *****
DATA G/32.1725/
XXX=.05*PONNOZ
IPLUG=0
PONNOZI=PONNOZ
RHEADI=RHEAD
RNOZI=RNOZ
PHEADI=PHEAD
DELTIT=DELTAT
DISM=MDIS
DELTAT=DELTIG
SUMABI=SUMAB
MNOZI=MNOZ
MNOZ=0.0
RHEAD=0.0
RNOZ=0.0
MDIS=0.0
ABI=0.0
TIGI=0.0
PCI=14.696
TIG=0.0

```

Table C-3 (Cont'd)

```

PCNEW=14.696
SUMAB=0.0
PCIG=14.696
PHEAD=14.696
PNOZ=14.696
SLOPE=SUMAB/L
G2=CAPGAM*CAPGAM
J2=JROCK*JROCK
GJ=G2*J2/2.
MIGAV=.2*AT/G
ASIG=4.*MIGAV*CSIG/(4.*PMIG-RRIG*(TI2-TI1))
MIGTOT=G*MIGAV*(5.*(TI2-TI1)/6.)
MIGAVE=MIGAV*G
WRITE(6,999) ASIG,MIGTOT,MIGAVE
WRITE(6,10)
18 NNN=0
WRITE(6,30) PCIG
CALL OUTPUT
9 CONTINUE
DO 8 N=1,4
IF(N.EQ.1) PC=PCI
IF(N.EQ.2) PC=PCI+B(2)*K(1)
IF(N.EQ.3) PC=PCI+B(5)*K(1)+B(6)*K(2)
IF(N.EQ.4) PC=PCI+B(7)*K(1)+B(8)*K(2)+B(9)*K(3)
TIG=TIGI+B(N)*DELTIG
SUMAB=ABI+SLOPE*UFS*B(N)*DELTIG
IF(SUMAB.GT.SUMAB1) SUMAB=SUMAB1
PHEAD=PC
IF(MDIS.NE.0.0) PHEAD=PC*(1.+GJ)
IF(PHEAD.LE.PTRAN)RHEAD=Q1*PHEAD**N1
IF(PHEAD.GT.PTRAN)RHEAD=Q2*PHEAD**N2
IF(TIG.LE.TI1) PCIG=PMIG*TIG/TI1
IF(TIG.GT.TI1.AND.PCIG.GT.PHEAD) PCIG=PMIG-RRIG*(TIG-TI1)
IF(PCIG.LE.PHEAD) PCIG=PHEAD
MIG=0.0
IF(PCIG.GT.PHEAD.AND.TIG.LE.TI2/2.) MIG=PCIG*ASIG/CSIG
CSTR=KA+KB*PC
MDIS=PC*AT/CSTR
IF(PC.LE.PBIG.AND.IPLUG.EQ.0) GO TO 7
IPLUG=1
MNOZ=MNOZI
PNOZ=PC*(1.-GJ)
ZIT=MDIS*X/APNOZ
RN1=RHEAD
AZ=ALPHA*ZIT** .8
XL=UFS*TIG
IF(XL.GT.L) XL=L
4 EX=XL** .2*EXP(BETA*RN1*RHO/ZIT)

```

Table C-3 (Cont'd)

```

    IF (PNOZ.LE.PTRAN)RNOZ=RN1-(RN1-Q1*PNOZ**N1-AZ/EX)/(1.+AZ*BETA*RHO/
2(ZIT*EX))
    IF (PNOZ.GT.PTRAN)RNOZ=RN1-(RN1-Q2*PNOZ**N2-AZ/EX)/(1.+AZ*BETA*RHO/
2(ZIT*EX))
    IF (ABS(RN1-RNOZ).LE.0.002) GO TO 5
    RN1=RNOZ
    GO TO 4
7 MDIS=0.0
  MNOZ=0.0
  PNOZ=PC
  RNOZ=RHEAD
5 CONTINUE
  MSRM=RHO*SUMAB*(RNOZ+RHEAD)/2.
  DENOM=(VCI/(12.*CSTR*CSTR*G2))*(1.-(2.*K8*PC)/CSTR)
  DPDT=(MIG+MSRM-MDIS)/DENOM
  IF (DPDT.LT.0.0.AND.PC.LT.20.0) DPDT=0.0
  K(N)=DELTIG*DPDT
8 CONTINUE
  PCNEW=PCI+A1*K(1)+A2*K(2)+A3*K(3)+A4*K(4)
  PHEAD=PCNEW
  IF (MDIS.GT.0.0) PHEAD=PCNEW*(1.+GJ)
  PONOZ=PCNEW
  XXY=ABS(PONOZ-PONOZ1)
  IF (PCNEW.LE.1.001*PCI.AND.SUMAB.EQ.SUMAB1.AND.XXY.LE.XXX) GO TO 13
  AB1=SUMAB
  TIG1=TIG
  PC1=PCNEW
  NNN=NNN+1
  IF (NNN.GE.5) GO TO 18
  GO TO 9
13 CONTINUE
  CALL OUTPUT
  WRITE(6,30) PCIG
  DELTAT=DELT
  MDIS=DISM
  SUMAB=SUMAB1
  PONOZ=PONOZ1
  RHEAD=RHEAD1
  RNOZ=RNOZ1
  PHEAD=PHEAD1
  MNOZ=MNOZ1
  IF (IPO.NE.2.AND.IPO.NE.3) GO TO 53
  NOUM=1
  CALL OUTPUT
  NOUM=0
53 CONTINUE
  IPT=0
  RETURN

```

Table C-3 (Cont'd)

```

999 FORMAT(///,20X,25HIGNITER SIZE CALCULATIONS,/,13X,5HASIG=,F7.2,/,
1 13X,7HWIGTOT=,F7.2,/,13X,6HMIGAV=,F8.3,///)
10 FORMAT(33X,28H*****Ignition Transient****,/,33X,28H**** IGNITION
1TRANSIENT ****,/,33X,28H*****Ignition Transient****)
30 FORMAT(13X,6HPCIG= ,1PE11.4)
END

```

```

SUBROUTINE INTRP1(Y,T,N,TT,DY,ICLK)
DIMENSION Y(N),T(N)
N1=N-1
DY=0.0
IF(ICLK) 2,2,3
2 DO 1 I=1,N1
IF(TT.GE.T(I).AND.TT.LT.T(I+1)) DY=((Y(I+1)-Y(I))/(T(I+1)-T(I)))
2*(TT-T(I))+Y(I)
IF(DY.NE.0.0) RETURN
1 CONTINUE
3 DO 4 I=1,N1
IF(TT.LE.T(I).AND.TT.GT.T(I+1)) DY=((Y(I+1)-Y(I))/(T(I+1)-T(I)))
2*(TT-T(I))+Y(I)
IF(DY.NE.0.0) RETURN
4 CONTINUE
RETURN
END

```

Table C-3 (Cont'd)

```

SUBROUTINE PLOTIT(X,XHDR,KX,Y,YHDR,NY,T,THDR,NT,NP,NPLOT,DUMMY,ND)
C *****
C * SUBROUTINE PLOTIT PLOTS TWO DEPENDENT VARIABLES, Y AND T, *
C * VERSUS AN INDEPENDENT VARIABLE, X *
C * XHDR, YHDR, AND THDR ARE THE HEADINGS FOR THE X, Y, AND T *
C * AXES, RESPECTIVELY *
C * KX, NY, AND NT ARE THE NUMBER OF CHARACTERS IN THE X, Y, AND *
C * T AXES HEADINGS, RESPECTIVELY (MAX OF 32 IN EACH) *
C * NP IS THE NUMBER OF POINTS TO BE PLOTTED PLUS 2 *
C * VALUES FOR NPLOT ARE *
C * 1 FOR Y ONLY PLOTTED VERSUS X *
C * 2 FOR Y AND T PLOTTED VERSUS X ON SAME AXES *
C * WITH INDIVIDUAL SCALES *
C * 3 FOR Y AND T PLOTTED VERSUS X ON SAME AXES *
C * WITH SAME SCALES *
C * DUMMY IS THE HEADING FOR THE DOUBLE AXIS (NPLOT=3) *
C * ND IS THE NUMBER OF CHARACTERS IN DUMMY *
C *****
DIMENSION XHDR(8),YHDR(8),THDR(8),DUMMY(8),X(NP),Y(NP),T(NP)
NX=-KX
NM=NP-1
NN=NP-2
IF(NPLOT.EQ.1) GO TO 9
CALL SCALE(T,4.,NN,1)
9 CALL SCALE(X,8.,NN,1)
CALL SCALE(Y,4.,NN,1)
IF(NPLOT.NE.3) CALL AXIS(0.,0.,YHDR,NY,4.,180.,Y(NM),Y(NP))
IF(NPLOT.EQ.3) CALL AXIS(0.,0.,DUMMY,ND,4.,180.,Y(NM),Y(NP))
CALL AXIS(0.,0.,XHDR,NX,8.,90.,X(NM),X(NP))
IF(NPLOT.EQ.1) GO TO 12
DO 11 I=1,NN
11 T(I)=-T(I)
12 DO 13 I=1,NN
13 Y(I)=-Y(I)
CALL LINE(Y,X,NN,1,0,1)
CALL PLOT(0.,0.,3)
IF(NPLOT.EQ.1) GO TO 24
IF(NPLOT.EQ.2) CALL PLOT(0.,-.5,2)
IF(NPLOT.EQ.2) CALL AXIS(0.,-.5,THDR,NT,4.,180.,T(NM),T(NP))
CALL LINE(T,X,NN,1,0,2)
DO 25 I=1,NN
25 T(I)=-T(I)
24 DO 26 I=1,NN
26 Y(I)=-Y(I)
IF(NPLOT.EQ.1) GO TO 32
CALL SYMBOL(-4.35,.52,.1,1,0.,0)
CALL SYMBOL(-4.2,.52,.1,2,0.,0)
CALL SYMBOL(-4.3,.65,.1,YHDR,90.,NY)
CALL SYMBOL(-4.15,.65,.1,THDR,90.,NT)
32 CALL PLOT(8.5,0.,-3)
RETURN
END

```